



MEDICAL UNIVERSITY
OF VIENNA

The role of calreticulin mutations in double mutated myeloproliferative neoplasms and as a potential target for immunotherapy

Doctoral thesis at the Medical University of Vienna for obtaining
the academic degree

Doctor of Philosophy (PhD)

Submitted by

DI Christina Maria Schüller

Supervisor:
Robert Kralovics, PhD

Klinisches Institut für Labormedizin
Medizinische Universität Wien
Währinger Gürtel 18-20, Leitstelle 5H
1090 Vienna, Austria

Vienna, 06/2023

Declaration

Experimental work for the present thesis was conducted in the Dr. Robert Kralovics lab at the Center for Molecular Medicine of the Austrian Academy of Sciences as well as the Institute of Laboratory Medicine of the Medical University of Vienna.

The article presented in chapter 3.1 was published in American Journal of Hematology. This study was a collaborative effort of the author and Andrea Majoros. All experiments were performed by Christina M. Schüller, Andrea Majoros and Harini Nivarthi. Data were analyzed by Christina M. Schüller, Andrea Majoros and the manuscript was written with input from Robert Kralovics.

Christina M. Schueller*, Andrea Majoros*, Harini Nivarthi, Robert Kralovics (2022) Co-expression of mutated Jak2 and Calr enhances myeloproliferative phenotype in mice without loss of stem cell fitness” published in American Journal of Hematology

Chapter 3.2 contains results from unpublished work comprising generation and testing of chimeric antigen receptors (CARs) specifically targeting mutant calreticulin (CALR). The study was carried out by the author, Christina Schüller.

All parts of this thesis were written by the author, Christina M. Schüller, with input from Robert Kralovics.

Table of contents

Declaration	II
Table of contents	III
List of figures	V
List of tables	VI
Abstract	VII
Zusammenfassung	VIII
Publications arising from this thesis	IX
Abbreviations	X
Acknowledgments	XII
1. INTRODUCTION	1
1.1 Pathophysiology of myeloproliferative neoplasms	1
1.1.1 <i>JAK2</i> mutations	3
1.1.2. <i>MPL</i> mutations	5
1.1.3 <i>CALR</i> mutations	6
1.1.4 Clonal evolution of MPN	7
1.1.5 The co-occurrence of MPN driver mutations	9
1.1.6 Aberrant cytokine signaling caused by MPN driver mutations	10
1.1.7 Lessons learned from mouse models	11
1.2. Clinical aspects of MPN	16
1.2.1 Risk stratification and prognosis	18
1.3 Therapeutic options for MPN	19
1.3.1 Hydroxyurea	20
1.3.2 Anagrelide	20
1.3.3 Interferon- α	21
1.3.4 <i>JAK</i> inhibitors	22
1.3.5 Allogeneic HSCT	22
1.3.6 Immunotherapy for calreticulin mutated MPN – a novel treatment approach	23
1.4 Chimeric antigen receptor T cell therapy	24

1.4.1 Structural elements of CARs	27
1.4.2 Limitations of CAR-T cell therapy	30
1.4.3 CAR-T cell therapy for hematological malignancies.....	33
1.5 AIMS.....	35
1.5.1 The influence of <i>JAK2/CALR</i> double mutation on HSC fitness and disease phenotype	35
1.5.2 Generation and testing of CARs targeting mutCALR	36
2. RESULTS.....	37
2.1 Manuscript #1: Co-expression of mutated Jak2 and Calr enhances myeloproliferative phenotype in mice without loss of stem cell fitness	37
2.2 Chimeric antigen receptor T cell therapy for myeloproliferative neoplasms with mutated calreticulin.....	42
2.2.1 Surface expression of mutCALR in different models.....	42
2.2.2 Generation and selection of a-mutCALR-CARs	43
2.2.3 Testing of selected CARs in primary T cells.....	44
2.2.4 The influence of perturbations <i>in vitro</i>	46
2.2.5 Generation of murine a-mutCALR CAR-T cells.....	47
2.2.6 <i>Ex vivo</i> targeting of primary murine Calr-del52 mutated cells	48
2.2.7 <i>In vivo</i> treatment of chimeric mice	50
2.2.8 Obstacles for <i>in vivo</i> efficacy	53
3. DISCUSSION.....	58
3.1 Co-expression of Jak2 and Calr oncogenes.....	58
3.2 CAR-T cells targeting mutCALR.....	62
4. METHODS	70
References.....	73
Curriculum vitae	98

List of figures

Figure 1: MPN driver mutations lead to cytokine-independent activation of myeloid cytokine receptors.	2
Figure 2: Frequency of MPN driver mutations among PV, ET and PMF.	2
Figure 3: <i>JAK2V617F</i> allele burden influences disease manifestation and progression.	4
Figure 4: Mutant CALR forms an oncogenic complex with MPL.	7
Figure 5: Clonal evolution of MPN.	9
Figure 6: CAR-T cells are autologous T cells equipped with synthetic receptors.	27
Figure 7: Target cells present mutCALR on their surface at different densities.	42
Figure 8: Jurkat CAR-T cells recognize mutCALR.	44
Figure 9: Primary T cells specifically recognize CALR mutated UT-7/Tpo target cells.	45
Figure 10: CAR-T cells can eliminate primary CD34+ patient cells.	46
Figure 11: Secreted mut-CALR does not influence CAR-T cell functionality.	47
Figure 12: Primary mouse CAR-T cells effectively eliminate mutCALR expressing target cells.	48
Figure 13: Murine anti-mutCALR CAR-T cells recognize and specifically target mutant cells <i>ex vivo</i>	49
Figure 14: Transplantation after <i>ex vivo</i> treatment leads to complete and durable remission.	50
Figure 15: <i>In vivo</i> CAR-T cell treatment of chimeric mice shows limited efficacy.	52
Figure 16: CD19-specific CAR-T cells are fully functional in Wt as well as Calr mutated mice.	53
Figure 17: PD-L1 expression is cell type specific and is increased after BMT.	54
Figure 18: Expression of exhaustion markers in a-mutCALR CAR-T cells depends on the recipients' genotype.	55
Figure 19: Expression of exhaustion markers is increased in CAR-T cells compared to Mock-T cells.	56
Figure 20: Antibody pre-treatment leads to increased availability of the CAR epitope.	57

List of tables

Table 1: Overview over different JAK2V617F mouse models..... 13
Table 2: Overview over different CALR mutated mouse models 15
Table 3: WHO diagnostic criteria for MPN, adapted from Arber et al., 2016²..... 17

Abstract

Myeloproliferative neoplasms (MPNs) are hematological disorders characterized by constitutive cytokine signaling caused by mutations in the *JAK2*, *CALR* and *MPL* genes. The discovery of *CALR* mutations in 2013 was the premise for the recognition of double mutated MPN and for the development of specific immunotherapies targeting mutant CALR (mutCALR). In this thesis we showed the influence of co-existing *CALR* and *JAK2* mutations on the MPN phenotype and generated the first chimeric antigen receptors (CARs) targeting mutCALR.

In the past, MPN driver mutations were believed to exclude each other. Yet, numerous reports described the concomitant presence of two mutations in one patient. Clonal analysis, however, showed that these mutations were acquired in two independent clones in most cases, which indicates that such mutations might be mutually exclusive on the cellular level. Thus, we set out to evaluate the influence of Jak2-V617F and Calr-del52 co-expression on hematopoietic stem cell (HSC) fitness. We generated a novel mouse model by crossing mice with *Jak2* or *Calr* single mutations and analyzed the disease phenotype as well as stem cell functionality in double mutant mice. Mice co-expressing both oncogenes had increased thrombocytosis, leukocytosis and reduced survival compared to single mutants. In bone marrow transplantation experiments, double mutated HSCs maintained their repopulation capacity and outgrew wild type competitors. Thus, our mouse model indicated that co-occurrence of *Calr* and *Jak2* mutations is associated with aggravated disease, while HSC fitness was not hampered.

Frameshift mutations in the *CALR* gene result in a protein with a novel amino acid sequence at the C-terminus. MutCALR interacts with the thrombopoietin receptor (MPL) forming an oncogenic complex, which leads to constitutive downstream activation and clonal hematopoiesis. Therefore, mutCALR constitutes a truly tumor-specific neoantigen, which is the disease driver and present at the cell surface and thus fulfills all criteria for an ideal immunotherapy target. Therefore, we developed CARs targeting mutCALR. We screened a small CAR library and could identify functional human and mouse CARs. Those were specifically activated by mutCALR expressing cells and led to selective and efficient killing of cell lines with mutated *CALR*, while wild type cells were spared. We could further show specific targeting of primary patient cells expressing mutCALR by human CAR-T cells. With this we delivered the first proof that CAR-T cells can selectively eradicate mutCALR expressing cells. Yet, the *in vivo* efficacy of murine CAR-T cells in a fully immunocompetent model is limited. Therefore, further research is needed to identify factors inhibiting CAR-T cell functionality *in vivo*.

Zusammenfassung

Myeloproliferative Neoplasien (MPN) werden durch *JAK2*, *CALR* oder *MPL* Mutationen ausgelöst. Die Entdeckung von *CALR*-Mutationen im Jahr 2013 war die Voraussetzung für die Erkennung doppelt mutierter MPN und für die Entwicklung spezifischer Immuntherapien gegen mutiertes *CALR* (mut*CALR*). In dieser Arbeit haben wir den Einfluss koexistierender *CALR*- und *JAK2*-Mutationen auf den Verlauf von MPN gezeigt und die ersten mut*CALR*-spezifischen chimären Antigenrezeptoren (CARs) generiert.

„Synthetic lethality“ beschreibt eine ungünstige Interaktion von zwei Mutationen, die das gleichzeitige Auftreten bestimmter somatischer Mutationen ausschließt. Obwohl MPN-Treibermutationen in der Vergangenheit als exklusiv beschrieben wurden, gibt es zahlreiche Berichte über das gleichzeitige Auftreten von zwei Treibermutationen. Diese wurden jedoch häufig in zwei unabhängigen Klonen erworben, was die Frage aufwirft, ob das gleichzeitige Auftreten beider Mutationen in einer hämatopoetischen Stammzelle (HSC) deren zelluläre Fitness verringert. In dieser Studie untersuchten wir die Auswirkung der Koexpression von Jak2-V617F und Calr-del52 auf die HSC-Fitness. Wir kreuzten Mäuse, mit Einzelmutationen und analysierten den hämatopoetischen Phänotyp von Doppelmутanten. Um die Stammzell-Fitness zu beurteilen, führten wir primären und sekundären Knochenmarktransplantationen durch. Doppelmutierte Mäuse hatten im Vergleich zu Einzelmutanten einen schwerwiegenderen MPN-Phänotyp und eine geringere Überlebensrate. Darüber hinaus übertrafen HSCs, die beide Mutationen exprimierten, nicht mutierte HSCs und behielten ihre Wettbewerbsfähigkeit in primären und sekundären Transplantationen bei.

Frameshift-Mutationen im *CALR*-Gen führen zur Veränderung der Aminosäuresequenz am C-Terminus des Proteins. Mut*CALR* interagiert mit dem Thrombopoietinrezeptor (MPL) und bildet einen onkogenen Komplex, der zu einer konstitutiven Downstream-Aktivierung und klonaler Hämatopoese führt. Daher stellt mut*CALR* ein tumorspezifisches Neoantigen dar, das auf der Zelloberfläche vorhanden ist und somit alle Kriterien für einen idealen Angriffspunkt gezielter Immuntherapie erfüllt. Aus diesem Grund haben wir CARs entwickelt, die auf mut*CALR* abzielen. Aus einer Reihe von CARs mit verschiedenen Antigenbindungsdomänen konnten wir funktionelle humane, sowie murine CARs identifizieren. Diese wurden spezifisch durch mut*CALR*-exprimierende Zellen aktiviert und führten zu einer selektiven und effizienten Zytotoxizität gegenüber Zelllinien und primären Zellen mit mutiertem *CALR*, während Wildtyp-Zellen verschont blieben. Murine CAR-T-Zellen zeigten jedoch begrenzte Wirksamkeit in einem vollständig immunkompetenten Modell. Daher sind weitere Untersuchungen erforderlich, um Faktoren zu identifizieren, die die Funktionalität von CAR-T-Zellen *in vivo* hemmen.

Publications arising from this thesis

Co-expression of mutated Jak2 and Calr enhances myeloproliferative phenotype in mice without loss of stem cell fitness

Christina M. Schueller, Andrea Majoros, Harini Nivarthi, Robert Kralovics

Published in American Journal of Hematology, 2022

Abbreviations

aa	amino acid
ADCC	antibody-dependent cellular cytotoxicity
ALL	acute lymphoblastic leukemia
AML	acute myeloid leukemia
APC	antigen-presenting cell
BBB	blood-brain barrier
BCMA	B-cell maturation antigen
BFU-E	burst forming unit erythroid
BMT	bone marrow transplantation
CAIX	carboanhydrase IX
CALR	calreticulin
CH	clonal hematopoiesis
CLL	chronic lymphocytic leukemia
CR	complete remission
CRISPR	clustered regularly interspaced short palindromic repeats
CRS	cytokine release syndrome
CTL	cytotoxic T lymphocyte
DC	dendritic cell
DIPSS	Dynamic International Prognostic Scoring System
DLBCL	diffuse large B cell lymphoma
EPO	erythropoietin
EPOR	erythropoietin receptor
ER	endoplasmic reticulum
ET	essential thrombocythemia
FL	follicular lymphoma
G-CSFR	granulocyte colony-stimulating factor receptor
GH	growth hormone
Hb	hemoglobin
HL	Hodgkin lymphoma
HSC	hematopoietic stem cell
HSCT	hematopoietic stem cell transplantation
HSPCs	hematopoietic stem and progenitor cells
HU	hydroxyurea
ICAN	immune effector cell-associated neurotoxicity syndrome
IFN	interferon
IM	idiopathic myelofibrosis
IPSET	International Prognostic Score for Thrombosis in ET
IPSS	International Prognostic Scoring System
ITAM	immunoreceptor tyrosine-based activation motif
JAK	janus kinase
LOH	loss of heterozygosity
LSK	Lin- Sca-1+ c-Kit+
MAPK	Ras-mitogen-activated protein kinase
MCL	mantle cell lymphoma
MDSC	myeloid-derived suppressor cell
MF	myelofibrosis

MHC	major histocompatibility complex
MIPSS	Mutation Enhanced International Prognostic Score System
MM	multiple myeloma
MPL	thrombopoietin receptor (myeloproliferative leukemia protein)
MPN	myeloproliferative neoplasm
mutCALR	mutant CALR
MZL	marginal zone lymphoma
NHL	non-Hodgkin lymphoma
OS	overall survival
PB	peripheral blood
PI3K	phosphoinositide 3-kinase
PMF	primary myelofibrosis
PRL	prolactin
PTK	protein tyrosine kinase
PV	polycythemia vera
STAT	signal transducer and activator of transcription
TAM	tumor-associated macrophage
TH	T helper cell
TLBL	T cell lymphoblastic lymphoma
TPO	thrombopoietin
TRAF	TNF-receptor-associated factor
Treg	regulatory T cell
TYK	tyrosine kinase
UPD	uniparental disomy
VAF	variant allele frequency
WBC	white blood cell
WT	wild type
ZAP-70	ζ-associated protein of 70 kDa

Acknowledgments

I received incredible support throughout my journey to this thesis and here I want to thank the people that were part of this journey.

First and foremost, I want to thank my supervisor, Robert Kralovics. I am grateful for the opportunity to work on such exciting projects and the guidance he provided throughout the evolution of these endeavors. His head never stops generating ideas and his enthusiasm is so big that it spreads throughout the whole lab. I am thankful for the immense trust Robert had in me. His support allowed me to follow my path, I could not have done it without him.

I want to thank my PhD committee members, Manfred Lehner and Christoph Bock. We had lively and fruitful discussions. I met Manfred during my master thesis in his lab and he had an open ear for me and my CARs ever since. Christoph offered me the support of his lab and provided me with the starting material for the CAR-T cell project.

Many thanks to the whole Kralovics lab, to the past members with whom I crossed paths and the current members. From sharing of reagents to sharing of chocolate, thank you for always helping each other out. I want to thank Andrea, not only for her amazing SOPs but also for her scientific and non-scientific input, for always having an open ear and for a fruitful collaboration on generating the double-positive mouse model. During my PhD, I had help from several ambitious students. Thank you for all your hard work, Antonia, Ines, Victoria and Isabella.

The whole CeMM community provided support, knowledge, fun and friendship. I want to thank Giulio Superti-Furga for his encouragement. I am thankful for the guidance by our PhD coordinator Matthew. Thank you to all my fellow CeMMies, who started their PhD with me and special thanks to Daria and Justine, "The cool kids", who became more than colleagues. I was lucky and had two great home institutes. Big thanks to all the KILMies. Work would not have been the same without the social life on 6th floor. Thank you to all the members of the Binder lab, who always had their doors open for me. Thanks to Maria, the mum of the whole floor and my Tullner mate.

As important as the support within the scientific community was the backing, I got from my friends and family. Foremost, I want to thank my amazing husband, Benjamin. His never-ending understanding and patience, his emotional support and all the fun we have, made everything better – the good and the hard times.

1. INTRODUCTION

1.1 Pathophysiology of myeloproliferative neoplasms

BCR-ABL-negative myeloproliferative neoplasms (MPNs), such as polycythemia vera (PV), essential thrombocythemia (ET), and primary myelofibrosis, are hematological cancers characterized by increased blood cell production, thromboembolic complications, hemorrhage, and evolution to acute leukemia (AML). While PV is characterized by panmyelocytosis with marked erythrocytosis, in ET and PMF the megakaryocyte lineage is affected leading to massive platelet production. In PMF, fibroblast activation and subsequent reticulin deposition additionally causes bone marrow (BM) fibrosis^{1,2}.

MPN oncogenesis is driven by acquired hematopoietic stem cell mutations in three genes, janus kinase 2 (*JAK2*), myeloproliferative leukemia protein (*MPL*) and calreticulin (*CALR*), which all trigger constitutive activation of cytokine receptors and downstream signaling³ (Figure 1). The most abundant is a point mutation in *JAK2* exon 14, *JAK2V617F*, which was identified as a driver occurring in PV, ET and PMF in 2005⁴⁻⁶. Two years later somatic mutations in exon 12 of the same gene were found in a small fraction of PV⁷. However, only 70 % of all MPN cases could be explained by *JAK2* mutations and thus, efforts to elucidate the emergence of these diseases were ongoing. From 2006 to 2008, alterations in exon 10 of the *MPL* gene, which encodes for the thrombopoietin receptor (MPL), were recurrently found in ET and PMF patients⁸⁻¹⁰. Nonetheless, a broad number of *JAK2*-negative, *MPL*-negative MPN cases remained enigmatic until 2013, when two groups reported mutations in the *CALR* gene causing ET and PMF. A large gap was closed with *CALR* alterations driving about 80% of *JAK*-negative, *MPL*-negative MPNs^{11,12} (Figure 2).

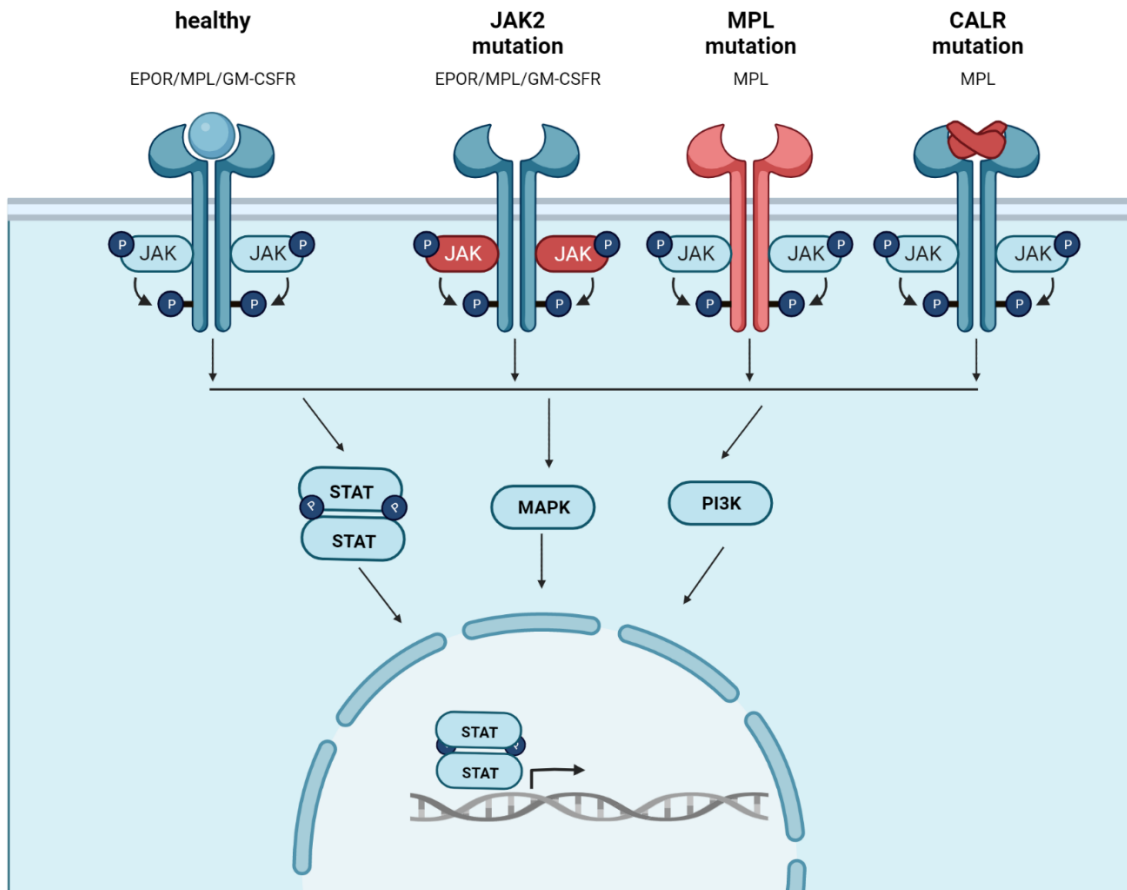


Figure 1: MPN driver mutations lead to cytokine-independent activation of myeloid cytokine receptors. In healthy individuals signaling via the EPOR, MPL and G-CSFR is dependent on interaction with the cognate ligand. MPN driver mutations in *JAK2*, *MPL* and *CALR* lead to constitutive activation of those receptors. *JAK2* can be seen as the catalytic unit of these receptors. Activated *JAK2* transphosphorylates the receptor, which leads to recruitment of molecules starting a downstream signaling cascade. STAT, MAPK and PI3K/AKT pathways affect proliferation and cell cycle progression. Generated with Biorender.

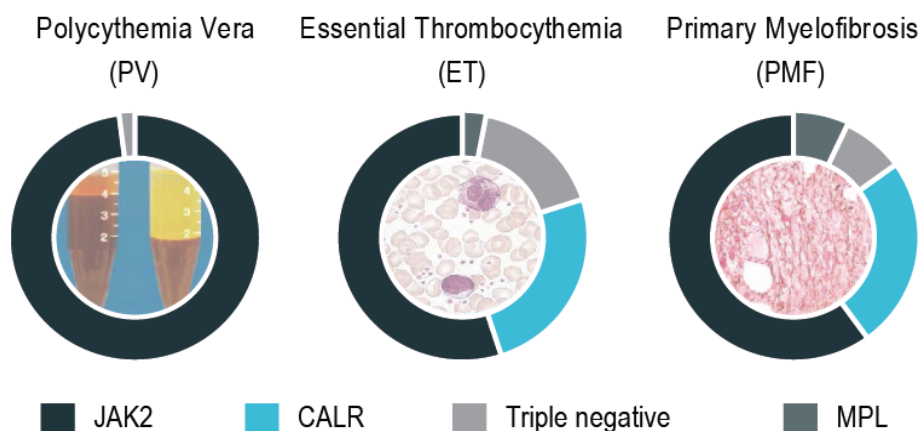


Figure 2: Frequency of MPN driver mutations among PV, ET and PMF. *JAK2* (V617F and exon 12) mutations occur in 98% of all PV and 50-60% of ET and PMF cases. *CALR* mutations account for 25-25% of ET and PMF

patients and MPL mutations occur in 1-4% of ET and 5-10% of PMF patients. Generated with Biorender.

1.1.1 JAK2 mutations

JAK2 belongs to the JAK family of non-receptor tyrosine kinases, which associate with the cytosolic part of cytokine receptors. JAK1, JAK2/tyrosine kinase 2 (TYK2) and JAK3 bind to heterodimeric cytokine receptors, whereas JAK2 binds to homodimeric cytokine receptors. The JAK2 protein consists of a C-terminal kinase domain, JH1, an adjacent pseudokinase domain JH2, an SH2 (JH3-4) and a FERM domain (JH5-7). The latter two comprise the functional unit, which interacts with box1 and 2 regions of cytokine receptors. JAK2 plays a vital role in hematopoiesis, as it binds to the erythropoietin receptor (EPOR), MPL and the granulocyte colony-stimulating factor receptor (G-CSFR). Upon ligand binding the dimeric receptor undergoes a conformation change. The JH1 domains of the JAK2 dimer phosphorylate each other in trans at two tyrosine residues, which leads to JAK activation. This in turn leads to transphosphorylation of the cytokine receptor and induction of downstream signaling via signal transducer and activator of transcription (STAT), Ras-mitogen-activated protein kinase (MAPK), and phosphoinositide 3-kinase (PI3K) pathways^{3,13,14}.

The majority of MPN patients (95 % in PV, 50-60% in ET and PMF) harbor a valine to phenylalanine substitution at position 617, which is located within the pseudokinase domain JH2. JH2 interacts with JH1 and thereby keeps the kinase in an inactive form. The V617F mutation, however, destabilizes the JH1-JH2 interaction and thus leads to constitutive JAK2 activation. A small fraction of PV patients (3 %) carries mutations in exon 12 of the *JAK2* gene, with the most prominent being N542-E543del, E543-D544del, F537-K539delinsL and K539L with frequencies of 23%, 11% and 10%, respectively³. These mutations affect a region adjacent to JH2 and seem to trigger constitutive activation of JAK2 via a different mechanism than V617F¹⁵.

The association of JAK2 with all three main myeloid cytokine receptors, EPOR, MPL and G-CSFR explains how the V617F mutation can occur in all three classical MPNs - PV, ET, and PMF. However, the mechanisms underlying this diverse disease manifestation are still under investigation. There are different hypotheses as to what might influence the phenotype of *JAK2*-mutated MPN, including allele burden, differential STAT signaling and host factors.

The *JAK2*V617F allelic burden or variant allele frequency (VAF) is usually low in ET, higher in PV, and highest in PMF. Notably in post-PV or post-ET myelofibrosis (MF) the VAF is close to 100%. Mitotic recombination frequently leads to uniparental disomy (UPD) at chromosome 9 (9p24) resulting in loss of heterozygosity (9pLOH). Homozygous *JAK2*V617F mutations were found in 25-30% of PV, 9-20% of PMF and only 0-3% of ET patients and homozygosity was associated with longer disease duration. This suggests that an increased VAF and 9pLOH is

associated with disease progression. Likewise, within the spectrum of PV, a higher allele burden is associated with a more severe phenotype, characterized by higher hemoglobin (Hb) and white blood cell (WBC) count, lower platelets (PLT) and erythropoietin (EPO) serum levels, as well as pronounced splenomegaly. These observations led to the conclusion that gene dosage dictates the disease ala “dosis facit venenum”. This was also shown in a transgenic mouse model where expression of human JAK2V617F at a low level led to ET, while higher expression led to PV¹⁶. ET, PV and PMF are tightly related with partially overlapping clinical presentation. A high JAK2V617F burden in ET leads to a more PV-like disease with higher WBC and increased Hb and ET can also evolve to PV. Both ET and PV can progress to MF and all three entities can develop into AML. Thus JAK2V617F-positive MPN might be seen as a continuum, where severity is regulated by allelic burden^{3,14} (Figure 3).

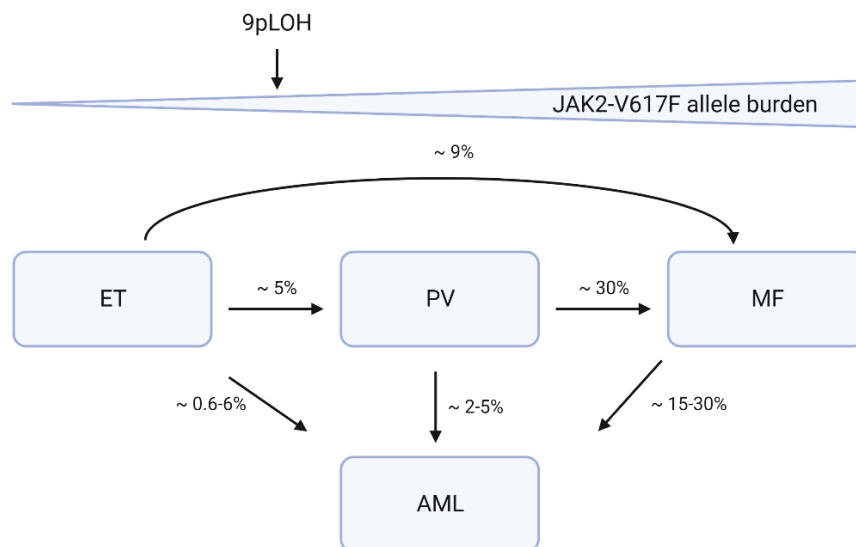


Figure 3: JAK2V617F allele burden influences disease manifestation and progression. ET is associated with low JAK2V617F burden and heterozygosity, while PV and MF are associated with a homozygous mutation due to 9pLOH and higher allelic burden. ET can evolve to PV, ET and PV can progress to MF and all three can escalate to AML. Generated with Biorender.

Apart from gene expression, differential patterns of STAT signaling were associated with different disease phenotypes. Teofili et al. analyzed STAT phosphorylation in BM biopsies and reported increased STAT3 and STAT5 phosphorylation in PV. In ET, however, STAT5 signaling was decreased compared to healthy controls, while STAT3 signaling was slightly increased. In idiopathic myelofibrosis (IM) both STAT3 and STAT5 signaling were decreased¹⁷. In contrast, Chen et al. observed increased STAT5 signaling in BFU-E (burst forming unit erythroid) colonies from PV and ET patients. In this study, however, increased megakaryopoiesis and decreased erythroid differentiation leading to an ET phenotype could

be attributed to increased STAT1 phosphorylation¹⁸. The importance of the individual STAT molecules was confirmed in mice expressing JAK2V617F in STAT1/3 or 5 deficient backgrounds. STAT5a/b signaling was indispensable in the pathogenesis of PV in two different mouse models^{19,20}. Loss of STAT3 did not affect erythrocytosis, but caused decreased neutrophilia and increased thrombocytosis²¹. However, increased STAT1 signaling was detected in these mice, which might be the driver of platelet formation. Deletion of STAT1 led to increased erythrocytosis and lower platelet counts²². Thus, differential activity of STATs 1/3/5 influences differentiation of hematopoietic progenitors in MPN with increased STAT1 leading to a megakaryocytic bias and an ET-like phenotype, and STAT5 being required for erythrocytosis, a hallmark of PV.

Moreover, patient to patient heterogeneity might influence the disease manifestation. Non-driver mutations can influence the disease phenotype and risk. There are also reports of single nucleotide polymorphisms (SNPs) in the JAK2 gene (rs7046736, rs10815148, and rs12342421), which were observed in PV and ET but not PMF. Three other JAK2 SNPs (rs10758669, rs3808850, and rs10974947) and one SNPs in EPOR (rs318699) in contrast were found in PV but not ET or PMF¹⁴. This suggests that genetic variability might influence disease manifestation. Moreover, other factors such as iron deficiency might play a role²³.

1.1.2. MPL mutations

MPL, like the EPO, growth hormone (GH), prolactin (PRL) and G-CSF receptors, is a type I homodimeric cytokine receptor. Its expression is limited to cells in hematopoietic tissues, such as hematopoietic stem cells (HSCs), megakaryocytes and their progenitors and platelets. It consists of an extracellular cytokine binding domain, a transmembrane domain, which is followed by a juxtamembrane domain and the cytoplasmic domains. The cytoplasmic domains are associated with JAK2 or TYK2, which lead to downstream signaling upon receptor activation. However, only JAK2 was associated with persistent cytokine signaling and a vital role in hematopoiesis. The ligand, thrombopoietin (TPO) regulates megakaryopoiesis and platelet formation. Binding of TPO leads to a conformational change, which brings the two JAK2 molecules in proximity, thereby causing their transphosphorylation. Activated JAK2 induces the JAK/STAT, PI3K/AKT and MAPK signaling pathways²⁴.

5-10 % of PMF patients and 1-4% of ET patients harbor mutations in the *MPL* gene. Most mutations occur in exon 10 of the *MPL* gene within the juxtamembrane cytoplasmic region. This domain is required to keep the receptor inactive in the absence of MPL. The most common are W515K or W515L but other substitutions, like W515A, W515G and W515R were also described^{8,25}. S505N were described in ET and PMF as well as hereditary thrombocythemia (HT) and stabilize the receptor in an active dimeric conformation²⁶. Rare mutations in the

extracellular or cytosolic part were observed in MPN as well. The common feature of these gain of function mutations is the induction of constitutive JAK2 activation^{3,24}.

1.1.3 CALR mutations

CALR consists of three domains, the N- and P-domain, which confer chaperone activity and a C-domain, which is responsible for lower calcium (Ca^{2+}) buffering. In contrast to JAK2 and MPL, it is not a signaling molecule but a chaperone that usually facilitates folding of N-glycosylated proteins within the endoplasmic reticulum (ER)²⁷. Hence, finding a causative relation between *CALR* mutations and myeloproliferative disorders was surprising.

CALR mutations occur in 25-30% of all ET and PMF cases. Pathologic mutations in exon 9, of which a 52 bp deletion (type 1) and a 5 bp insertion (type 2) are the most prevalent, all lead to a +1 (-1/+2) frameshift. Transcription from this alternative reading frame completely changes the amino acid composition within the C-domain, leading to a novel sequence of about 40 amino acids and loss of the KDEL (Lys-Asp-Glu-Leu) ER retention signal^{11,12}. Those alterations caused by type 1 and 2 mutations enable a unique interaction of mutant CALR (mutCALR) with MPL leading to its activation and oncogenic transformation^{28,29}.

Of the homodimeric type I cytokine growth factor receptors, mutCALR only induces activation of MPL and to a much weaker extent of the G-CSFR but not of the EPOR^{29,30}. These differences might be caused by the fact that only MPL presents two sets of extracellular domain, whereas the others have only one³¹. Indicated by differential localization with a preference to the ER to Golgi intermediate compartment of mutCALR opposed to wild type (WT) CALR, interaction with MPL is presumably happening during MPL maturation²⁹. This is also in concordance with the finding that the fraction of mature MPL is reduced in *CALR* mutated cells^{29,32}. At the cell surface, mutCALR-bound MPL activates the JAK/STAT, MAPK PI3K/AKT pathways leading to proliferation and clonal expansion (Figure 4).

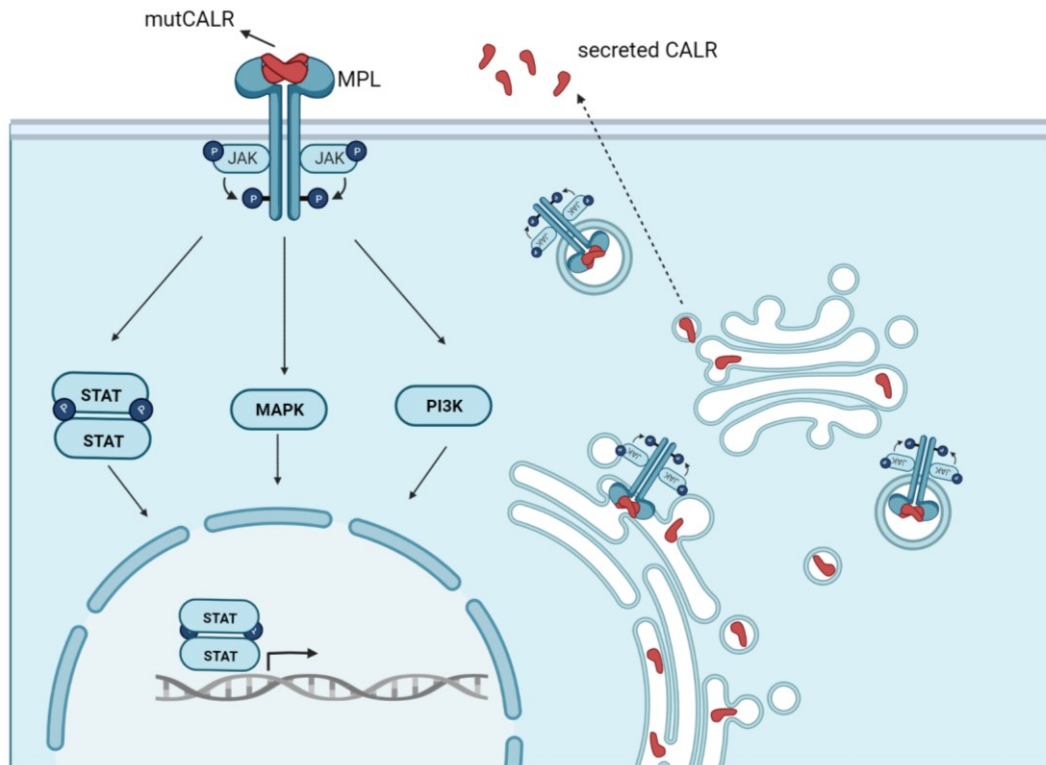


Figure 4: Mutant CALR forms an oncogenic complex with MPL. MutCALR binds to immaturely glycosylated MPL in the ER. By vesicular transport via the Golgi the complex reaches the plasma membrane, where mutCALR activates MPL resulting in JAK/STAT, MAPK and PI3K/Akt signaling. Partially, mutCALR is also secreted.

It was proposed that CALR engages with MPL during its maturation by binding to immature glycans^{29,32}. The CALR N-domain harbors oligosaccharide binding capacity, which initiates folding of glycoproteins in the ER. MPL, as a glycoprotein, also poses a substrate for WT CALR. The interaction of mutCALR with MPL, however, is much stronger due to a lack of negative inhibition, which is conferred by the P-domain in WT CALR but not in mutCALR. Further, the mutant specific domain was shown to induce homo-multimerization of mutCALR molecules. This complex stabilizes MPL in a multimeric state³³. The mutCALR-MPL complex is subsequently transported to the cell surface³⁴. In fact, it was reported that surface localization is a prerequisite for oncogenic signaling³³. Due to the loss of the KDEL sequence, CALR is also partially secreted. Yet, as immature glycans are required for the unique MPL-mutCALR interaction, the secreted form cannot activate MPL in WT cells in a paracrine way^{28,35}. However, it was recently reported that soluble mutCALR can induce MPL activation from outside in mutCALR cells but at non-physiologic concentrations³⁶.

1.1.4 Clonal evolution of MPN

While normal hematopoiesis is highly polyclonal, hematopoietic stem and progenitor cells (HSPCs) can acquire a growth and or differentiation advantage leading to clonal

hematopoiesis (CH). CH can occur at all ages but is frequently observed in the elderly population. It is associated with increased risk for hematopoietic malignancies as well as cardiovascular disease^{37,38}. Premalignant CH, also called clonal hematopoiesis of indeterminate potential (CHIP), is associated with distinct mutations. The most frequent mutations in myeloid CHIP occur in the *TET2*, *DNMT3A* or *ASXL1* gene³⁹. These mutations are called clonal drivers and are not restricted to MPN. While such mutations alone do not cause MPN, they give clonal advantage and can modify the disease phenotype.

MPN driver mutations are defined as genetic aberrations that induce the manifestation of an MPN phenotype in mouse models. Known driver mutations occur in the *CALR*, *JAK2* and *MPL* genes and were already discussed in the previous sections. These mutations lead to the onset of MPN with variable penetrance and latency. Interestingly, the *JAK2*V617F mutation is one of the most frequently found genetic aberrations in the healthy population with CH. Thus, driver mutations can also be seen as clonal drivers in the premalignant state. Moreover, recent publications showed that *JAK2* mutations are acquired early in life, in some individuals even in utero, with a long latency of decades until MPN manifestation^{40,41}. In contrast, the occurrence of *CALR* mutations in CHIP is much less frequent, suggesting that de-novo *CALR* mutations are either recognized and cleared more efficiently by the immune system or that this mutation harbors stronger oncogenic potential³⁹.

Recurrent mutations in epigenetic regulators (*ASXL1*, *EZH2*, *IDH1*, *IDH2*), transcription factors (*TP53*, *NFE2*, *RUNX1*), splicing factors (*SRSF2*, *U2AF1*) and signaling proteins (*NRAS*, *KRAS*) are associated with disease progression³. These are usually missense and loss of function mutations and have a high prevalence in post-MPN AML. The number of mutations shows a direct correlation with prognosis. In the chronic phase of PV and ET the driver mutation is often the only mutation. In PMF, however, the number of somatic mutations is higher.

Thus, the development of MPNs is a dynamic process and the phenotype is shaped by outgrowth and clonal evolution of malignant HSPCs. Manifestation of MPN is often preceded by a CHIP phase, which is associated with clonal driver mutations and increased cardiovascular risk. MPN driver mutations induce oncogenic signaling leading to a chronic myeloproliferative disease with classical changes in peripheral blood (PB) count and BM morphology. Further genetic aberrations lead to disease progression and an increased risk for leukemic transformation. A simplified linear model of clonal evolution in MPN is depicted in Figure 5. However, disease development and progression are far more complex. Clonal driver mutations can precede MPN or be acquired to a clone with a disease driver mutation or to a separate clone leading to biclonal evolution^{41,42}. ET can evolve into PV and PV and ET can evolve into secondary MF. And all entities have potential to transform to AML.

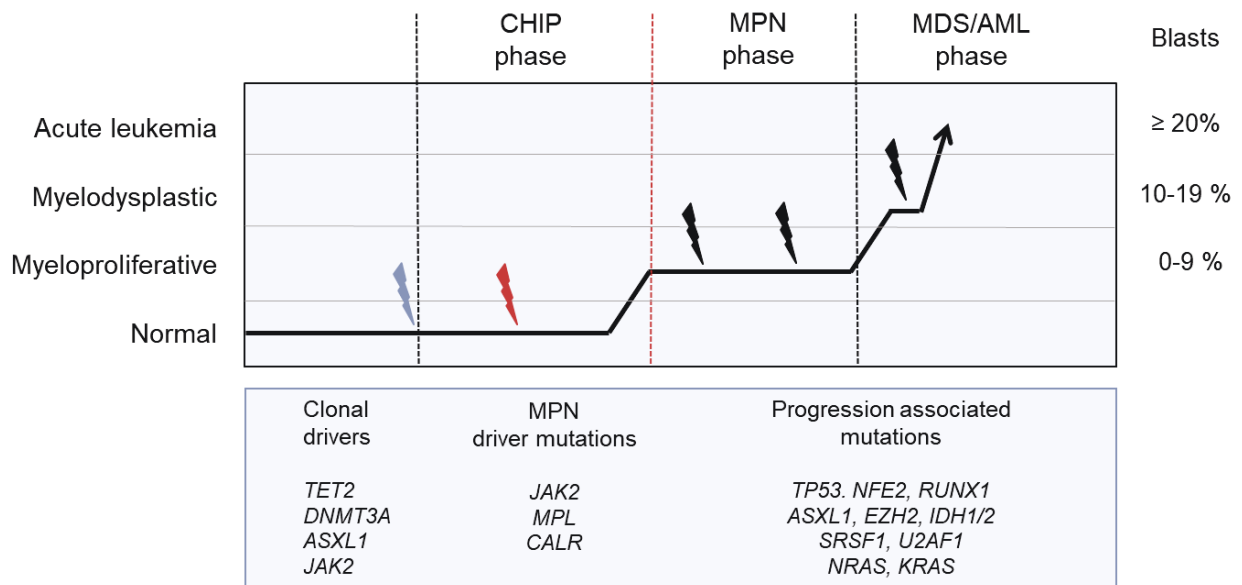


Figure 5: Clonal evolution of MPN. Clonal driver mutations promote CH, which increases the risk of developing MPN. The occurrence of an MPN driver mutation in a HSC provides the cell with clonal advantage resulting in outgrowth and increased production of terminally differentiated blood cells indicative of MPN. Acquisition of additional mutations is associated with MPN progression. The presence of blasts in peripheral blood is diagnostic for the evolution to MDS or AML.

1.1.5 The co-occurrence of MPN driver mutations

MPN driver mutations were described as mutually exclusive in the past^{43,44}. However, since 2014 the co-occurrence of *JAK2*, *CALR* and *MPL* mutations in MPN patients has been reported in numerous publications^{42,45-67}. Usseglio et al. reported significantly increased thrombocytosis in *JAK2/MPL* and *JAK2/CALR* double-mutated ET compared to *JAK2* or *CALR* single-mutated patients⁶¹. Likewise, Mansier et al. described a slightly higher PLT count and decreased Hb in double mutated compared to single mutated ET, albeit not at a significant level. They also found no significant difference in the frequency of thrombotic events or the progression to secondary PMF or AML⁶³. In contrast in the study by Lim et al. the incidence of thrombotic events was increased in double mutated compared to *JAK2* or *CALR* single mutated patients⁵⁰. Interestingly, additional *CALR/MPL* or *JAK2* exon 12 mutations were frequently found in patients with low *JAK2V617F* burden^{48,55-57,61,68}. A low mutant burden in *JAK2V617F*⁺ PMF has been previously associated with lower overall survival compared to patients with a higher burden, which might be explained by the presence of undetected additional mutations^{69,70}.

While these studies and case reports give insight into the clinical relevance of the co-existence of two MPN driver mutations, the true implications of double mutation for treatment and prognosis remain unknown. First, the rarity of such patients hampers a systematic investigation. Second, within the small group of patients with two mutations there might be

several subgroups with distinctive clinical features, divided by i.e. different combinations of mutations, the range of mutant burden of each mutation, clonal vs. biclonal occurrence of the mutations.

While many authors described the co-existence of two or even three MPN driver mutations, the clonality was rarely determined. In most cases both mutations seem to be present in independent clones^{42,71,72}. Mansier et al. showed that *CALR* burden is lower in double-mutated compared to single-mutated MPN. The lower allele frequencies might be indicative of two competing clones^{56,63}. The distinction between co-existence of two mutations in one or two clones might play a major role in the clinical outcome. Recently, three case reports were published, in which two mutations were acquired in the same clone^{65,66,73}. Nishimura et al. detected a *JAK2V617F* mutation secondary to a *CALR* type 1 mutation in one patient at the onset of progression from ET to MF. Partouche et al. and Zhou et al. described the acquisition of *MPL* mutations to *CALR* mutant clones in PMF, which was associated with accelerated disease progression in both patients and unresponsiveness to ruxolitinib in one patient^{73,74}. Thus, these three case reports indicate that co-occurrence of driver mutations in the same clone might be associated with disease acceleration. In two of these cases the second mutation was acquired into a *CALR* mutated clone years after initial diagnosis. This is in concordance with the results of Lundberg et al., who found that *CALR* mutations are usually early events in MPN evolution.

Over the past years it became eminent that MPN driver mutations are not mutually exclusive. While double mutation was described with frequencies ranging from below 1 to 6.8 %, the true frequency might be underrepresented as screening for MPN driver mutations is usually a sequential process, which stops after detection of one mutation^{58,75}. In addition, case reports showed that a second driver mutation can be acquired years or even decades after initial diagnosis. In the past, patients were rarely re-analyzed for driver mutations. However, it seems that acquisition of a second mutation might be associated with disease acceleration and therefore might be an important prognostic indicator.

1.1.6 Aberrant cytokine signaling caused by MPN driver mutations

Based on shared clinical features and common morphological changes Dameshek already described MPNs as a group of diseases driven by an “*hitherto undiscovered stimulus*” in 1951¹. By now it became eminent that the common hallmark of PV, ET and PMF is clonal hematopoiesis driven by constitutive signaling of the JAK/STAT pathway.

Four different JAK (JAK1, 2, 3 and TYK2) and seven STAT proteins (STAT 1-6 with STAT5a and b) act as intracellular mediators of cytokine receptors after the interaction with extracellular ligands. JAK proteins associate with cytokine receptors lacking intrinsic tyrosine kinase

capacity. Ligand binding induces activation of JAK proteins by autophosphorylation. Activated JAK trans-phosphorylates tyrosine residues at the receptor, which then serve as docking sites for STATs. Phosphorylated STAT proteins form homo- or heterodimers and after translocation to the nucleus act as transcription factors involved in metabolic processes, immunological responses, and hematopoiesis. The abundance of blood cells is tightly regulated and needs to be adapted to external stimuli, such as stress or infection. Cytokines, including EPO, TPO and G-CSF trigger the production of erythrocytes, thrombocytes, and granulocytes, respectively. Their receptors are all associated with JAK2 and the JAK/STAT pathway is vital for productive hematopoiesis. The known MPN driver mutations in the *JAK2*, *CALR* and *MPL* genes lead to constitutive signaling via JAK2, which consequently triggers STAT phosphorylation. STAT5/3 and 1 were identified as major downstream signaling molecules in MPN with differential involvement in the distinct disease entities as discussed in part 1.1.1. STAT5 is required for development of PV, STAT 3 ameliorates thrombocytosis and STAT1 induces thrombocytosis and inhibits erythrocytosis^{3,76}. The importance of JAK/STAT signaling in MPN pathogenesis is also utilized therapeutically by blocking this pathway (see chapter 1.3.4).

Apart from the JAK/STAT pathway, PI3K/Akt and MAPK signaling has been shown to play a role in the pathogenesis of MPN. While JAK-inhibitors like ruxolitinib effectively block the JAK/STAT signaling pathway, PI3K/Akt and MAPK pathway activation persists and thus combination therapy might lead to improved results⁷⁷⁻⁸¹.

1.1.7 Lessons learned from mouse models

MPNs are disorders, which arise from a mutated HSC. These cells are low in frequency and their life span *in vitro* is limited and requires cytokine supplementation at a non-physiological level. *In vivo*, mutated HSCs expand and differentiate leading to a progressive disease with increased myelopoiesis with distinct lineage specificity, possible splenomegaly and/or bone marrow fibrosis. These complex processes make mouse models indispensable for studying stem cell disorders, such as MPNs. In addition, mouse models are essential for the definition of driver mutations, as formal proof for such mutations is disease initiation after introduction into preclinical models.

To date there are several mouse models available for each of the known driver mutations, which were generated using different strategies. A fast way to introduce a specific mutation into HSCs is *ex vivo* retroviral (RV) transduction and transplantation into lethally irradiated mice. The disadvantage of such models is that neither expression level nor the viral integration site can be controlled. This usually leads to expression above the physiological level and random integration might influence the expression of other genes leading to artefacts. Moreover, the need for transplantation exposes HSCs to an irradiation-related cytokine storm,

which leads to increased replication and oxidative stress during engraftment. Transgenic (TG) animals harbor the advantage of germline transmission of the mutation and thus do not require transplantation. The promoter use influences the expression level and tissue distribution but again the expression level is non-physiologic, and the integration is random. The most physiologically relevant models are knock-in (KI) models. The transgene is introduced into the locus of the target gene by homologous recombination. Thus, expression is driven by the endogenous promoter. The use of the Cre-loxP system allows for a conditional KI as the transgene is only expressed in presence of Cre-recombinase. By using tissue specific promoters for the expression of Cre, a transgene can be directed to specific tissues. Frequently used Cre strains in MPN research are Vav-Cre and MxCre. The Vav promoter is expressed in all hematopoietic tissues with minor leakage in endothelial cells. MxCre is only expressed in response to interferon and thus allows inducible transgene expression⁸².

Early mouse models from an era before the discovery of MPN driver mutations were based on cytokine overstimulation. HSCs were RV transduced with plasmids leading to high EPO or TPO expression. Mice exposed to EPO developed erythrocytosis. Transplantation of TPO^{high} cells resulted in a fibrosis model with a severe phenotype. Mice underwent a plethoric phase defined by thrombocytosis, leukocytosis, and anemia, followed by a spent phase associated with extramedullary hematopoiesis and severe pancytopenia. These mice died within less than a year after transplantation and a subset of mice developed AML resulting in premature death. Thus, this model recapitulated the evolution of human PMF and enabled testing of drugs for MF⁸².

JAK2 mouse models

After the discovery of the *JAK2V617F* mutation in MPN several RV models were established (Table 1). Introduction of the murine *Jak2V617F* led to a PV-like phenotype in all models with progression to MF in most. These studies delivered the first proof that *JAK2V617F* is an MPN driver mutation. Interestingly, the genetic background of different mouse strains significantly influenced the disease phenotype. BALB/c mice developed increased leukocytosis, splenomegaly and BM fibrosis compared to C57BL/6 mice⁸³. This might underline the role of genetic variability as a cause of disease heterogeneity observed in humans. Two of these models had a transient non-transplantable disease, which points towards limited self-renewal capacity of JAK2 mutated cells^{84,85}.

Starting from 2008 TG models emerged, which stably expressed human or murine JAK2V617F under different promoters (Table 1). In these models expression of the mutant protein was much lower than in RV models. While all RV models rapidly developed PV, all three diseases ET, PV and PMF could be recapitulated in TG models. Modulating the ratio of WT JAK2 to JAK2V617F directly influenced the disease phenotype. A low mutant to WT ratio preferentially

resulted in development of ET or PV, whereas high expression of the mutant gene resulted in an aggravated PV-like disease or PMF. Similarly, the *JAK2V617F* VAF correlates with varying degree of severity in MPN patients. While ET patients have the lowest mutant burden, PV and PMF are associated with increased VAF and *JAK2V617F* homozygosity^{3,39}. Together these observations formed the basis for the gene dosing theory. In 2019, Chapeau et al. generated an additional TG model using the SCL-tTA-2S tet-off system, which enables conditional, inducible expression. Mice developed disease reminiscent of MPN, which was reversible after switching off the transgene expression. Notably, disease manifestation was influenced by sex in this model with females predominantly developing ET whereas males had PV, the opposite of what is observed in humans⁸⁶.

Several KI models were published between 2010 and 2013 (Table 1). Murine or human *JAK2V617F* were expressed at the *Jak2* locus using different strategies including constitutive, conditional, and inducible KI. All mice expressing murine *Jak2V617F* developed PV and some progressed to MF. In contrast, the use of human *JAK2V617F* resulted in an ET-like disease in the heterozygous state. Homozygous mice, however, developed PV, as observed in humans⁸⁷. Although these mice had the mildest phenotype the human protein seemed to impair HSC renewal evidenced by decreased number of Lin⁻ Sca1⁺ c-Kit⁺ (LSK cells). While heterozygous *JAK2* mutations are associated with ET in humans, all mice expressing murine *Jak2V617F* developed PV in a heterozygous state. Yet, homozygotes had a more severe phenotype compared to heterozygotes. One major disadvantage of KI models is the fact that *JAK2V617F* is uniformly expressed in all HSCs. Thus, in these models MPN is driven by a polyclonal population as opposed to the monoclonal or oligoclonal disease origin in humans. This problem was addressed by Mansier and colleagues by generating a conditional KI mouse using PF4iCre⁸⁸. In this model only a minority of HSCs express *Jak2V617F* and mice develop a PV-like disease at an age of 10 weeks.

Table 1: Overview over different *JAK2V617F* mouse models

	Oncogene	Mouse strain	Phenotype	Additional disease characteristics	Reference
RV	m <i>Jak2V617F</i>	C57BL/6	PV	strain-specific phenotypic differences	Wernig et al., 2006 ⁸³
		BALB/c	PV to MF		
	m <i>Jak2V617F</i>	C57BL/6	PV to MF	strain-specific phenotypic differences PV resurrected from fibrotic BM by secondary BMT	Zaleskas et al., 2006 ⁸⁹
		BALB/c			
m <i>Jak2V617F</i>	C57BL/6	PV to MF	transient thrombocytosis in mice with low expression	Lacout et al., 2006 ⁸⁴	
m <i>Jak2V617F</i>	BALB/c	PV to MF	increased TNF- α , transient disease, not transplantable	Bumm et al., 2006 ⁸⁵	

TG	huJAK2V617F Vav promoter	C57BL/6	mild PV/ET PV or ET to MF	low expression high expression	Xing et al., 2008 ⁹⁰
	huJAK2V617F Vav-Cre/MxCre	C57BL/6	ET to MF PV to MF	V617F:WT = 0.5:1 V617F:WT = 1:1	Tiedt et al., 2008 ¹⁶
	mJak2V617F H2kb promoter	BDF1	ET or PV PMF	V617F:WT = 0.45:1, 20% ET-like and 30% PV-like disease V617F:WT = 1.35:1	Shide et al., 2008 ⁹¹
	huJAK2V617F TetOCMV	C57BL/6	ET or PV	reversible disease, sex bias	Chapeau et al., 2019 ⁸⁶
KI	mJak2V617F constitutive	C57BL/6	PV to MF	-	Marty et al., 2010 ⁹²
	mJak2V617F E2A-Cre	C57BL/6	PV	low competitive advantage in BMT	Mullally et al., 2010 ⁹³
	mJak2V617F MxCre	C57BL/6	PV to MF	homozygous JAK2 ^{V617F} led to more severe phenotype	Akada et al., 2010 ⁹⁴
	huJAK2V617F MxCre	C57BL/6	ET	V617F:WT = 1:1, transplantable disease, impaired HSC renewal	Li et al., 2010 ⁹⁵
	mJak2V617F Vav-Cre	C57BL/6	PV to MF	HSC amplification and competitive advantage	Hasan et al., 2013 ⁹⁶
	mJak2V617F PF4iCre	C57BL/6	PV	low number of HSCs expressing JAK2V617F	Mansier et al., 2019 ⁸⁸

MPL mouse models

Pikman et al. established a MPLW515L RV model, which is characterized by a rapid onset of MPN⁹. Mice developed thrombocytosis, leukocytosis, and splenomegaly before progressing to a lethal MF. Interestingly, both WT MPL and MPLW515L led to increased erythropoiesis caused by expression of MPL in erythroid progenitors, a population that usually does not express this receptor. As of now this is the only available mouse model for MPL mutations⁸².

CALR mouse models

The first mouse models with mutated *CALR* were established few years after the discovery of such mutations in MPN patients. RV models were generated by expression of different versions of human mutated *CALR* (Table 2). CALRdel52 and other type 1-like *CALR* variants (del34 and del46) induced ET-like disease with thrombocytosis caused by megakaryocyte hyperplasia and at a later stage progression to MF. CALRins5 and type 2-like CALRdel19 were associated with a milder phenotype and mice expressing these proteins did not show signs of fibrosis even one year after transplantation. Likewise, in humans type 1 mutations are more frequent in PMF than type 2 mutations. However, patients with type 2 mutations have increased thrombocytosis compared to patients with type 1 mutations, which is in direct

contrast to the observations made in RV mouse models. Transplantation of CALRdel52 expressing HSCs into MPL deficient recipients prevented development of MPN, which proved that mutant CALR induces thrombocytosis through MPL³².

A single TG model expressing human CALRdel52 under control of the H-2Kb promoter showed a milder phenotype with moderate thrombocytosis but absence of splenomegaly and MF⁹⁷.

As mutations at the homologous position in murine and human CALR do not result in the same amino acid change, KI models in which human exon 9 was inserted into the otherwise murine *Calr* gene locus were developed (Table 2). Chimeric CALRdel52 and CALRins5 induced an ET-like phenotype. As observed in the RV models, CALRins5 had a milder effect than del52. Homozygous mice developed an aggravated disease compared to heterozygous mice, characterized by increased thrombocytosis, additional leukocytosis, moderate fibrosis, and splenomegaly.

The insight that charge rather than amino acid (aa) sequence is the denominator for mutant CALR-MPL interaction led to the development of fully murine frameshift models (FS) (Table 2). In these mice mutations were introduced using CRISPR/Cas9. Type 1-like mutations including del19, del52 and del61 were tested. While mice with the del61 variant had similar blood counts as their WT littermates, del52 and del19 induced thrombocytosis and splenomegaly. FS models showed a milder phenotype, which can be explained by different potential of human and murine CALR variants to activate MPL. These frameshift models also showed that heterozygous mutation is embryonic lethal due to problems in cardiac development. A similar observation was previously made in CALR-deficient mice showing the importance of CALR during later embryogenesis^{98,99}.

Expansion of HSCs, megakaryocyte progenitors and myeloid progenitors was observed in RV as well as KI models. By using single-cell transcriptomics Prins et al. confirmed that the *CALR* mutation had the strongest effect on HSCs with some contribution of the megakaryocyte lineage. In addition, we and others used KI mouse models to investigate the effect of *CALR* mutations on the hematopoietic stem and progenitor compartment. *CALR* mutated HSCs were characterized by increased JAK-STAT signaling, cell-cycle, unfolded protein response and cholesterol biosynthesis^{100,101}.

Table 2: Overview over different CALR mutated mouse models

	Oncogene	Mouse strain	Phenotype	Disease characteristics	Reference
RV	huCALRdel52	C57BL/6	ET	BM megakaryocyte hyperplasia, MPL dependence	Elf et al., 2016 ³²

	huCALRdel52		ET to MF	marked thrombocytosis	Nguyen et al., 2016 ¹⁰²
	huCALRdel52 huCALRins5		ET to MF ET	competitive advantage of megakaryocyte lineage, del52 led to more severe phenotype	Marty et al., 2016 ³⁰
	huCALRdel19		ET	type 2 like	Toppaldoddi et al., 2019 ¹⁰³
	huCALRdel34 huCALRdel46		ET to MF	type 1 like	
TG	huCALRdel52 H-2Kb promoter		ET	no competitive advantage of HSCs	Shide et al., 2017 ¹⁰⁴
KI	chCALRdel52 Mx1 Cre		ET to MF	no competitive advantage of HSCs, homozygous mutation led to more severe disease	Li et al., 2018 ¹⁰⁵
	chCALRdel52 chCALRins5 Sci Cre		ET to MF ET	competitive advantage, homozygous mutation led to more severe disease	Benlabiod et al., 2020 ¹⁰⁶
	chCALRdel52 Vavi Cre		ET	competitive advantage, homozygous mutation led to more severe disease	Achyutuni et al., 2021 ¹⁰⁰
FS	mCalrdel19		ET	low clonal advantage	Shide et al., 2019 ¹⁰⁴
	mCalrdel52 mCalrdel61		ET mild ET	del61 is less active than del52, low competitive advantage	Balligand et al., 2020 ¹⁰⁷

1.2. Clinical aspects of MPN

The incidence of PV is 2-3/100000/year and most frequently diagnosed in patients between 60-65 years. Almost all patients harbor mutations in the *JAK2* gene, which leads to constitutive signaling of the EPOR, MPL and G-CSFR. Therefore, PV is characterized by trilineage myeloproliferation, leading to erythrocytosis, leukocytosis and thrombocytosis. Massive erythrocytosis leads to increased blood viscosity and volume. Consequently, complications include disturbances of microcirculation and thromboembolic events. Patients frequently develop splenomegaly and can also suffer from pruritus and erythromelalgia¹⁰⁸.

ET occurs with a frequency of 2.5/100000/year and has two peaks in age distribution one from 20 to 40 and the second from 60-70 years. This disease is associated with *JAK2*, *CALR* and *MPL* mutations leading to increased megakaryopoiesis in the BM. Therefore, ET is characterized by isolated thrombocytosis. Complications include thromboembolic events due to spontaneous aggregation but also hemorrhage due to thrombopathy or acquired Van Willebrand disease in case of high thrombocytosis. Additionally, microcirculation can be disrupted as well¹⁰⁸.

PMF has an incidence of 0.5-1.5/100000/year. It is characterized by progressive loss of hematopoietic capacity due to BM fibrosis. The early phase is marked by a hyperproliferative phenotype. In the late phase increased BM fibrosis leads to pancytopenia with the usual complications such as fatigue caused by anemia, increased risk for infections and bleeding. Due to extramedullary hematopoiesis liver and spleen are massively enlarged and PB shows a leukoerythroblastic phenotype¹⁰⁸.

Diagnosis of MPN is based on hematological, morphological, and genetic parameters. The WHO defined major and minor criteria for each disease, which are summarized in Table 3.

Table 3: WHO diagnostic criteria for MPN, adapted from Arber et al., 2016²

	Major criteria	Minor criteria
PV	A1: Hb > 16 g/dL (male) or 16.5 g/dL (female) A2: BM histology: trilineage myeloproliferation with pleomorphic megakaryopoiesis A3: detection of a <i>JAK2</i> mutation	B1: Decreased serum EPO levels
	Diagnosis of PV requires all major criteria, or the first two major and the minor criterium.	
ET	A1: thrombocytosis > 450000/ μ L A2: BM histology: increased number of mature hyperlobulated megakaryocytes without significant granulopoiesis or erythropoiesis, no or minimal increase in reticulin fibers A3: criteria for other MPNs (CML, PV, PMF) are not met A4: detection of a <i>JAK2</i> or <i>CALR</i> or <i>MPL</i> mutation	B1: detection of another clonal marker B2: no evidence for reactive thrombocytosis
	Diagnosis of ET requires all major criteria, or the first three major criteria combined with the minor criteria.	
PMF	A1: BM histology: proliferation and atypical megakaryopoiesis, grade 2 or 3 reticulin or collagen fibrosis A2: criteria for other MPNs (CML, PV, PMF) are not met A3: detection of a <i>JAK2</i> or <i>CALR</i> or <i>MPL</i> mutation or another clonal marker	B1: anemia B2: palpable splenomegaly B3: WBC > 11000/ μ L B4: increased LDH B5: leukoerythroblasts in peripheral blood
	Diagnosis of PMF requires all major criteria and at least one minor criterium.	

1.2.1 Risk stratification and prognosis

Prognosis is significantly different for each MPN subtype. ET can be seen as the most benign form with highest overall survival (OS) and lowest progression rate to MF or AML. It is followed by PV, and PMF has the worst prognosis. Median OS is 20 years, 14 years and 6 years for ET, PV and PMF, respectively. The 15-year risk of fibrotic transformation is 4-11% for ET and 6-14% PV¹⁰⁹. Leukemic transformation is most frequent in PMF with a 10-year risk of 10-20%. For PV and ET the risk is significantly lower with 1-14% of PV and 1-3% of ET patients evolving to secondary AML^{109,110}. Secondary AML shows distinct features from de-novo AML and treatment remains a major challenge leading to a poor median survival of about 6 months¹¹¹.

After categorization into a specific MPN subtype further risk stratification is needed to make treatment decisions. Thus, disease scores were developed to assign patients to risk groups. In ET and PV, criteria for shortened survival include age above 60, previous thromboembolic event, such as ischemia, embolism or hemorrhage, and leukocytosis. The strongest risk factor for thrombotic events is prior thrombosis. In addition hypertension is associated with an increased risk for arterial thrombosis and higher age was defined as a risk factor for venous thrombosis in PV¹¹². In ET risk factors for thrombosis are summarized in the IPSET (International Prognostic Score for Thrombosis in ET) scoring system and include age older than 60 years, prior thrombotic event, cardiovascular risk factors and the presence of a *JAK2V617F* mutation¹¹³⁻¹¹⁵. For PMF the International Prognostic Scoring System (IPSS) and Dynamic International Prognostic Scoring System (DIPSS) were developed to define risk groups with distinct OS at the diagnosis or at any time during disease course, respectively^{116,117}. Risk factors involve hematological parameters (Hb < 10 g/dL, WBC > 25x10⁹/L and blasts in PB ≥ 1%) as well as constitutional symptoms. The DIPSS-plus score includes three further criteria: PLT < 100x10⁹/L, transfusion dependent anemia, and unfavorable karyotype. It has four categories, low (0 criteria), intermediate-1 (1 criterium), intermediate-2 (2-3 criteria) and high (≥4 criteria), with median survivals of 15.4, 6.5, 2.9 and 1.3 years¹¹⁷.

As previously eluded to (chapter 1.1.4 Clonal evolution of MPN), the mutational landscape has a major influence on disease course. This includes driver as well as non-driver mutations. Alvarez-Larrán et al. compared the impact of driver mutations on leukemic transformation in ET and PV. Cumulative incidence for transformation to AML was lowest for *CALR* mutated patients, followed by *JAK2*⁺, *MPL*⁺ and triple negative patients¹¹⁸. Tefferi et al. also reported inferior leukemia-free survival in patients with triple negative and *JAK2*⁺ PMF compared to *MPL* or *CALR* mutated PMF⁴⁷. Genetic risk factors were incorporated in addition to clinical parameters in the Mutation Enhanced International Prognostic Score System for transplantation-age (under 70 years) PMF patients (MIPSS70, MIPSS70-plus, MIPSSv2.0).

These include similar clinical parameters as the DIPPS-plus score with additional focus on high molecular risk mutations, such as *ASXL1*, *SRSF2*, *EZH2*, *IDH1*, and *IDH2* and unfavorable or very high-risk karyotype^{119,120}. The Genetically Inspired Prognostic Scoring System for PMF is based solely on genetic markers and includes very-high risk karyotype, unfavorable karyotype, absence of type1-like *CALR* mutation, and presence of three different high molecular risk mutations (*ASXL1*, *SRSF2*, *U2AF1Q157*)¹²¹. GIPSS and MIPSSv2.0 allow accurate prediction, which underlines the importance of molecular information for risk stratification.

1.3 Therapeutic options for MPN

Therapeutic interventions are adapted to the disease and risk profile of each patient. These range from patient monitoring without therapeutic intervention in low-risk cases to stem cell transplantation in severe cases.

In ET and PV, increased production of terminally differentiated blood cells frequently leads to thromboembolic complications. Thus, treatment focus for ET and PV patients lies on prevention of thrombotic events. This can either be achieved by inhibition of platelet aggregation by low-dose acetyl salicylic acid or by reducing the blood cell mass with cytoreductive agents, such as hydroxyurea, busulfan, anagrelide and interferon- α . In PV, phlebotomy is an additional frequently used option to decrease the erythrocyte count. Ruxolitinib, a JAK1/2 inhibitor is also used as second line therapy to achieve hematological responses and reduction of splenomegaly in PV.

While PV, ET and the early phase of MF are characterized by a hyperproliferative phenotype, the progressive loss of BM functionality due to increased fibrosis results in pancytopenia in the later stages of MF. MF-associated anemia can be treated with androgens, thalidomide, pomalidomide, epoetins, danazol, and prednisone to reduce transfusion dependency. Extramedullary hematopoiesis leads to splenomegaly. Symptomatic splenomegaly can be alleviated with cytoreductive agents including hydroxyurea and ruxolitinib. In cases of drug-resistant splenomegaly, splenectomy can be taken into consideration as a palliative measure. While cytoreductive therapy can lead to a full hematological response and partially achieves molecular responses, i.e. decrease of the mutant clone, the only curative option for MPN is allogeneic hematopoietic stem cell transplantation (HSCT). Transplantation is indicated in patients with intermediate-2 or high risk DIPSS scores, but should also be considered for patients with a lower risk score and other negative prognostic markers.

While the pathophysiology of MPN is well studied, therapeutic options are still scarce, and their benefits and drawbacks are reviewed in this chapter. With allogeneic HSCT being the only

option to eliminate the mutant clone, further research is needed to develop disease modifying therapies. The discovery of the *CALR* mutation opened new possibilities for targeted immunotherapy. This is a currently heavily studied area and progress will be discussed in the last part of this section.

1.3.1 Hydroxyurea

Hydroxyurea (HU) or hydroxycarbamide inhibits the ribonucleotide reductase. Thereby it prevents DNA synthesis in the S-phase of the cell cycle and leads to accumulation of cells at the G1-S checkpoint. HU is frequently used as a cytoreductive drug in MPN and is also applied for the treatment of sickle cell disease.

HU has proven effective to elicit hematological responses, i.e. reduction of thrombocytes, leukocytes and erythrocytes, prevent arterial thrombosis and to reduce splenomegaly.

While HU is usually well tolerated side effects include reversible myelosuppression, macrocytosis, cystitis, fever, and gastrointestinal symptoms¹²². In addition, cutaneous adverse events, such as ulceration, erythema, skin dryness and nail pigmentation, are associated with long-term HU treatment and a minor increase skin cancer incidence was observed¹²³. The influence of HU on leukemic transformation is under controversial discussion. Some studies reported a higher rate of progression to leukemia in patients treated with HU compared to the control group^{124–126}. However, in other studies such an association was not observed^{127–129}.

1.3.2 Anagrelide

Anagrelide was developed as an inhibitor of platelet aggregation due to its inhibition of phosphodiesterase III. However, administration of the drug led to species-specific thrombocytopenia in early studies. This potential to reduce a single hematopoietic lineage was then exploited to treat patients with thrombocytosis and anagrelide is now widely used in ET. While anagrelide treatment does not influence platelet survival, it leads to a decrease in megakaryocyte size and ploidy. *In vitro* studies showed that the drug prevents megakaryocyte maturation and differentiation by cell cycle interference^{130–133}. In studies comparing anagrelide to HU, both drugs led to comparable efficacy in normalizing platelet counts. However, HU seemed to be more effective in preventing arterial thrombosis. Anagrelide on the other hand lowered the incidence of venous thrombosis¹³⁴. In another study, the combined incidence of minor or major thrombohemorrhagic complications was comparable in both treatment groups¹³⁵. Discontinuation rates due to side effects were similar. However, the profile of adverse events is different for anagrelide, including cardiac symptoms (tachycardia, hypotension), gastrointestinal events (nausea, diarrhea, abdominal pain), noncardiac edema, headache and cardiomyopathy. Interestingly, Harrison et al. reported a higher incidence of transformation to

myelofibrosis under treatment with anagrelide compared to the HU group probably, which might be caused by pro-fibrotic factors secreted by immature megakaryocytes¹³⁴. Thus, HU remains first line treatment for high-risk ET.

1.3.3 Interferon- α

Type I interferons (IFNs), such as IFN- α , are cytokines that activate the JAK/STAT pathway and exert immunomodulatory, antiproliferative and antiangiogenic potential. In the 1980s the potential of IFN- α 2 for the treatment of hematological diseases was discovered in several studies in which complete and lasting remissions were achieved in patients with hairy cell leukemia and CML. Albeit the normalization of hematologic parameters of MPN patients upon treatment with IFN- α 2 in early studies, it did not prevail as a treatment strategy for MPN due to a high dropout rate caused by side effects. However, interest in IFN- α 2 was renewed for two reasons. First, a change in formulation (pegylation) led to increased stability allowing less frequent dosing as well as better tolerability. With these new formulations adverse events include flu-like symptoms, fatigue, cytopenia and liver enzyme elevation. Second, with the discovery of molecular markers, i.e. MPN driver mutations, it became eminent that long-term treatment with IFN- α 2, not only leads to hematologic but also molecular responses, meaning a reduction of the mutant burden. This might be caused by a direct effect on HSCs combined with enhanced immune surveillance. IFN- α 2 has been shown to induce apoptosis in *JAK2V617F*⁺ CD34⁺ cells of PV patients and led to increased differentiation of mutant HSCs in a *JAK2V617F* mouse model^{136,137}. Further, IFN- α 2 activates quiescent stem cells, which might favor recognition of mutant cells by the immune system leading to a decrease of the mutant HSC pool. MPN leads to immune dysregulation including downregulation of major histocompatibility complex (MHC) I expression and PD-L1 upregulation, both of which are modulated by IFN- α treatment. In addition, IFN- α leads to a change in immune cell frequency with an increase in CD56^{bright} NK cells as well as regulatory T cells (Tregs). The increase in Tregs might be a counteractive measure to the immunostimulatory drug. However, there are also speculations that the increase of Tregs in circulation might represent a shift of Tregs out of the bone marrow niche. Thus, IFN- α treatment might contribute to immunological clearance of mutant cells^{138,139}.

IFN- α showed similar rates of hematological response compared to HU in ET and PV. In addition, it also led to a decrease of the mutant burden in a fraction of patients and even induced complete molecular remission in some. IFN- α can also be used as a cytoreductive agent and to improve symptoms such as splenomegaly in low- and intermediate-risk MF patients. However, treatment of advanced MF was less successful and limited by cytopenias^{138,139}.

1.3.4 JAK inhibitors

Activation of the JAK/STAT pathway is a hallmark of MPN pathogenesis. Thus, blockade of this pathway can be of therapeutic use for this group of diseases. Ruxolitinib is a JAK1/2 inhibitor docking to the ATP binding site in its active conformation. It led to improvement of constitutional symptoms and reduction of splenomegaly and therefore was approved as first line treatment for MF-related splenomegaly and as a second line for PV patients refractory or intolerant to HU¹⁴⁰⁻¹⁴². However, about half of the patients become resistant to ruxolitinib within 1.5 years¹⁴⁰. Fedratinib, a JAK2 inhibitor was approved for intermediate-2 and high risk MF a few years after ruxolitinib and might alleviate symptoms in patients refractory to ruxolitinib¹⁴¹. However, interaction with the human thiamine transporter led to occurrence of Wernicke encephalopathy in few individuals. Thus, fedratinib was approved with a warning about severe Wernicke encephalopathy and monitoring of thiamine levels is recommended^{141,143}. Nevertheless, the JAK/STAT pathway plays a vital role in normal hematopoiesis and current JAK inhibitors are not selective for mutant JAK. This leads to dose limiting side effects like anemia, thrombocytopenia, neutropenia, association with infections and an increased risk of developing secondary leukemias. Additional adverse reactions are headache, dizziness elevation of liver function parameters and hypercholesteremia. To improve hematological side effects, further JAK inhibitors are under development with momelotinib and pacritinib as alternative JAK inhibitors for patients with anemia or thrombocytopenia, respectively¹⁴⁰⁻¹⁴².

1.3.5 Allogeneic HSCT

Allogeneic HSCT is the only treatment with curative potential. Conditioning by high dose chemotherapy or radiation leads to ablation of hematopoietic cells, including the origin of MPNs, the mutated HSCs. At the same time the immune system is suppressed allowing the engraftment of exogenous HSCs. In addition, donor cells might exert a so-called graft versus leukemia effect by recognizing and eliminating mutant stem cells after engraftment. Factors influencing transplantation outcome are manifold and include patient age and comorbidities, conditioning regimen, mutation status, HSC donor type and leukemic transformation¹⁴⁴. Therefore, HSCT requires detailed assessment of each patient. The European Leukemia Network (ELN) recommended the consideration of HSCT for intermediate-2 and high-risk MF patients as well as for patients in the intermediate-1 risk group under 65 years with at least one of the following attributes: refractory, transfusion dependent anemia, more than 2% blasts in PB, adverse cytogenetics (as defined in DIPSS-plus), *JAK2/CALR/MPL* triple negative mutation status, *ASXL1* mutation¹⁴⁴. While HSCT can be curative, relapse is a major cause for treatment failure with incidence ranging from 10-43% in different studies¹⁴⁴.

1.3.6 Immunotherapy for calreticulin mutated MPN – a novel treatment approach

With a novel stretch of about 40 amino acids, mutCALR is a true neoantigen leading to high immunogenicity, which suggests importance in tumor control. Holmström et al. reported evidence for both tumor immune surveillance as well as a potential for therapeutic application in MPN^{145–147}. They reported circulating memory T cells with specificity for mutCALR in healthy donors and with a lower frequency in patients, indicating emergence followed by immunological clearance of *CALR* mutations in healthy patients and failure of this surveillance in MPN patients. Still, they isolated reactive CD4⁺ T cells from patients, which also showed a cytotoxic effect against mutCALR expressing cells, leading to the assumption that there is a therapeutic window for T-cell based immunotherapy in MPN. Holmström et al. as well as Tubb et al., however, failed to isolate reactive CD8⁺ T cells from patients with mutated *CALR*^{146,148}. This might be caused by defects in processing or presentation of mutCALR-derived peptides by MHC class I molecules. Tubb et al. found no evidence for mutCALR neoepitopes presented by common European/Caucasoid HLA class I alleles. In concordance, in the study by Holmström et al. CD8⁺ cytotoxic T lymphocytes failed to show a response against a mutCALR peptide, while CD4⁺ T cells showed reactivity against the peptide as well as target cells in an HLA II restricted manner. As part of the peptide-loading complex CALR plays an important role in HLA I assembly. Recently, it was reported that MHC I expression is reduced and peptide loading compromised upon mutation of *CALR*¹⁴⁹. Further, secreted mutCALR has been shown to inhibit phagocytosis of dying cancer cells by dendritic cells (DCs), which might further hinder the emergence of mutCALR-specific immune cells as antigen presentation by DCs is compromised¹⁵⁰. Thus, mutCALR drives oncogenesis by autologous constitutive MPL activation and at the same time its soluble form contributes to escaping immune surveillance.

Naturally, MPL is located at the plasma membrane, suggesting presentation of mutCALR at the cell surface^{34,100}. A recent study also presented evidence that membrane association of the mutCALR-MPL complex is required for oncogenic transformation³³. Both MHC I deficiencies as well as surface expression of a truly tumor-specific neoantigen indicate that targeting the surface antigen would be advantageous in *CALR* mutated MPN. Immunotherapies targeting tumor-associated antigens include among others antibody treatment. So far, three studies presented evidence for the feasibility of antibody-based treatment of *CALR* mutated MPN in preclinical models. Our group showed that frequent injections of a naked antibody targeting the mutant tail of *CALR* led to a transient decrease in PLT count and normalized the number of LSK cells in a Calrdel52 KI mouse model¹⁰⁰. The PLT reduction lasted only for several hours and thus required frequent antibody dosing. Further, the observation time was very short and hence long-term effects of antibody treatment could not be evaluated. Yet, in this short time

frame the antibody seemed to have an effect on HSPCs indicated the reduction of LSK cells to the level of WT mice. Likewise, Kihara et al. achieved a reduction of megakaryocyte and PLT counts by mutCALR-specific antibody treatment in a RV mouse model¹⁵¹. In this report, the authors introduced the cleavage of mutCALR at the cell surface as a potential obstacle for antibody treatment. They developed an antibody which detects the cleaved as well as the uncleaved version of mutCALR. This antibody led to inhibition of thrombocytosis over a time period of at least two months. While both antibodies led to a hematological response in mouse models, the mechanism of action, i.e. antibody-dependent cellular cytotoxicity (ADCC), complement-dependent cytotoxicity (CDC) or antiproliferative capacity effects due to receptor blockade, was not characterized in the mentioned studies. The low surface density of mutCALR at the cell surface of primary cells is probably limiting ADCC and CDC. As MPN can be associated with a certain degree of immunodeficiency, using an antibody that blocks oncogenic signaling is advantageous because of its indecency of immune-mediated effects. Tvorogov et al. developed an antibody that specifically inhibits the mutCALR-MPL interaction. This antibody diminished proliferation of hematopoietic progenitor cells of CALR mutated patients and prolonged survival of mice engrafted with a CALRdel61 cell line¹⁵². This was the only study showing an effect of the antibody on primary patient material. The in vivo experiments, however, were performed in xenograft models with a rapidly growing tumor cell line. Therefore, characterization of this antibody in KI models would be interesting.

1.4 Chimeric antigen receptor T cell therapy

The recognition and rejection of malignant cells by the immune system is the basis for cancer immunotherapy. T lymphocytes play an important role in immune surveillance and exhibit the potential to control tumor growth. Recognition of non-self-antigens is based on the interaction of the T cell receptor (TCR) with a peptide loaded MHC. MHC I and II present peptides from intracellular proteins that were synthesized in or ingested by a cell. MHC I is expressed by all nucleated cells, including cancer cells. MHC II expression is restricted to professional antigen-presenting cells (APCs), such as DCs, macrophages, and B cells, and thymic epithelial cells. MHC molecules interact with their corresponding co-receptor on the T cell surface. MHC I engages with CD8, thus enabling recognition and clearance of virus infected or malignant cells by cytotoxic T lymphocytes (CTLs). MHC II is bound by CD4 on T helper (T_H) cells, which play a role in elimination of extracellular pathogens by activating macrophages or enhancing the antibody production by B cells. Both CD4 and CD8 T cell response is dependent on TCR ligation by a specific MHC-peptide complex. The most common form of the TCR is a heterodimer consisting of one α and one β chain, which are each composed of one constant and one variable immunoglobulin-like domain. The variable domains of the α and β chain form one binding site, which determines antigen specificity. The $\alpha\beta$ -heterodimer is integrated in the

CD3 signal transduction complex, which consists of three dimers, $\epsilon\delta$, $\zeta\zeta$, and $\epsilon\gamma$. The interaction of the variable antigen binding site and the corresponding co-receptor (CD4 for MHC II and CD8 for MHC I) with the peptide loaded MHC complex leads to phosphorylation of the immunoreceptor tyrosine-based activation motifs (ITAMs) of the CD3 domains by Src protein tyrosine kinases (PTKs). The ζ -associated protein of 70 kDa (ZAP-70) is recruited to the phosphorylated ζ chains and equips the CD3 complex with kinase activity, leading to downstream signaling by phosphorylation of numerous substrates^{153–155}.

Initiation of a T cell response requires two signals. Signal 1 is provided by TCR-MHC interaction and CD3 mediated stimulation. Costimulatory domains, such as CD28, 4-1BB, ICOS, CD27 and OX-40 are responsible for signal 2. These molecules interact with their respective ligands on APCs, which can be either stimulatory or inhibitory and thereby balance the T cell response. CD28, the best studied costimulatory domain, binds to CD80/86 on APCs, which leads to increased T cell differentiation, proliferation and survival and promotes cytokine production. The T cell response is further modulated by cytokines which can be seen as a third, soluble signal. Naïve T cells are activated by APCs in secondary lymphoid organs and differentiate into effector and memory cells. These effector cells exert specific functions when presented with the same antigen in any tissue^{153,154}.

CTLs induce apoptosis in infected or neoplastic cells by two different cell-contact dependent mechanisms. The primary mechanism is a calcium-dependent release of lytic granules into the immunological synapse, a specialized spatiotemporal membrane structure between the T cell and the tightly bound target cell. These granules contain perforin and serine proteases, called granzymes. Polymerized perforin forms pores in the target cell membrane and granzymes can enter the cell via these channels. Granzyme B induces caspase-dependent and -independent apoptotic pathways by cleavage of caspase 3 and BCL-2. Activated CTLs further express the Fas ligand on their surface. Cell contact between activated T cells and their target cell can mediate interaction of the Fas ligand with Fas, a death protein expressed by a range of cell types. Upon binding, an adaptor protein is recruited to the cytosolic tail of the Fas receptor and leads to cleavage of procaspase 8. The following caspase cascade leads to programmed cell death. The production of IFN- γ directly interferes with viral replication and can further enhance the T cell reaction by increasing the expression of MHC I and Fas on the target cell. Cytokines of the tumor necrosis factor (TNF) family contribute to cytotoxicity as their interaction with TNF receptors on target cells induces apoptosis. IFN- γ and TNFs also lead to activation and recruitment of macrophages and are thereby at the interplay between innate and adaptive immunity¹⁵³.

CD4⁺ effector cells activate other immune cells in an antigen-specific manner by secretion of cytokines and interaction with CD40 on the surface of APCs. The three major types are T_H1,

T_H2 and T_H17 cells, which are distinguished by their cytokine profile. The main role of T_H1 cells is activation of macrophages by the production of IFN- γ , which plays a role in clearance of intracellular pathogens. T_H2 cells are important in the defense against extracellular parasites such as helminths. IL-4, IL-5 and IL-13 stimulate IgE production, activate eosinophils and mast cells and contribute to alternative macrophage activation. T_H17 cells are involved in infections with extracellular bacteria and fungi. IL-17 mobilizes neutrophils and monocytes and together with IL-22 increases the barrier function of tissue cells. Another CD4⁺ T cell subset are the Tregs. These dampen the immune response by secretion of inhibitory cytokines (IL-10, TGF- β) and antigen-specific modulation of DC function by direct cell contact¹⁵³.

The potency of the immune system in the treatment of cancer was established in 19th century by Busch and Fehleisen, who observed spontaneous regression of tumors after stimulation of the immune system by infections¹⁵⁶. Tumor infiltrating lymphocytes have been recognized as crucial for the control of development and progression of cancers¹⁵⁷. Especially CTLs and T_H1 cells are associated with prolonged OS and improved treatment success¹⁵⁸. However, cancer cells acquire the capability to avoid immunological clearance. Persisting tumors dampen the T cell response by different mechanisms including downregulation of MHC I, the formation of a hostile tumor microenvironment and the expression of inhibitory receptors^{159,160}. T cell-based immunotherapies can overcome these hurdles by redirecting T cells to malignant cells or by reactivating and/or enhancing a natural T cell response. Such therapies include cancer vaccination, checkpoint blockade and adoptive cell transfer. In this chapter the basics, current development, and limitations of chimeric antigen receptor (CAR) T cells will be reviewed.

CARs are synthetic receptors that combine antigen binding properties of an antibody with the stimulatory domains of a T-cell receptor. One major advantage of these receptors compared to TCRs is the independence of antigen presentation via MHC I. While natural CTL responses and chimeric TCRs are limited to MHC-presented peptides, CARs can target any kind of surface molecule including non-proteinogenic molecules such as carbohydrates or lipids. Thus, antigens that would otherwise not be immunogenic can be made visible for T cells by equipping them with a CAR. Besides, downregulation of MHC I is a common mechanism by which cancer cells escape destruction by CTLs. In addition, CAR-T cells deliver selective cytotoxicity at much lower antigen densities present on tumor cells when compared to conventional antibody therapeutics. Induction of ADCC or complement activation requires antigen densities of >10,000 molecules/cell, whereas CAR-T cells can recognize and eliminate target cells with antigen surface expression in the range of few hundred molecules/cell¹⁶¹. Thus, CAR-T cell therapy combines the versatility of antibodies with the effector function of T cells.

For CAR-T cell immunotherapy autologous T cells are harvested by leukapheresis. T cells are then stimulated and genetically modified by viral transduction, which leads to stable expression of the CAR. These engineered T cells are further expanded *ex vivo* in a bioreactor (Figure 6). After concentration and quality testing the final product can be cryopreserved, which enables shipment to distant treatment sites. Patients receive lymphodepleting chemotherapy before the cells are administered¹⁶². Kymriah (tisagenlecleucel) and Yescarta (axicabtagene ciloleucel), two CAR-T cell products targeting CD19 have shown unprecedented response rates in the treatment of B cell leukemias, which led to approval of the first cell-based gene therapies by the American Food and Drug Administration (FDA) in 2017. The success of these therapies paved the way for this rapidly progressing field.

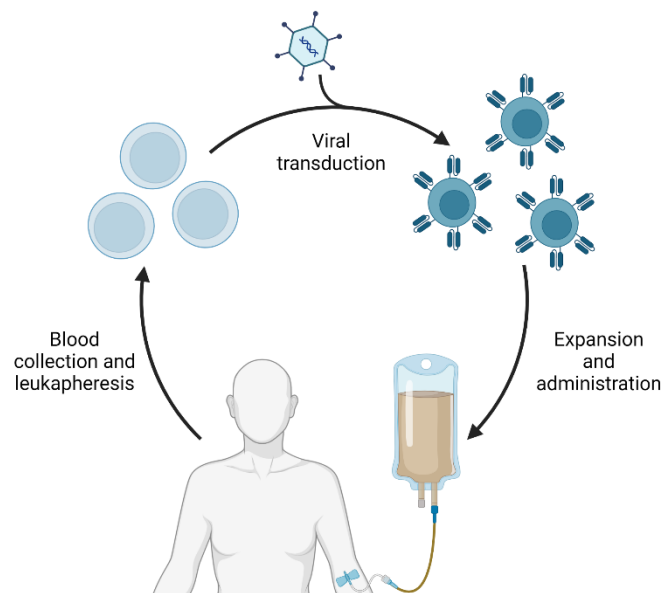


Figure 6: CAR-T cells are autologous T cells equipped with synthetic receptors. Generation of CAR-T cells is based on viral transduction of autologous T cells. These are administered to the patient after expansion and quality testing.

1.4.1 Structural elements of CARs

CARs are surface receptors that link an extracellular antigen binding scaffold to intracellular stimulatory domains via a linker and transmembrane domain. Each of these building blocks modulates T cell activation and influences CAR-T cell efficacy.

Antigen recognition domain

The antigen binding domain endows CAR-T cells with specificity towards a tumor associated antigen. In most CARs single chain variable fragments (scFvs), consisting of the variable light (V_L) and heavy (V_H) chain of an antibody connected via a flexible linker, are used.

Characteristics of the binding scaffold, such as the affinity for the target antigen, are detrimental for CAR efficacy. While the ideal target is a neoantigen exclusively expressed on cancer cells, such antigens are rare, and antigens not restricted to but overexpressed by the tumor are often targeted. T cell activation is influenced by the binding strength of a CAR which results from binding affinity and antigen surface density on the target cell^{161,163}. Thus, affinity must be optimized for each target to ensure recognition of malignant cells while sparing healthy cells. Yet, affinity is not the only criterion affecting the choice of an scFv. Depending on the linker between V_H and V_L and the antibody framework, interaction between the chains might lead to multimerization of scFvs and thereby to CAR clustering. It has been shown that scFvs prone to clustering can induce ligand-independent activation of CAR-T cells, which can lead to T cell exhaustion in CARs with a CD28 costimulatory domain^{164,165}. Interestingly, a recent study showed a beneficial effect of tonic signaling for the efficacy of 4-1BB CARs¹⁶⁶. To prevent clustering single domain antigen binding scaffolds such as V_{HH} domains of camelid antibodies or affibodies were incorporated into CARs^{163,167}. Another factor influencing suitability of the antigen recognition domain for a CARs is immunogenicity. The use of a fully human binding scaffold might increase CAR-T cell persistence^{168,169}.

Hinge and transmembrane domain

The hinge and transmembrane domains connect the extracellular binding scaffold to the intracellular signaling domains. The interaction of T cells and target cells is tightly regulated, and the spatial characteristics of target epitope and binding domain influence the formation of an immune synapse. The immune synapse formed between T cells and APCs is determined by the TCR-MHC interaction, which results in a cell-to-cell distance of about 15 nm¹⁷⁰. This distance was also found to be the maximal length for a functional CAR extracellular domain. The hinge region is a linker between antigen binding and transmembrane domain. It determines the distance between CAR-T and target cell and provides flexibility, an important denominator of epitope accessibility. It was shown that long spacers are advantageous for targeting membrane proximal epitopes, while short spacers are suited for membrane distal epitopes¹⁷¹⁻¹⁷⁴. The Fc part of IgG1 and IgG4 are frequently used as stabilizing linkers. However, interaction with Fc-γ receptors decreases *in vivo* persistence and leads to toxicities. These problems can be overcome by mutating the CH2 part or by incorporation of other linkers derived from CD8 or CD28¹⁷⁴. The transmembrane domain not only anchors the CAR in the cell membrane but also influences signal transduction. Commonly used stalks are derived from CD28, CD8 and CD3. They can induce homo- or heterodimerization and influence association with components of the signaling machinery^{175,176}. Both hinge and transmembrane domain can influence CAR expression and stability¹⁷⁷. Moreover, the choice of these domains allows fine tuning of the signaling threshold^{178,179}.

Stimulatory domains

In 1993 the pioneer of nowadays CARs, a so called first-generation CAR, was generated: a scFv fused to a transmembrane domain and a CD3 ζ -derived stimulatory domain¹⁸⁰. Although such first-generation CARs activated T cells leading to cytokine secretion and target cell lysis *in vitro*, *in vivo* efficacy and persistence was limited^{181–185}.

Second-generation CARs were equipped with a costimulatory domain derived from CD28, CD134/OX40, CD137/4-1BB or CD27 to prevent T-cell anergy. The most used costimulatory domains are CD28 and 4-1BB. While both CD28-CD3 ζ (28z) and 4-1BB-CD3 ζ (BBz) CARs led to substantial T cell expansion and strong and durable remissions *in vivo*, their kinetics and safety profile are different. Long et al. postulated that 28z CARs are more prone to tonic signaling which leads to T cell exhaustion¹⁶⁴. Gomes-Silva and colleagues, however, also observed tonic signaling in BBz CAR-T cells caused by high CAR expression. In this study T cell exhausting was influenced by the expression vector and the CAR surface density¹⁸⁶. In a small cohort of patients with non-Hodgkin lymphoma BBz and 28z CD19 CAR-T cells expanded at a comparable rate and had similar antitumor activity. The BBz CAR, however, increased T cell persistence and differentiation towards central memory T cells. CD28, on the other hand, induced a stronger signal, which drove differentiation into effector memory cells and promoted cytokine secretion. Thus, the 28z CAR was also associated with increased risk for cytokine release syndrome (CRS) and immune effector cell-associated neurotoxicity syndrome (ICAN), while BBz CARs had a favorable safety profile¹⁸⁷. In a larger cohort of patients with relapsed or refractory (r/r) diffuse large B cell lymphoma axicabtagene ciloleucel outperformed tisagenlecleucel. CRS and ICANS were more frequent in the group with axicabtagene ciloleucel¹⁸⁸. In conclusion, both CD28 and 4-1BB CARs are incorporated in approved CAR-T cell products and lead to comparable anti-tumor responses overall. While differences were observed in preclinical and clinical trials, consistent superiority of one of these CAR designs over the other has not been observed¹⁸⁹.

To further enhance the costimulation effect, third generation CARs were provided with two costimulatory domains targeting different signaling pathways. CD28 activates the PI3K pathway and 4-1BB and OX40 activate T cells via TNF-receptor-associated factor (TRAF) adaptor proteins. Therefore, combination of CD28 with 4-1BB or OX40 can have a synergistic effect on T cell activation. However, results in preclinical models were ambiguous. While a third-generation CAR outperformed its second-generation pendant in a lymphoma model, incorporation of an additional costimulatory domain did not improve *in vivo* efficacy in mouse models for leukemia and pancreatic cancer^{190–192}. So far, all FDA- approved use are second-generation format with either CD28 or 4-1BB¹⁹³.

1.4.2 Limitations of CAR-T cell therapy

Despite the remarkable success of CAR-T cells in the treatment of hematological malignancies, certain limitations remain that hinder broader applications. These include adverse events following CAR-T cell infusion, tumor cell escape by antigen modulation and limited T efficacy due to impeded tumor accessibility and/or an immune suppressive tumor microenvironment.

CAR-T cell associated toxicities

While infusion of a live therapy enables durable remission, it also comes with the risk of uncontrolled immune effector function leading to toxicities. Excessive production of pro-inflammatory cytokines, such as IFN- γ , IL-6, IL-10 and GM-CSF, causes CRS, one of the main side effects associated with CAR-T cell therapy. The onset of CRS occurs early after T cell infusion and is associated with fever and constitutional symptoms like fatigue, rigor, and myalgia. A systemic inflammatory response goes hand in hand with endothelial damage. This results in severe symptoms including hypotension, hypoxia, and organ failure. To prevent organ damage close monitoring and early intervention in case CRS symptoms is necessary. Treatment with corticosteroids and tocilizumab, an IL-6 blocker, have proven effective in the management of CRS¹⁹⁴. Immune-mediated activation of endothelial cells can also lead to intravascular coagulation, capillary leakage, and disruption of the blood-brain barrier (BBB). Increased permeability resulting in elevated cytokine levels and presence of immune cells in the cerebrospinal fluid is involved in the occurrence of neurotoxicity¹⁹⁴. Apart from a systemic immune reaction, the role of antigen-specific CAR-T cell reactions in the development of ICANS is discussed. High affinity CARs can recognize cells with low antigen expression, which might lead to on-target/off-tumor toxicities. CD19 expression in brain mural cells was detected by RNA sequencing and thus might be involved in neurotoxicity observed in anti-CD19 CAR-T cell trials¹⁹⁵. Likewise, post-mortem analysis of the brain tissue revealed expression of BCMA in a proportion of neurons and astrocytes of a patient who developed parkinsonism following treatment with anti-BCMA CAR-T cells¹⁹⁶. On-target/off-tumor toxicities apart from the central nervous system have been reported for several CARs, inducing side effects with different severity. The paragon CD19 is a B cell marker expressed on healthy cells as well as leukemic cells. Therefore, anti-CD19 CARs lack specificity for malignant cells resulting in complete B-cell aplasia. This, however, is a well manageable side effect, which can be counterbalanced by intravenous immunoglobulin administration. Expression of target antigens on vital tissues, however, can result in severe organ damage. In a study testing CAR-T cells directed against CAIX (carboanhydrase IX) for the treatment of renal cell carcinoma, patients developed cholestasis due to expression of CAIX by the biliary bile duct epithelium¹⁸². In one case, reactivity of HER-2 specific CAR-T cells given at a high dose even had lethal consequences

due to on-target/off-tumor targeting of lung cells¹⁹⁷. This illustrates the importance of specificity in CAR design. As tumor-specific neoantigens are rare, antigens overexpressed in tumor cells are an important target group. Therefore, most CARs are directed against antigens that are also expressed in healthy tissues albeit at lower levels. CARs directed at such antigens must be designed in a way that the signal strength is adequate to trigger a reaction against tumor cells, while antigen expression levels of healthy cells are below the activation threshold. Improving discrimination of tumor from healthy tissue by combining dual target antigens in logic gates, such as AND- or NOT-gates is subject of extensive ongoing research and might increase the repertoire of targetable antigens. Further approaches to include CAR-T cell safety include the use of suicide switches, which would allow CAR-T cell depletion upon observation of adverse events.

Antigen modulation leads to resistance

Resistance to anti-CD19 CAR-T cell therapy in pediatric B-ALL and patients with large B cell lymphoma is associated with antigen loss or downregulation below the threshold for current CAR-T cell formats in about half of all cases^{198,199}. To overcome this problem dual antigen targeting is under investigation. This can be achieved by generation of a mixed cell product, co-transduction of different CAR constructs, bicistronic expression or incorporation of two binding domains in one CAR. In fact, ciltacabtagene autoleucl, a recently approved anti-BCMA CAR, contains two V_{HH} domains targeting different BCMA epitopes¹⁶⁷. In trials with bispecific CARs targeting CD19 and CD20, antigen-negative relapse rates were diminished showing the potential for such approaches^{200,201}. The combination of CD19 and CD22, however, was less effective. In one study inferior reactivity against CD22 allowed the emergence of CD19^{-low} tumor cells²⁰². In other studies, relapse was associated with loss of both antigens in about one third of patients^{203,204}.

The antigen threshold correlates with CAR signaling strength and is therefore modulated by scFv affinity, structure and length of the hinge and transmembrane region, the choice and modification of signaling domains, and the CAR expression level. Increasing sensitivity towards low antigen expression might prevent relapse by antigen modulation. However, this approach comes with a severe risk of increased toxicities. Therefore, CAR optimization for low antigen expression should only be considered for antigens not expressed in vital tissues. For some targets, antigen downregulation can be counteracted by application of small molecules. CD22, for example, is upregulated by bryostatin and BCMA surface expression can be increased by using γ -secretase inhibitors, which prevent the cleavage from the tumor cell surface^{205,206}. Thus, γ -secretase inhibitors increase the amount of BCMA retained on the surface and prevent the shedding of soluble BCMA into the tumor environment, two important prerequisites for CAR-T cell efficacy²⁰⁶.

The immunosuppressive tumor microenvironment

During cancer progression a pro-tumorigenic but immune suppressive tumor microenvironment is shaped, which interferes with T cell migration, infiltration, and functionality. Migration of immune cells into the tumor microenvironment is dictated by chemokine expression. Expression patterns, however, are modulated by tumor cell intrinsic oncogenic and epigenetic pathways as well as metabolic reprogramming resulting in impaired infiltration of effector cells and increased recruitment of immunosuppressive cells like myeloid-derived suppressor cells (MDSCs), tumor-associated macrophages (TAMs) and Tregs¹⁵⁹. Moreover, stromal and endothelial cells can directly interfere with tumor penetration. Within the tumor microenvironment, a combination of different factors including the expression of inhibitory receptors, secretion of immunomodulatory cytokines and metabolic challenges directly constrain T cell functionality. The tumor cells often express inhibitory ligands, such as PD-L1 and CTLA-4, which induce T cell exhaustion in a cell-contact dependent manner. Soluble factors such as the immunosuppressive cytokines IL-10 and TGF- β further inactivate T cells. In addition, rapidly dividing tumor cells deplete their environment of nutrients and at the same time produce suppressive metabolites. Tumor cells undergo metabolic reprogramming which allows flexibility and gives those cells an advantage in an environment with insufficient nutrient levels. The harsh metabolic conditions in the tumor microenvironment impair T cell development, proliferation, survival and effector function¹⁶⁰.

To overcome the hurdles posed by the tumor microenvironment, combination therapies or modification of CAR-T cells can be beneficial. The expression of chemokine receptors adapted to the chemokine profile of the tumor might increase T cell trafficking and migration^{207,208}. CAR-T cells directed against the supportive tissue, such as CARs degrading components of the extracellular matrix or CARs with specificity for cancer-associated fibroblasts, increased tumor infiltration and cytotoxic function in preclinical models^{209,210}. Moreover, locoregional application into the central nervous system improved responses in glioma patients²¹¹. To increase persistence and functionality at the tumor site by secretion of pro-inflammatory cytokines “armoured CARs” were developed^{207,212}. The secretion of IL-12 by CAR-T cells at the target cell site for example had beneficial effects including resistance to Tregs and stimulation of immune cells²¹². Another approach is to render T lymphocytes immune to inhibitory signals by genetic modification or pharmacological intervention. Genetic disruption or expression of a dominant negative form of the TGF- β , PD-1 or Fas receptors can act as a sink for the immunosuppressive signals^{213–217}. Combination with immune checkpoint inhibitors, such as ipilimumab or pembrolizumab can overcome T cell exhaustion induced by PD-1 and CTLA-4 signaling^{218–220}. These signals can even be reverted into positive signals by fusing PD-1 to the co-stimulatory CD28 domain²²¹.

1.4.3 CAR-T cell therapy for hematological malignancies

Currently, there are six approved CAR-T cell therapies, which are all in use for the treatment of late-stage hematological diseases. CD19-specific tisagenlecleucel (Kymriah) and axicabtagene ciloleucel (Yescarta) were the first gene therapies approved in 2017 for the treatment of B-cell acute lymphoblastic leukemia (B-ALL) and B-cell non-Hodgkin lymphoma (NHL) or B-ALL and follicular lymphoma (FL), respectively. In 2020 and 2021 two more CD19 CARs followed with brexucabtagene autoleucel (Tecartus) and lisocabtagene maraleucel (Breyanzi). Brexucabtagene autoleucel is used for the treatment of mantle cell lymphoma (MCL) and B-ALL, while lisocabtagene maraleucel was approved for patients with B-cell NHL. Idencabtagene vicleucel (Abecma) and ciltacabtagene autoleucel (Carvykti) are BCMA-specific CARs that were approved for the treatment of multiple myeloma (MM) in 2020 and 2021. The clinical response to these CARs and novel CAR constructs that showed evidence for clinical efficacy will be reviewed within this chapter.

B-cell and plasma cell malignancies

Anti-CD19 CARs have shown remarkable efficacy in the treatment of NHL, B-ALL and chronic lymphocytic leukemia (CLL). NHL is a heterogenous group of diseases comprised of diffuse large B cell lymphoma (DLBCL), FL, marginal zone lymphoma (MZL) and MCL. Most types of NHL arise from degenerate B cells and thus express classical B cell markers, such as CD19 and CD20, and are therefore susceptible to targeted therapies using a CD20-specific antibody rituximab and anti-CD19 CAR-T cells. Further indications for anti-CD19 CAR-T cell therapy are CLL and B-ALL. All four currently approved products were able to induce deep initial remission with complete response (CR) rates of 28-68% in patients with NHL and CLL and 62-86% in B-ALL. Long-term remissions over two years were observed in different types of NHL and CLL, suggesting that CD19 CAR-T cell therapy can have curative potential for these indications. Although initial response rates are higher in B-ALL, the median relapse-free survival of adult patients is in the range of half a year. Thus, consolidative allogeneic HSCT is recommended following CAR-T cell treatment. More than half of all patients developing B-ALL are children and tisagenlecleucel is also approved for patients younger than 25 years. In the ELIANA study, pediatric patients treated with tisagenlecleucel showed better response rates (82% CR) compared to adults and durable remissions (median event free survival 24 months) were observed. Therefore, in adult B-ALL patients, CAR-T cell therapy plays a significant role as bridging therapy before HSCT, while in children long-term remission might be achieved with CAR-T cells alone^{193,199}.

Apart from CD19 other B cell-specific markers are under investigation as CAR-T cell targets. Those include CD20 for LBCL, and CD22 for B-ALL and LBCL. Hodgkin lymphoma (HL) is caused by malignant cells called Reed-Sternberg cells, which, although stemming from B

lymphocytes, are often CD19 and/or CD20-negative^{222,223}. CD30, a typical marker for these cells, is targeted by brentuximab vedotin. This antibody-drug conjugate showed promising overall response rates as a monotherapy, which also raised interest in targeting this antigen with CAR-T cells. The κ -light chain is expressed on certain B-cell lymphomas and leukemias, while only part of nonmalignant B cells bears κ chains. Thus, targeting this antigen will avoid complete B-cell aplasia. Overall, expanding the antigen repertoire is an important step towards targeting CD19⁻ lymphoma or leukemia cells^{193,198}.

Recently, two BCMA-specific CARs were approved for the treatment of MM. CR rates in studies with idencabtagene vicleucel and ciltacabtagene autoleucel ranged from 33% to 83%. While a subset of patients achieved long-term remission ≥ 1 year, the progression free survival was highly variable ranging from a median of 5 months to 27 months. Thus, anti-BCMA CARs have shown to enable a long intervention-free period in patients with r/r MM with superior efficacy of ciltacabtagene autoleucel^{193,224}.

Historically, CAR-T cells were previously only used for the treatment of refractory malignancies in heavily pretreated patients. Previous therapies, however, might lead to lymphopenia and reduce T cell fitness. Moreover, malignant cells that do not respond to chemotherapy might outgrow during the CAR-T cell manufacturing process. Application of CAR-T cells at an earlier stage resulted in an improved response and increased CAR-T cell persistence in the patients with aggressive B cell lymphomas¹⁹³.

T cell malignancies

The CD7 glycoprotein is a marker for mature T cells. Targeting of T cell specific antigens requires additional engineering to prevent fratricide. Transduction with an anti-CD7 binding scaffold, that is coupled to an ER/Golgi retention signal retains CD7 intracellular. Thus, surface expression is prevented, and T cells are rendered fratricide-resistant. Such CD7 CAR-T cells were tested in patients with T-ALL or T cell lymphoblastic lymphoma (TLBL) in two small studies^{225,226}. Both trials achieved very high CR rates around 90%. While these studies had relatively short follow up times, durable remissions were observed in some patients over a time of up to 9 months. While B cell aplasia after CD19 CAR-T cell treatment is a well tolerable and manageable side effect, T cell aplasia is more severe due to the lack of interventions. Thus, CD7 CAR-T cell treatment renders patients immunocompromised and bears the risk of severe infections. The presence of CD7⁻ normal T cells can lead to reconstitution of the immune system and thereby dampen the risk of infections. Another factor complicating the use of T cells against malignant T cells is the potential contamination of CAR-T cells with malignant T cells. Thus, the final product needs stringent quality control to ensure the purity of the T cell population.

Myeloid malignancies

AML is associated with poor prognosis and limited therapeutic opportunities. Besides high-dose chemotherapy, allogeneic HSCT is the most promising approach. Heterogeneity and potential cytopenia due to on-target/off-tumor toxicity complicated the identification of an ideal target for the immunotherapeutic treatment of AML. CD38 is expressed on most AML and MM cells but is absent from HSCs. Clinical safety and efficacy of daratumumab, a monoclonal anti-CD38 antibody used in the treatment of MM, makes CD38 an interesting target for CAR-T cells. A third-generation anti-CD38 CAR was tested in six patients who relapsed after HSCT, a cohort with dismal outcomes. CR was observed in four out of six patients with median OS of 7.9 and median leukemia free survival of 6.4 months²²⁷.

As CAR-T cell engineering will improve safety and side effect profiles in the future, CAR-T cell therapies will be available for a much larger indication range including chronic diseases with a longer treatment window such as MPN. MutCALR is a neoantigen expressed on the cell surface of mutated cancer cells and its interaction with MPL at cell surface drives oncogenesis. Therefore, it fulfills all criteria of an ideal immunotherapy target. Due to their sensitivity and versatility, we believe that CAR-T cells can be of therapeutic relevance for *CALR*-positive MPN, especially primary myelofibrosis – the most severe form of MPN with greatest unmet medical need.

1.5 AIMS

In 2013 *CALR* mutations were discovered as driver mutations in myeloproliferative neoplasms¹¹. Since then, major progress has been made in elucidation of the oncogenic transformation driven by mutant *CALR* variants. This thesis comprises two independent aims. The first aim was to elucidate the influence of concomitant *CALR* and *JAK2* mutation. The second goal was the generation of CARs for targeted treatment of *CALR* mutated MPN.

1.5.1 The influence of *JAK2/CALR* double mutation on HSC fitness and disease phenotype

Based on early publications MPN driver mutations were considered mutually exclusive^{43,44}. However, the co-occurrence of driver mutations has been described in numerous publications since then. While clonal hierarchy was rarely investigated in these studies, those providing such data found the mutations in independent clones. This prompted the question, whether MPN driver mutations are mutually exclusive on a single cell level. Recently, the first case report about a patient who progressed from ET to MF after acquiring a *JAK2* mutation into a *CALR* mutated clone was published. This study implicated that *JAK2* and *CALR* mutations can

co-exist in a single cell and that co-occurrence might promote disease progression. Yet, the influence of dual mutation on HSC functionality remained elusive. Further, the scarcity of such patients hinders evaluation of the consequences of *JAK2/CALR* co-mutation on the disease. Therefore, the first aim was to investigate the impact of *CALR/JAK2* double mutation on disease phenotype and HSC fitness in a novel mouse model.

1.5.2 Generation and testing of CARs targeting mutCALR

Due to the novel amino acid sequence at the C-terminus and surface presentation of the mutant protein, *CALR* mutations provide a unique opportunity for targeted treatment. However, there has been little progress on delivering targeted therapies for MPN despite the great unmet medical need especially for PMF (shortest overall survival among different MPNs and frequent leukemic transformation). Therefore, in the second part we explored the use of CAR-T cells for *CALR* mutated MPN.

2. RESULTS

2.1 Manuscript #1: Co-expression of mutated Jak2 and Calr enhances myeloproliferative phenotype in mice without loss of stem cell fitness

Christina M. Schueller, Andrea Majoros, Harini Nivarthi, Robert Kralovics

Published in *American Journal of Hematology*, 2022

In this publication we addressed the first aim of this thesis. We generated a novel mouse model by co-expression of Jak2 and Calr mutations in the hematopoietic system. This model for the first time allowed to investigate the influence of Jak2/Calr double mutation on MPN phenotype. Further, we assessed the effect of dual mutation on stem cell fitness to rule out synthetic lethality as a cause for the rarity of such patients.

The open-access PDF is reprinted on the following pages.



CORRESPONDENCE

Co-expression of mutated Jak2 and Calr enhances myeloproliferative phenotype in mice without loss of stem cell fitness

To the Editor:

Myeloproliferative neoplasms (MPNs) are a group of acquired hematopoietic stem cell (HSC) disorders driven by mutations that constitutively activate physiologic signal transduction pathways essential for hematopoiesis. Most patients with classical MPNs harbor mutations within the Janus activated kinase 2 (JAK2), calreticulin (CALR), or thrombopoietin receptor (MPL) genes. The occurrence of driver mutations was thought to be mutually exclusive, but double-positive cases have been reported. However, in rare cases where clonal analysis was performed both mutations occurred in independent clones, suggesting mutual exclusivity at the single cell level.^{1–3} Recently, a single report described one patient who acquired a JAK2 mutation in a CALR mutant clone.⁴ Although the JAK2 mutation could be detected in HSCs as well as myeloid progenitors, the variant allele frequency was lowest in the HSC population. Although this report suggests that JAK2-V617F and CALR-del52 mutations can occur in a single clone, the effect on HSC fitness remains elusive.

In this study, we tested the hypothesis that Jak2-V617F and Calr-del52 mutations are synthetic lethal if they occur in the same HSC. Since synthetic lethality at the HSC level can manifest as loss of competitive fitness over time or cell death, the only means by which such genetic interaction can be detected is using primary genetically engineered HSCs. Therefore, we generated a mouse model in which both mutations are co-expressed in the hematopoietic system, which allowed us to assess the phenotype of such animals and enabled evaluation of HSC fitness in transplantation experiments.

We generated conditional knock-in mice that co-express Jak2 and Calr mutations in the presence of Cre recombinase in hematopoietic lineages (vav-iCre) and analyzed their phenotype (Figure 1A). C57BL/6 vav-iCre and Ly5.1/CD45.1 mice were purchased from Charles River Laboratories. Mice carrying Jak2-V617F mutation were previously published,⁵ and the Calr-del52 transgenic mice were generated in our laboratory.⁶ The Calr-del52 vav-iCre mice were further bred with Jak2-V617F mutant mice to generate mice expressing both mutations in the hematopoietic compartment. Blood parameters were measured on hematology analyzer scil Vet abc™ (Horiba ABX, Montpellier, France). Single cell suspensions of bone marrow, spleen, and blood were stained, with relevant panels of antibodies (Tables S1–S3), measured at BD LSRFortessa™ (Flow Cytometry - Core Facilities, Medical University

of Vienna, Vienna, Austria) and analyzed using FlowJo software (Version 10.7.1; Ashland, Oregon, USA).

Double positive offspring were born at expected Mendelian frequency comparable to the single positive littermates, suggesting no signs of synthetic lethality in utero (Figure 1B). The phenotype of the Calr/Jak2 double positive mice was significantly more severe compared to the single mutant mice. Notably, double positive mice showed more pronounced splenomegaly and higher platelet, leukocyte, granulocyte, monocyte, and lymphocyte count in peripheral blood compared to non-mutated or single mutated mice (Figures 1C–G and S1a). Hematocrit, red blood cell count, and hemoglobin were increased compared to non-mutated and Calr mice but did not exceed the values of Jak2 mice (Figures 1H and S1b,c). In line with the thrombocytosis, double mutant mice showed an increased frequency of megakaryocytes in the bone marrow (Figure 1I). Flow cytometry analysis of the blood and spleen revealed an altered cellular composition with a shift toward myeloid lineages (Figures S1d–i and S2a–f). While the stem cell frequency in double mutant mice seemed unaltered, the myeloid progenitor compartment showed a significant expansion of different progenitor types further explaining the excessive production of terminally differentiated myeloid cells (Figures S2g–j and S3a–i). Spleen and bone marrow of double positive mice also showed morphological changes. More obscured follicular architecture and enhanced extramedullary hematopoiesis was detected in the spleen. The bone marrow presented with more prominent megakaryocyte dyspoiesis and altered myeloid to erythroid ratios with no signs of myelofibrosis (Figure S4, reticulin staining not shown). Most importantly, the aggravated myeloproliferative phenotype of double positive mice manifested in lower overall survival compared to the Jak2 and Calr single mutated mice (Figure 1J). Our results are further supported by the report of a double mutant MPN patient who evolved from essential thrombocythemia to advanced myelofibrosis after acquisition of the JAK2-V617F mutation in a CALR-del52 mutated clone.⁴

To gain further insight into the cellular processes affected by Calr/Jak2 double mutation we compared gene expression of single and double mutated LSK (Lin- Sca-1+ c-Kit+) cells. While double mutated cells showed a very similar gene expression signature as the Jak2 single mutated cells, differential expression in comparison to Calr mutated cells was more pronounced (Figure S5a–d). Gene sets upregulated in double mutated versus Calr single mutated cells, such as coagulation, IL-2/STAT5 signaling, and IL-6/JAK/STAT3 signaling, are consistent

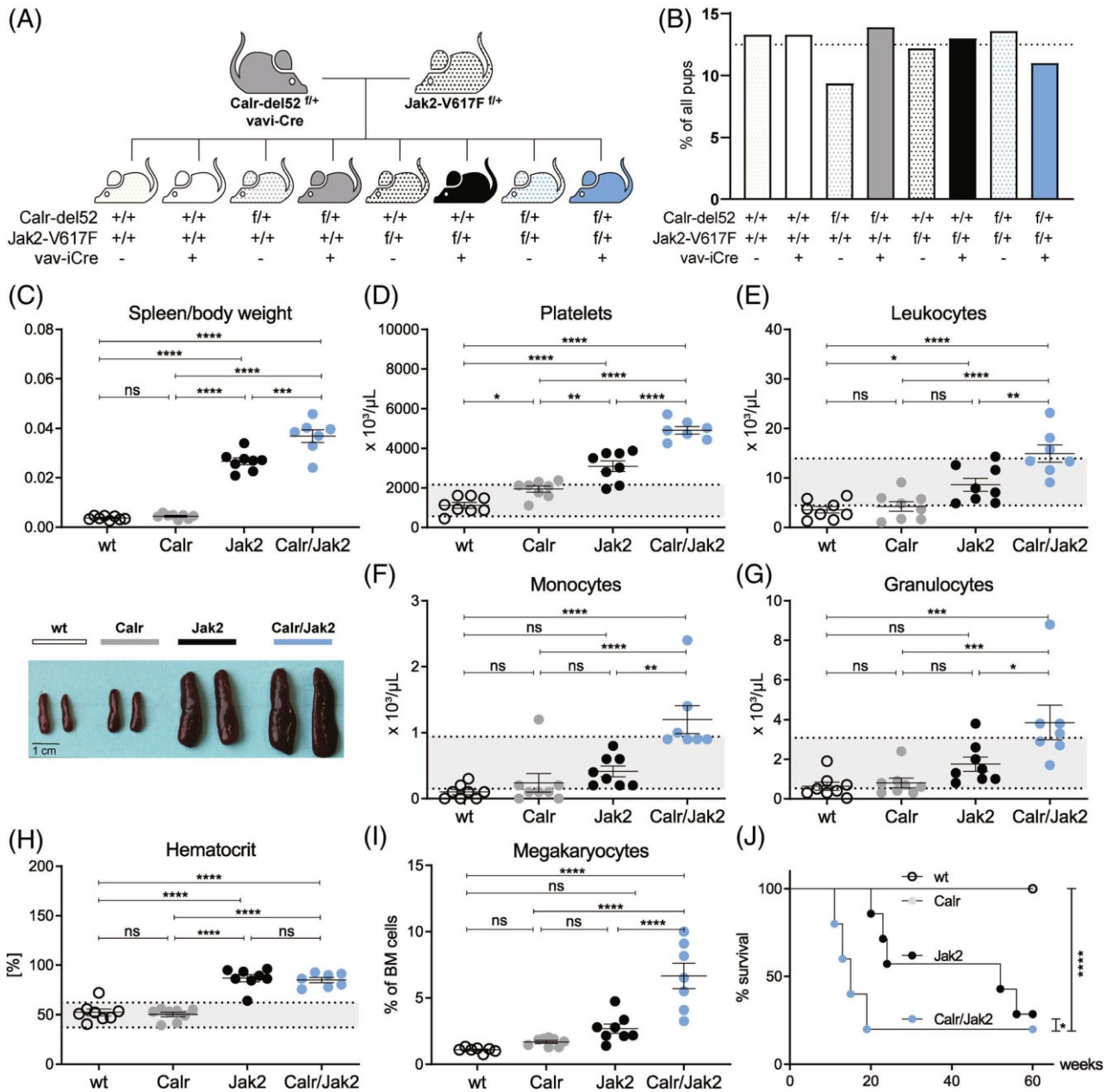


FIGURE 1 Mice bearing Calr-del52 and Jak2-V617F double mutation develop more severe MPN compared to single mutated mice. (A) Breeding scheme. (B) The genotype of 353 pups was determined and the frequency of each genotype was calculated (expected frequency = 12.5%, dotted line). Statistical analysis was performed using Chi-squared test. (C)–(I) 8 to 9 week old mice of different genotypes, wt vav-iCre (wt), Calr-del52^{fl/+} vav-iCre (Calr), Jak2-V617F^{fl/+} vav-iCre (Jak2), and Jak2-V617F^{fl/+}/Calr-del52^{fl/+} vav-iCre (Calr/Jak2), were examined for phenotypic differences: Spleen size (spleen to body ratio) (C), peripheral blood parameters from automated blood counting (D)–(H), FACS analysis of bone marrow megakaryocytes (I). (K) Survival curve analysis. Statistical analysis was performed using Log-Rank (Mantel-Cox test). The dots represent values for individual animals; Lines represent mean values for the group and the error bars represent standard error of the mean (SEM); asterisks denote the level of statistical significance (ns, $p > 0.05$; * $p \leq 0.05$; ** $p \leq 0.01$; *** $p \leq 0.001$; **** $p \leq 0.0001$); unless stated otherwise the p -values were calculated using ordinary one-way ANOVA test. The gray area between dotted lines represents physiological levels for wt C57BL/6 mice.

with the increased disease phenotype. Although apoptosis is also among the enriched gene sets, the two genes clustering in this set, *Btg2*, and *Ltb* are also associated with maintenance of hematopoietic stem cells. Among the downregulated genes, three were associated with mTORC1 and hedgehog signaling. Compared to Jak2 single

mutated cells, significantly downregulated genes clustered in heme metabolism and TNF-alpha signaling. Both genes categorized into the pancreas beta cell pathway, *Mafb* and *Pklr* are also involved in erythrocyte differentiation and metabolism. High expression of *Ebi3* and *STAT5* induced genes, that is *Socs2* and *Cish* in the double mutant cells

suggest that phenotypic differences are driven by JAK/STAT signaling (Figure S5e).

To examine the impact of double mutation on HSC fitness, we performed competitive primary and secondary bone marrow transplantation (Figure S6a). Double positive bone marrow engrafted into recipients equally well as single positive cells suggesting no functional defect at the HSC level. We observed outgrowth of mutant cells in blood, spleen, and bone marrow with most prominent expansion of mutant cells in the myeloid compartment (Figures S6b–c and S7). Transplanted mice also developed an MPN phenotype reminiscent of the one observed in the transgenic animals (Figures S6d–f and S8). To further test if the double positive HSCs maintained their self-renewal capacity over time, we performed secondary transplantation. Double mutant HSCs efficiently engrafted in secondary recipients and mice developed peripheral blood changes indicative of myeloproliferative disease, further suggesting the absence of any long-term defect (Figures S6g, S9 and S10). Thus, the presence of both mutations in HSCs is unlikely to cause synthetic loss of HSC fitness.

To date, with a single case being reported, there is no sizable *JAK2/CALR* double mutated patient cohort available to evaluate the disease phenotype and estimate survival. Our mouse model allowed phenotypic assessment of *JAK2/CALR* double mutated MPN. We observed a severely aggravated phenotype in double mutated compared to single mutated animals with increased hematocrit similar to *Jak2* mutated mice and aggravated megakaryopoiesis and myelopoiesis compared to all other groups. Likewise, the reported patient also progressed to myelofibrosis after acquisition of the second mutation. Therefore, we conclude that the co-occurrence of both mutations might be a negative predictive indicator.⁴

HSCs did not show any signs of reduced fitness, ruling out mutual exclusivity due to synthetic lethality. Transplantation experiments using *Calr-del52* or *Jak2-V617F* single mutated knock-in mice have been performed in previous studies and are in line with our results. While *Jak2* mutant cells were reported to outgrow wt competitors, heterozygous *Calr* mutated HSCs did not show a significant proliferative advantage compared to wt cells.^{6–8} In this study we observed a steady increase in myeloid peripheral blood chimerism in all groups with little expansion in the *Calr* group and strongest expansion in mice that received double mutant bone marrow. The results were similar on the HSC level. In the *Jak2* and double mutated group two mice each reached full mutant HSC chimerism in the secondary transplant. In short, double mutant HSCs engrafted equally well or better than their single mutant equivalents. Therefore, we can rule out reduced stem cell fitness as a reason for rare occurrence of double mutant patients.

We hypothesize that patients carrying both mutations in one clone might be underdiagnosed as the most common diagnostic routine is single gene analysis for driver mutations in *JAK2*, *CALR*, and *MPL* at diagnosis. In the reported case, a *JAK2-V617F* mutation was acquired in a *CALRdel52* mutated clone 18 years post initial diagnosis.⁴ This shows that a second driver mutation can be acquired decades later, which might be another factor leading to such patients being undetected since driver mutations are rarely re-analyzed after

initial molecular diagnostics. In addition, establishing if the two mutations are monoclonal or bi-clonal, requires an in vitro colony assay. Presence of colonies with both mutations is the formal proof of monoclonal acquisition of the two mutations. However, this procedure is very time consuming and therefore rarely performed.

AUTHOR CONTRIBUTIONS

Andrea Majoros and Robert Kralovics designed the study; Christina M Schueller, Andrea Majoros, and Harini Nivarthi performed experiments and collected the data; Christina M Schueller and Andrea Majoros analyzed the data; Christina M Schueller, Andrea Majoros, and Robert Kralovics wrote the manuscript.

ACKNOWLEDGMENTS

This study was supported by the Austrian Science Fund, FWF P34451-B granted to Robert Kralovics and P30041-B26 granted to Harini Nivarthi as well as the Austrian Academy of Sciences, DOC fellowship 26008 granted to Christina M Schueller. We thank Jakob Weinzierl and Elisabeth Fuchs for their technical assistance. We also thank Agnieszka Piszczek, Tamara Engelmaier, Julia Klughofer, and Mihaela Zeba for tissue processing and histochemical staining and Anoop Kavirayani for histopathological assessment. Moreover, we thank the CeMM Biomedical Sequencing Facility and Michael Schuster for performing RNA sequencing and data processing.

FUNDING INFORMATION



This study was supported by the Austrian Science Fund, FWF P34451-B granted to Robert Kralovics and P30041-B26 granted to Harini Nivarthi as well as the Austrian Academy of Sciences, DOC fellowship 26008 granted to Christina M Schueller.

CONFLICT OF INTEREST

The authors declare that there is no conflict of interest.

DATA AVAILABILITY STATEMENT

The data that support the findings of this study are available from the corresponding author upon reasonable request.

Christina M. Schueller^{1,2} , Andrea Majoros², Harini Nivarthi²,
Robert Kralovics¹ 

¹Department of Laboratory Medicine, Medical University of Vienna,
Vienna, Austria

²CeMM Research Center for Molecular Medicine of the Austrian
Academy of Sciences, Vienna, Austria

Correspondence

Robert Kralovics, Department of Laboratory Medicine, Medical
University of Vienna, Währinger Gürtel 18-20, Vienna 1090, Austria.
Email: robert.kralovics@meduniwien.ac.at

Christina M. Schueller and Andrea Majoros contributed equally to this study.

ORCID

Christina M. Schueller  <https://orcid.org/0000-0001-7618-6815>

Robert Kralovics  <https://orcid.org/0000-0002-6997-8539>

REFERENCES

1. Mansier O, Migeon M, Etienne G, Bidet A, Lippert E. JAK2V617F and CALR double mutations are more frequently encountered in patients with low JAK2V617F allelic burdens. *Leuk Lymphoma*. 2016;57:1949-1951.
2. Thompson ER, Nguyen T, Kankanige Y, et al. Clonal independence of JAK2 and CALR or MPL mutations in comutated myeloproliferative neoplasms demonstrated by single cell DNA sequencing. *Haematologica*. 2021;106:313-315.
3. Lundberg P, Karow A, Nienhold R, et al. Clonal evolution and clinical correlates of somatic mutations in myeloproliferative neoplasms. *Blood*. 2014;123:2220-2228.
4. Nishimura M, Nagaharu K, Ikejiri M, et al. Acquisition of JAK2 V617F to CALR-mutated clones accelerates disease progression and might enhance growth capacity. *Br J Haematol*. 2021;194:e89-e92.
5. Marty C, Lacout C, Martin A, et al. Myeloproliferative neoplasm induced by constitutive expression of JAK2V617F in knock-in mice. *Blood*. 2010;116:783-787.
6. Achyutuni S, Nivarthi H, Majoros A, et al. Hematopoietic expression of a chimeric murine-human CALR oncoprotein allows the assessment of anti-CALR antibody immunotherapies in vivo. *Am J Hematol*. 2021;96:698-707.
7. Hasan S, Lacout C, Marty C, et al. JAK2V617F expression in mice amplifies early hematopoietic cells and gives them a competitive advantage that is hampered by IFN α . *Blood*. 2013;122:1464-1477.
8. Li J, Prins D, Park HJ, et al. Mutant calreticulin knockin mice develop thrombocytosis and myelofibrosis without a stem cell self-renewal advantage. *Blood*. 2018;131:649-661.

SUPPORTING INFORMATION

Additional supporting information can be found online in the Supporting Information section at the end of this article.

2.2 Chimeric antigen receptor T cell therapy for myeloproliferative neoplasms with mutated calreticulin

In this chapter, unpublished data addressing the second aim are presented. We generated CARs targeting mutCALR and tested their efficacy *in vitro* and *in vivo*.

2.2.1 Surface expression of mutCALR in different models

Surface expression of the targeted antigen is indispensable for successful CAR-T cell therapy. Therefore, we tested all model systems (Figure 7A,C and D) for stable surface expression using mutCALR-specific antibodies. FACS analysis confirmed the presentation of mutCALR on the surface of the different proposed models, i.e. CRISPR/Cas9 edited UT-7/Tpo cells, Ba/F3 cells overexpressing human MPL and mutCALR and bone marrow cells derived from transgenic Calr-del52^{fl/fl},yav-iCre mice¹⁰⁰. We further analyzed mutCALR on the cell surface of each patient samples used within this project (Figure 7B). We quantified the number of mutCALR molecules on the surface of CALR mutated UT-7/Tpo cells and patient CD34⁺ cells using QIFIKIT (Agilent). The antigen density on the cell surface of patient cells (200-2000 molecules/cell) was comparable to those of UT-7/Tpo cells ($CALR^{mut/mut}$: 6400 molecules/cell, $CALR^{wt/mut}$: 1300 molecules per cell), confirming the validity of this model system.

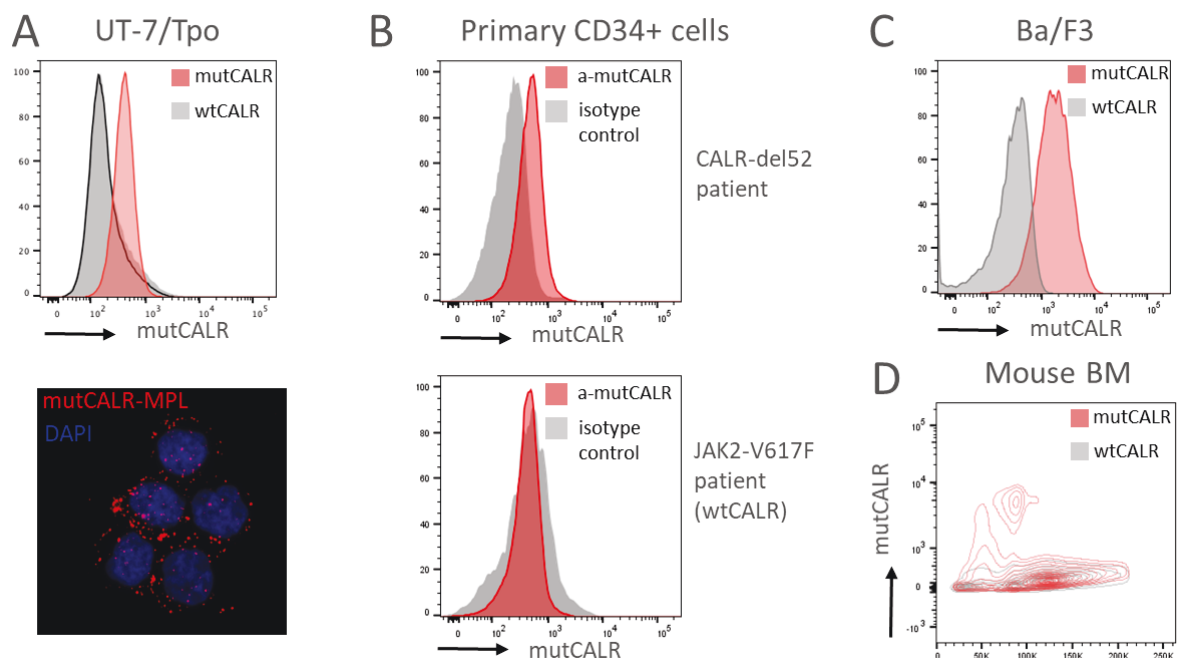


Figure 7: Target cells present mutCALR on their surface at different densities. FACS staining was performed using mutCALR-specific antibodies (A-D). A) FACS staining (top) and proximity ligation assay (bottom) of CRISPR-Cas9 edited mutCALR UT-7/Tpo cells. Proximity ligation assay was performed using mutCALR and MPL specific antibodies. Complexes were analyzed using a confocal microscope, 40x objective, and are shown here in red. Nuclei were stained with DAPI (blue). B) Example FACS plots of primary CD34⁺ cells isolated from a mutCALR

(CALR-del52) or wtCALR (JAK2-V617F) patient. C) FACS staining of a Ba/F3 mutCALR overexpression cell line. D) FACS analysis of total bone marrow (BM) of a transgenic CALR-del52 fl/fl, vav1-cre mouse.

2.2.2 Generation and selection of α -mutCALR-CARs

A small library of mutCALR specific monoclonal antibodies (mAbs) generated from immunized mice or rabbits by hybridoma fusion or phage display, respectively, was provided by MyeloPro Diagnostics and Research GmbH. Those antibodies served as an analytical tool for the detection of mutCALR and most importantly constituted the basis for generation of mutCALR-specific CARs. Two second generation α -CD19-CARs containing a 4-1BB (BBz-CAR) or CD28 (28z-CAR) costimulatory domain were kindly provided by the group of Dr. Christoph Bock. Those CARs were used as a positive control and served as a basis for α -mutCALR-CAR generation. In total, fourteen different rabbit scFvs and one mouse scFv were incorporated into the 28z backbone in a lentiviral vector (Figure 8A). As a first line of testing all CARs were expressed in Jurkat cells by lentiviral transduction. In Jurkat CAR-T cells, I tested antigen binding by staining with a FITC-labelled 22 amino acid peptide, which mimics the C-terminus of mutCALR. Except for one clone, all tested CARs showed proper antigen binding (Figure 8B). Next, to assess the binding capacity to mutCALR in its native conformation at the cell surface and to test CAR functionality I performed an arrayed activation screen using CD69 expression as a readout (Figure 8C). From this initial screen, we could identify CARs which are well expressed, able to bind mutCALR and trigger activation upon recognition of the cognate antigen on the cell surface.

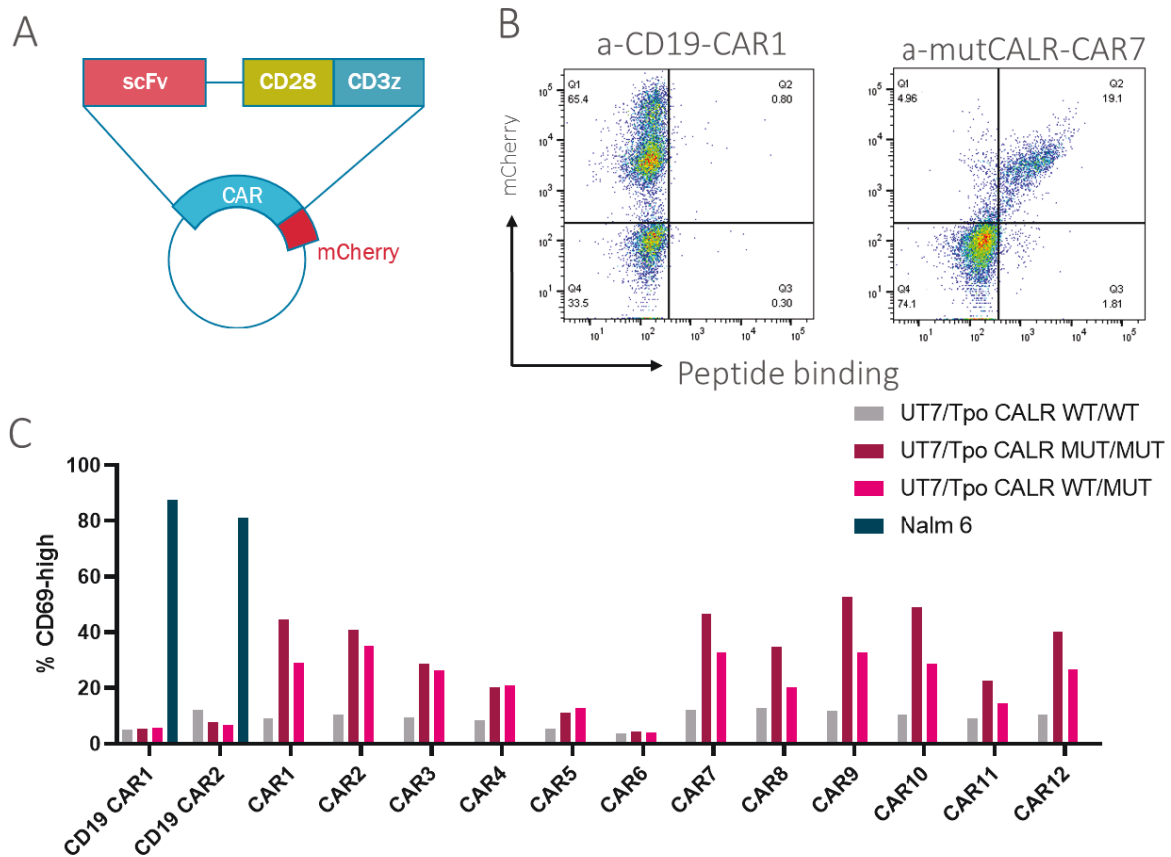


Figure 8: Jurkat CAR-T cells recognize mutCALR. A) Schematic drawing of the CAR design. An scFv was linked to a standard second generation 28z backbone. As a proxy for CAR expression mCherry was linked to the CAR via a P2A site. B) After transduction, unsorted Jurkat CAR-T cells were tested for their ability to bind an antigen-mimicking peptide (at 413 nM). Example FACS plots for an irrelevant (α -CD19) and one mutCALR-specific CAR (CAR 7) are shown here. C) Jurkat activation screen. Sorted Jurkat CAR-T cells were co-cultured with target cells for 16 hours. wtCALR, homozygous or heterozygous mutant UT-7/Tpo cells were used to test CALR-specific CARs. Nalm 6 cells were used as positive control for targeting with established α -CD19 CARs with a BBz (CD19 CAR1) or 28z (CD19 CAR2) backbone. The percentage of CD69-high cells (compared to Jurkat CAR-T cells without target cells) was determined using flow cytometry. Here only one assay is shown, CARs that were produced at a later time point were tested similarly but are not depicted in this graph.

2.2.3 Testing of selected CARs in primary T cells

Selected CARs were further used to transduce primary T cells and tested in cytotoxicity assays. Here, I want to highlight the results of the lead CAR (α -mutCALR-CAR 7) candidate (Figure 9). Initially the CAR was generated using a 28z backbone. However, I also produced the BBz version of this CAR (α -mutCALR-CAR 7.2). UT-7/Tpo cells expressing mutCALR in a heterozygous or homozygous manner were selectively killed by anti-mutCALR CAR-T cells whereas wild type CALR expressing cells (parental UT-7/Tpo or Nalm 6) were not killed (Figure 9 A,B). Control anti-CD19 CAR-T cells only targeted Nalm6 cells that express CD19 (Figure 9A). Further, activation assays showed that CAR-T cells are specifically activated by mutCALR

expressing cells. Both IFN- γ secretion as well as CD25 expression were increased in CAR-T cells after co-culture with mutCALR UT-7/Tpo cells (Figure 9 C,D).

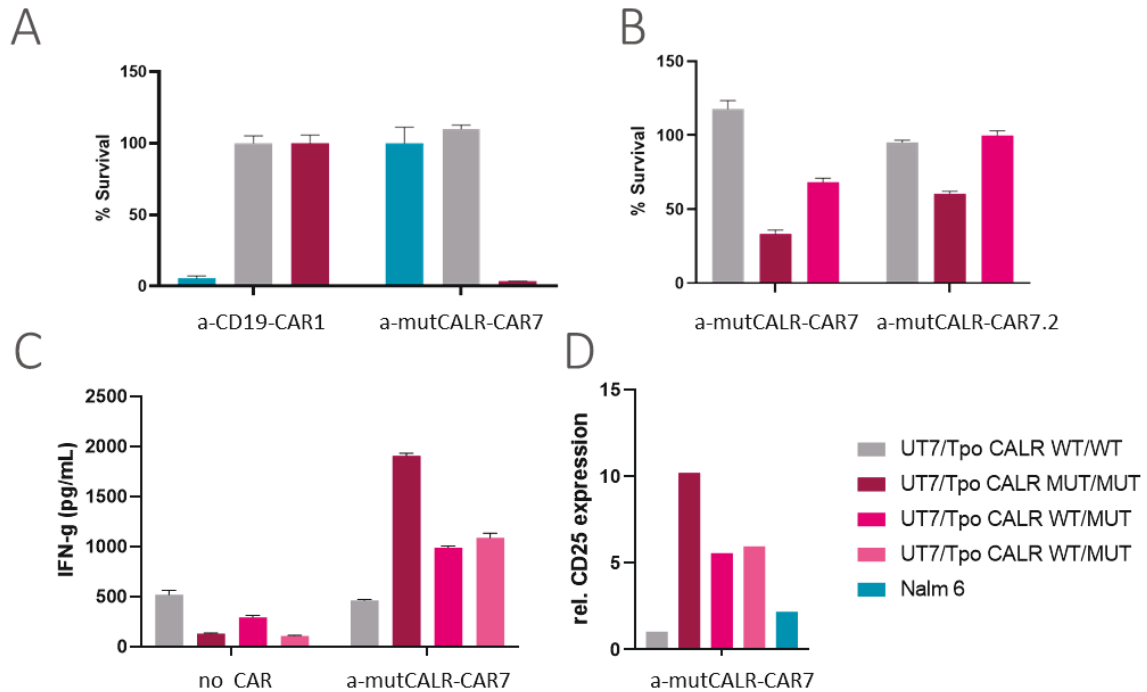


Figure 9: Primary T cells specifically recognize CALR mutated UT-7/Tpo target cells. A and B) Luciferase cytotoxicity assays were performed at an E:T of 10:1. Luminescence was measured after 24 hours. Here the % survival compared to the irrelevant CAR (a-CD19-CAR) is shown. A and B depict two independent experiments in different T cell donors. C) Cytokine secretion assay. CAR-T cells were co-cultured with UT-7/Tpo cells at an E:T of 5:1 for 72 hours. IFN-g in the supernatant was measured by ELISA. Two different heterozygous mutCALR clones were used (two separate bars in pink). D) Activation assay. CAR-T cells were co-cultured with UT-7/Tpo cells at an E:T of 1:1 for 48 hours. CD25 expression was measured by FACS. Here the relative increase in MFI compared to Mock-T cells with the same UT-7/Tpo cells is shown. Two different heterozygous mutCALR clones were used (two separate bars in pink).

Next, we used primary CD34⁺ cells from patients that carried the CALR-del52 or CALR-ins5 mutation for the cytotoxicity assay (Figure 10). The clone CAR7 that showed best killing of UT-7/Tpo cells also delivered cytotoxicity towards CALR mutated CD34⁺ cells. This data for the first time demonstrated that anti-CALR CAR-T cells can direct cytotoxicity to CALR mutated myeloid progenitor cells and validates the potential of CAR-T cells for targeting primary malignant cells.

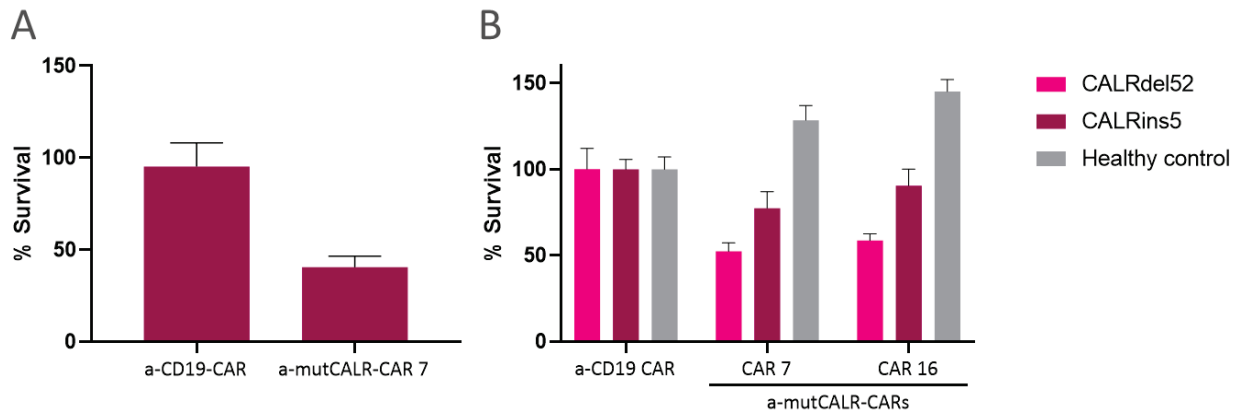


Figure 10: CAR-T cells can eliminate primary CD34+ patient cells. A and B) Primary CD34+ cells were cultured in STEMspan II SFM medium and transduced with a lentiviral luciferase construct three days before the assay. Luciferase cytotoxicity assays were performed at an E:T of 10:1. Luminescence was measured after 24 hours. Here the % survival compared to the irrelevant CAR (a-CD19-CAR) is shown. A and B depict two independent experiments in different T cell donors.

2.2.4 The influence of perturbations *in vitro*

Secreted mutCALR might interfere with immunotherapies directed against mutCALR covering the paratope and blocking CAR-T cell functionality or by triggering target-cell independent activation. To dissect the effect of soluble mutCALR on primary CAR-T cells we added soluble mutCALR from different sources to cytotoxicity assays: We added supernatant collected from UT-7 Tpo cells, recombinantly produced CALRins5 or patient plasma to the cytotoxicity assays. UT-7 Tpo cells with a homozygous CALR mutation secreted the antigen at a concentration of 5 ng/mL. The recombinant CALRins5 was added at a concentration of 200 ng/mL, thereby exceeding the plasma levels of CALR mutated patients. By adding patient plasma we assessed the combinatorial effect of secreted antigen and other potentially inhibiting factors present in patient plasma, such as immunomodulatory cytokines. By using cell culture supernatants, as well as patient plasma we ensured the conservation of the natural conformation of secreted mutCALR. We did not observe any difference when comparing cytotoxicity and activation of CAR-T cells incubated with supernatant from either WT or mutant UT-7 Tpo cells (Figure 11 A, B). Likewise, adding recombinant CALRins5 at a high concentration did not lead to unspecific activation (Figure 11 B). Neither the addition of patient serum nor recombinant CALRins5 did suppress CAR-T cell functionality or lead to unspecific killing (Figure 11 C). The combined results suggest that secreted CALR up to 200 ng/mL does not influence CAR-T cell functionality.

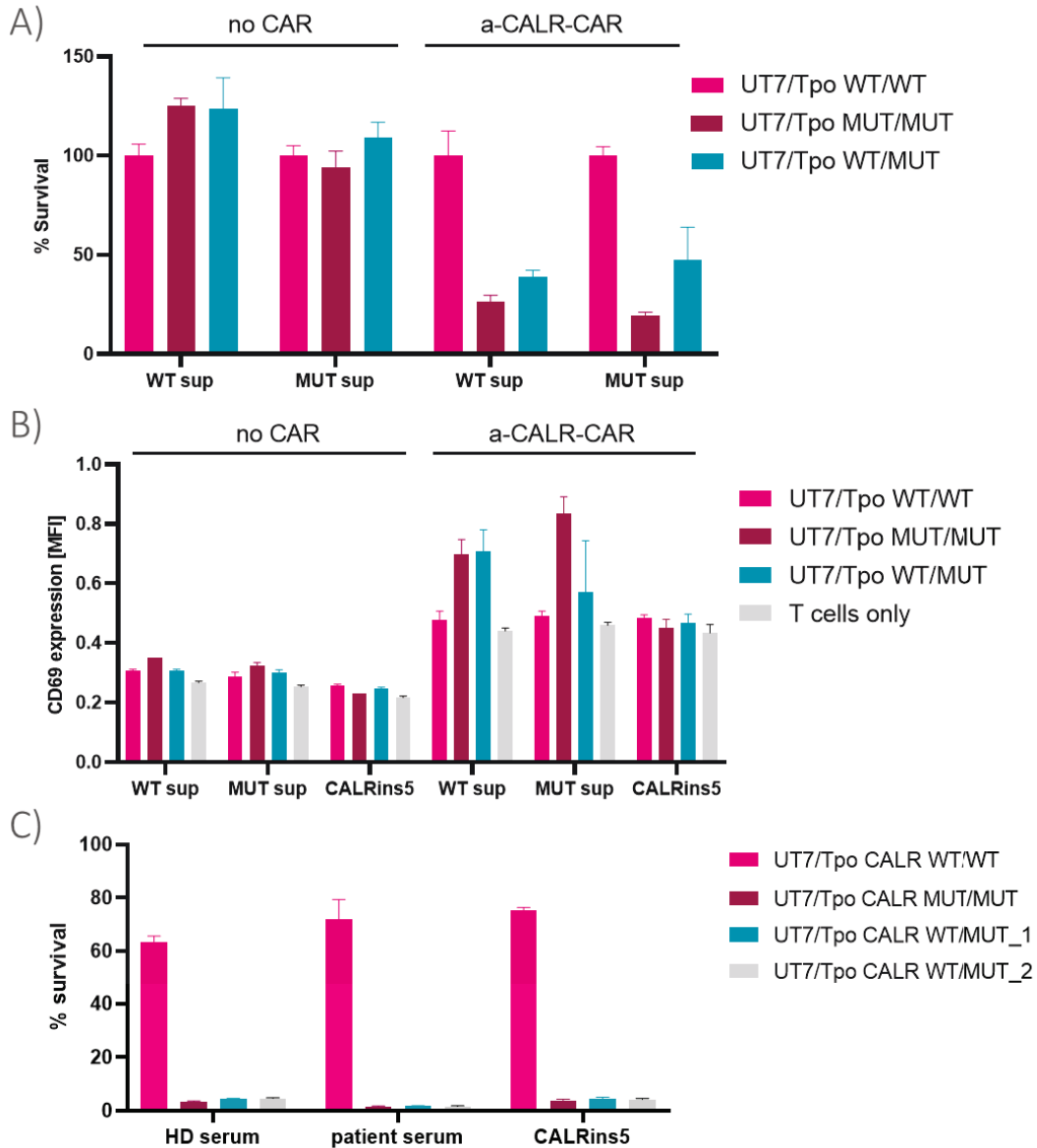


Figure 11: Secreted mut-CALR does not influence CAR-T cell functionality. Luciferase cytotoxicity assays were performed at an E:T of 10:1. Luminescence was measured after 24 hours. Here the % survival compared to the Mock-T cells is shown. A) Cytotoxicity assay using UT-7 Tpo cells and supernatant (sup) collected from the same cells. B) CD69 expression corresponding to part A. In addition, CD69 expression was measured after incubation with CALRins5 at 200 ng/mL. C) Cytotoxicity assay using UT-7 Tpo cells and healthy donor (HD) serum or patient serum at 50% or CALRins5 at 200 ng/mL.

2.2.5 Generation of murine a-mutCALR CAR-T cells

In order to establish a fully murine a-mutCALR-CAR, we cloned an scFv derived from a mouse a-mutCALR mAb into a murine 28z CAR backbone in a retroviral vector developed by James Kochenderfer²²⁸. Splenic T cells isolated from a C57BL/6 wt mouse were transduced with the CAR and expression was verified by FACS (Figure 12 A). On day seven after isolation, T cells were co-cultured with either mutCALR expressing target BaF/3 cells or CALR wild type BaF/3

cells. Murine anti-mutCALR CAR-T cells selectively killed target cells expressing mutCALR (Figure 12 B). This poses the foundation for *in vivo* experiments using immunocompetent mouse models.

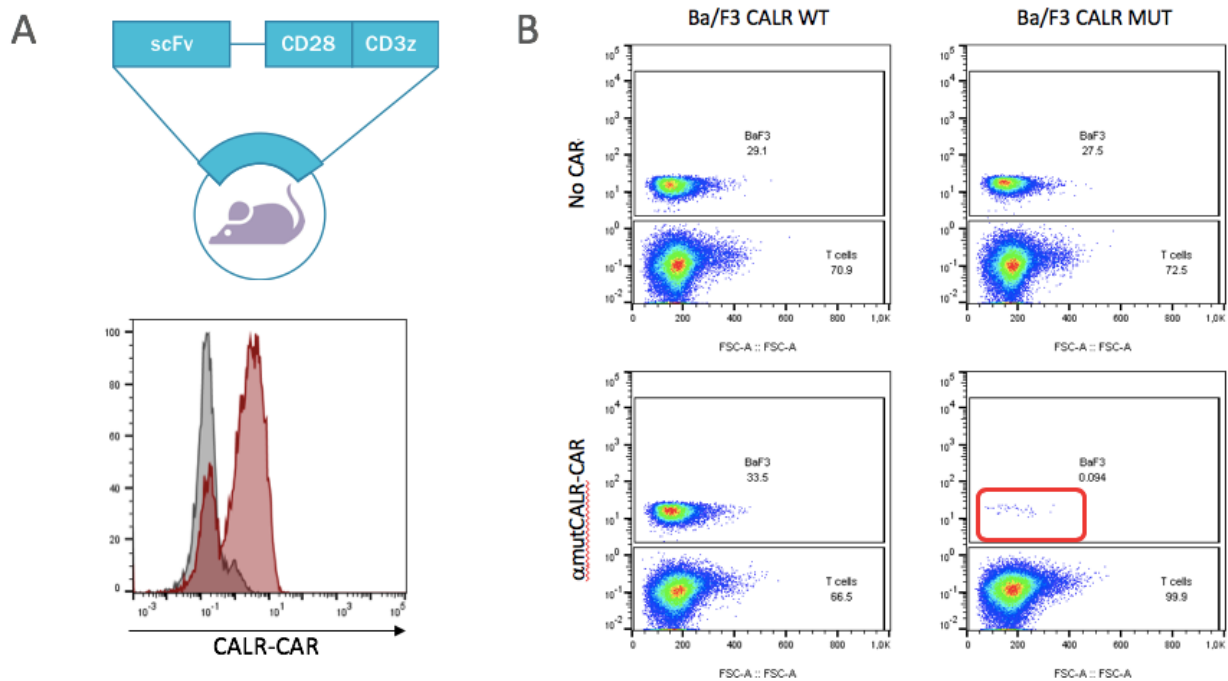


Figure 12: Primary mouse CAR-T cells effectively eliminate mutCALR expressing target cells. A) CAR clone consisting of a scFv derived from a mouse monoclonal Ab specific for mutCALR was fused with a CAR CD28-CD3z backbone and retrovirally transduced to CD3⁺ mouse T cells. FITC-labeled antigen FACS staining of CAR-T cells (red) is shown on the lower panel together with unstained cells (gray). B) Cytotoxicity assays were performed by co-culturing CAR-T cells with GFP-positive BaF/3 target cells (WT or expressing CALR-del52 mutant). Red box indicates the selective killing of mutCALR expressing target cells. Effector:target ratio of 5:1, 24 hours co-culture.

2.2.6 *Ex vivo* targeting of primary murine Calr-del52 mutated cells

As we aimed at using a competitive bone marrow transplantation (BMT) model for testing of murine CAR-T cells *in vivo*, we first tested the recognition of primary cells expressing mutCALR by murine CAR-T cells *ex vivo*. We isolated lineage negative (Lin⁻) cells from Calrdel52 *f/f* vav-iCre mice and simulated the competitive BMT *ex vivo* (Figure 2). CD45.1 WT and CD45.2 mutant lin⁻ cells were mixed in a 50:50 ratio (MUT/WT) and CAR-T cells or Mock-T cells were added at an E:T ratio of 10:1 (Figure 13 A). As a control, an equal mixture was prepared with WT cells only (CD45.1 and CD45.2; WT/WT). CAR-T cells led to decrease of CD45.2 cells in the MUT/WT mixture but not in the WT/WT control (Figure 13 B-C). Moreover, CAR-T cells showed increased expression of activation markers in the presence of mutant cells (Figure 13 D-E).

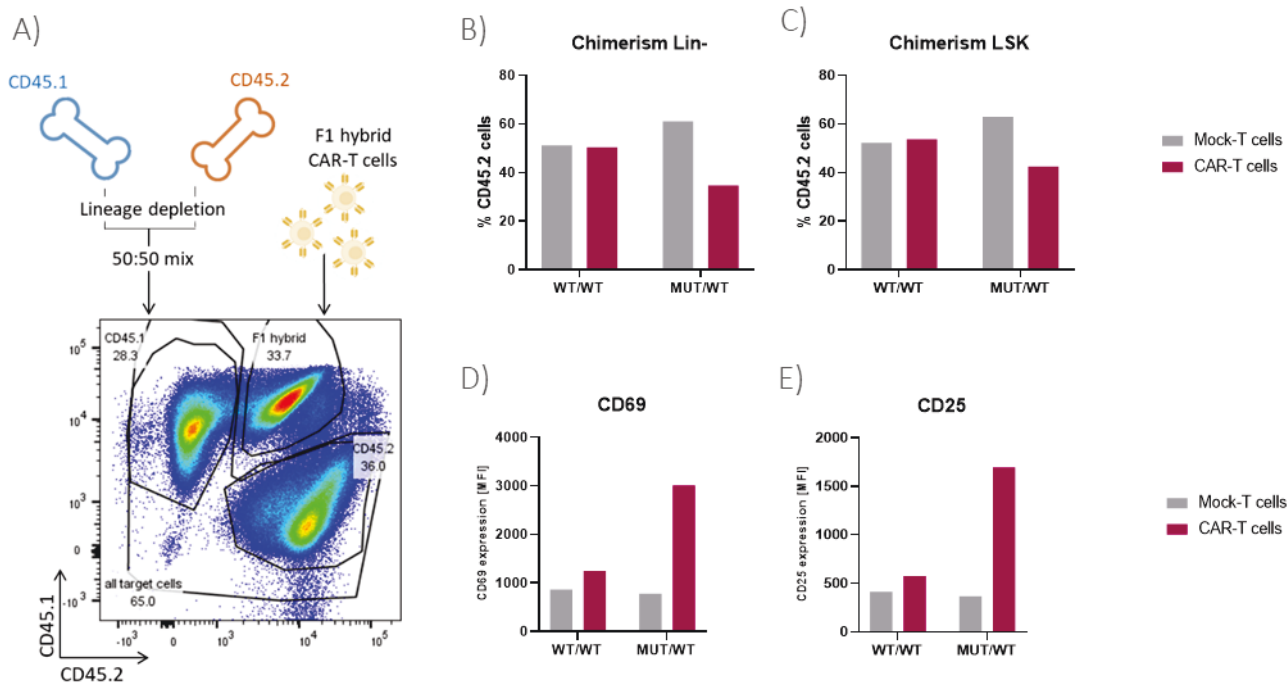


Figure 13: Murine anti-mutCALR CAR-T cells recognize and specifically target mutant cells ex vivo A) Setup of the ex vivo treatment. Lin⁻ cells of different origin (CD45.1 WT, CD45.2 WT or CD45. MUT) were isolated from the BM and mixed in a 50:50 ratio. Cytotoxicity assays were performed in STEMspan SFEM II with human CD34⁺ supplement for 48 hours at an E:T of 10:1. B and C) Quantification of CD45.2 cells after incubation for 48 hours. D and E) Expression of activation markers (CD69 – D and CD25 – E) after incubation for 48 hours.

Presentation of mutCALR on the cell surface is dependent on MPL. Thus, the actual targetable population are only cells which express MPL, such as HSCs, a minute fraction of Lin⁻ and LSK cells. Those cells are so rare that one can hardly perform an assay using a pure MPL-positive fraction. However, transplantation is a very sensitive readout for the presence of HSCs. Therefore, we transplanted the *ex-vivo* treated mixture of WT and mutant cells into lethally irradiated CD45.1 mice and evaluated the chimerism as well as the phenotypic changes. In mice which received the Mock-T cell treated graft, WT and mutant cells engrafted properly. The myeloid chimerism (% of mutant derived cells) in PB was 60 % at week four post transplantation and reached almost 100 % until the end of the experiment. On the contrary, mice which received CAR-T cell treated cells almost exclusively harbored WT derived myeloid cells in PB (Figure 14 A). The minute fraction of CD45.2 cells present at the beginning depleted overtime. The origin of this population was most likely short term repopulating cells, which are part of the Lin⁻ cells but not targetable by our CAR-T cells due to the lack of MPL expression. Further, only mice transplanted with the Mock-T cell conditioned cells, developed severe thrombocytosis indicative of myeloproliferative disease (Figure 14 B). We observed the mice for 22 weeks to test whether mutant stem cells were completely depleted. Should any residual mutant stem cells engraft, they would outgrow over time. However, this was not the case. Few

mutant derived cells were only detected in the lymphoid lineage in the spleen (Figure 14 C). Notably, long-term hematopoietic stem cells were exclusively of WT origin in the CAR-T cell pre-treated group, while in the Mock-T cell conditioned group, all LT-HSCs were mutant (Figure 14 D). Thus, murine CAR-T cells specifically eradicated mutant HSCs and spared WT HSCs. After transplantation of the *ex-vivo* treated mixture, complete and durable remission was observed in the CAR-T cell pre-treated group.

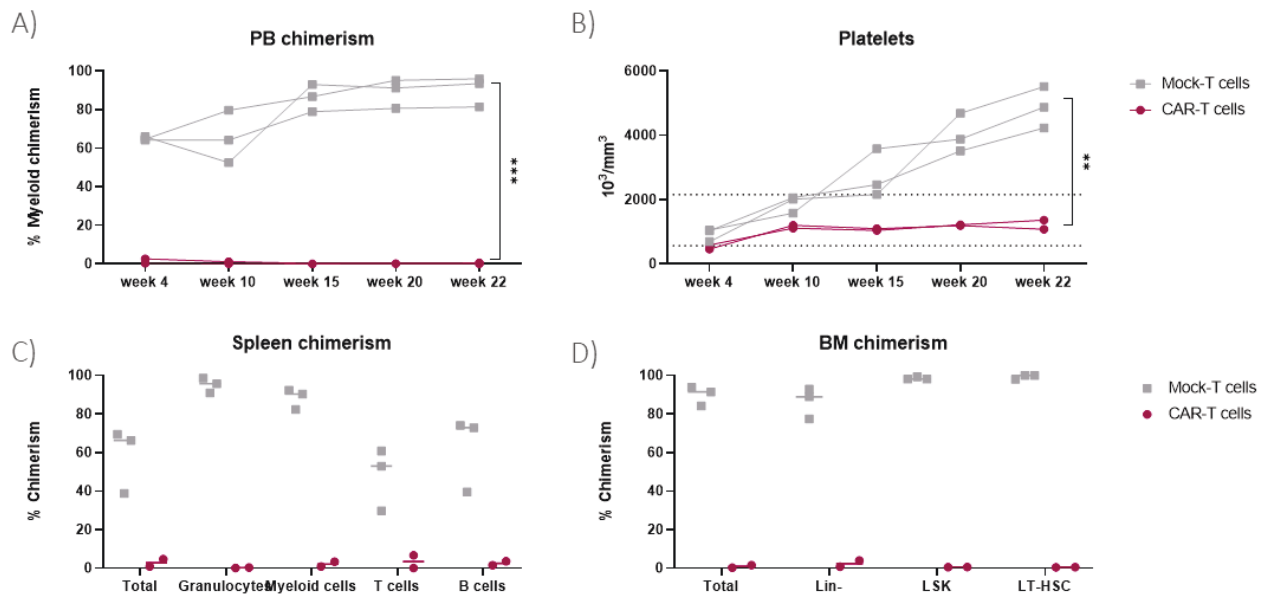


Figure 14: Transplantation after *ex vivo* treatment leads to complete and durable remission. A) Myeloid chimerism in PB over time. B) Platelet (PLT) count over time. C) Chimerism in different populations of the spleen 22 weeks (endpoint) post transplantation. D) Chimerism in different populations of the BM 22 weeks (endpoint) post transplantation. Lin⁻ - lineage-negative, LSK – Lin⁻ Sca-1⁺ c-Kit⁺, LT-HSC - Lin⁻ c-Kit⁺ Flt-3⁻ CD48⁻ CD150⁺. Statistical analysis was performed in Graphpad using an unpaired t test. ** P ≤ 0.01, *** P ≤ 0.001

2.2.7 *In vivo* treatment of chimeric mice

Next, we sought out to test the CAR-T cell treatment in the competitive BMT model *in vivo*. As lymphodepleting conditioning was reported to be essential for CAR-T cell treatment of immunocompetent mice, we first chose an early intervention model, where CAR-T cells were injected one week post transplantation, a timepoint at which lymphocytes are still depleted from the lethal irradiation²²⁹. In the first experiment, we administered two doses of CAR-T cells and monitored the chimerism in PB (Figure 15 A). We saw a decrease in myeloid chimerism in PB in two of five CAR-T cell treated mice (Figure 15 B). Those mice were also the only animals with normal platelet counts and had the lowest chimerism in BM (Figure 15 C, D). One mouse in the control group also showed a low chimerism. However this mouse had the lowest

chimerism from the beginning, which stayed stable over time. Since only two mice in the CAR-T cell group showed a decrease in chimerism, the results were inconclusive. Thus we repeated the experiment, but in the second run CAR-T cells did not show any effect (data not shown). We also tested two different time points of CAR-T cell injection, co-injection with Lin⁻ cells at the day of transplantation and treatment of established chimeric mice with lymphodepleting conditioning (data not shown). However, the adoptively transferred CAR-T cells did not lead to a decrease in chimerism in any of those attempts.

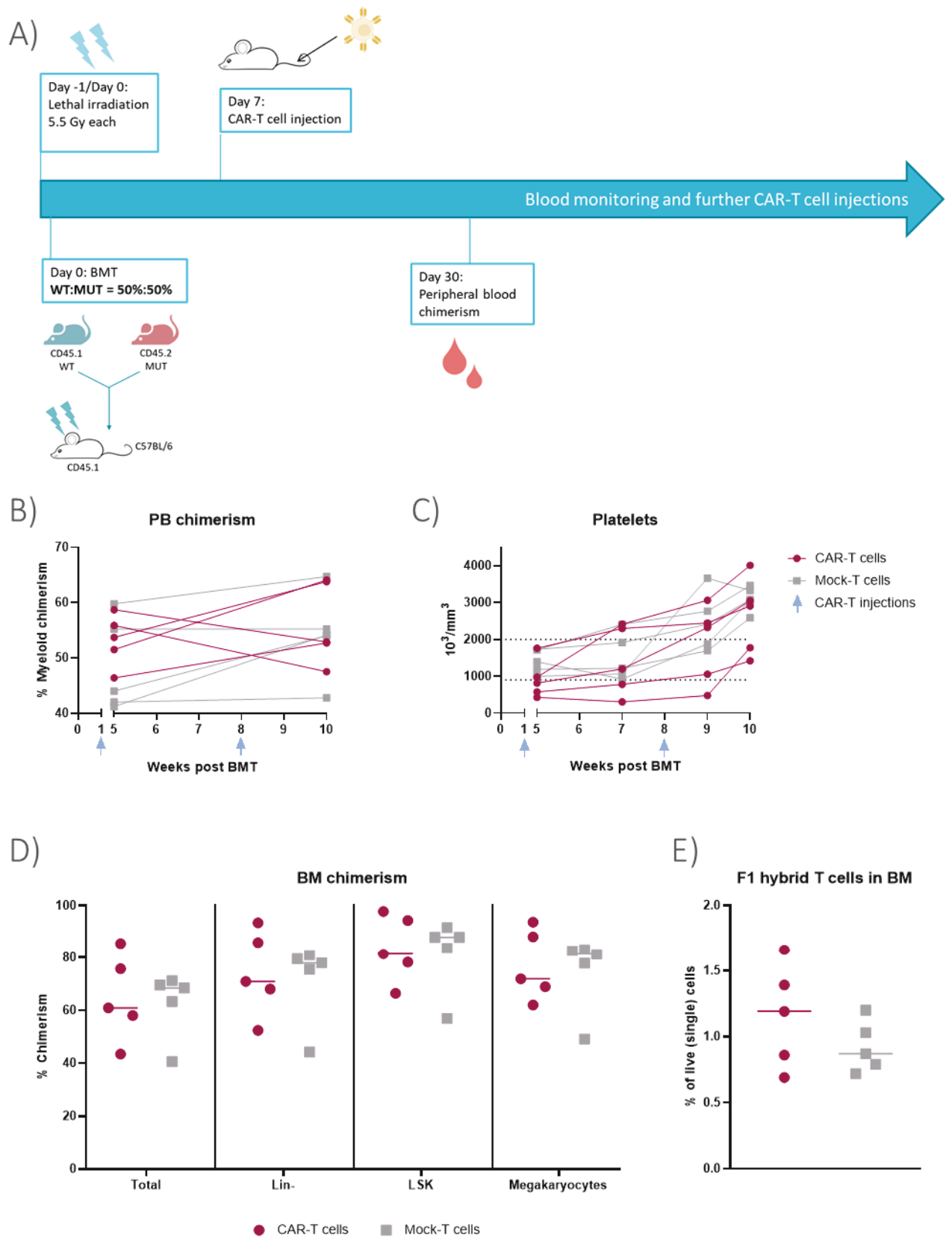


Figure 15: *In vivo* CAR-T cell treatment of chimeric mice shows limited efficacy. A) Experimental setup. B) Myeloid chimerism in PB five (first blood analysis) and ten (endpoint) weeks post transplantation (BMT). C) Platelet count over time. D) Chimerism in different populations of the bone marrow ten weeks post transplantation.

2.2.8 Obstacles for *in vivo* efficacy

Due to a lack of efficacy of the anti-mutCALR CAR-T cells *in vivo*, we sought out to quality control the CAR-T cell preparation by using an established murine a-CD19 CAR. We injected CD19 CAR-T cells that were generated in the same manner as the a-mutCALR CAR-T cells into C57BL/6 mice after sublethal irradiation as a lymphodepleting step. These cells were fully functional and led to complete ablation of B cells (data not shown). We repeated the anti-CD19 CAR-T cell treatment in *Calr* mutated mice with homozygous (Hom) and heterozygous (Het) *Calr* mutation. In both cases, a-CD19 CAR T cells led to eradication of B cells in blood, spleen and bone marrow. Thereby, we can exclude a general T cell suppression in CALR mutated mice.

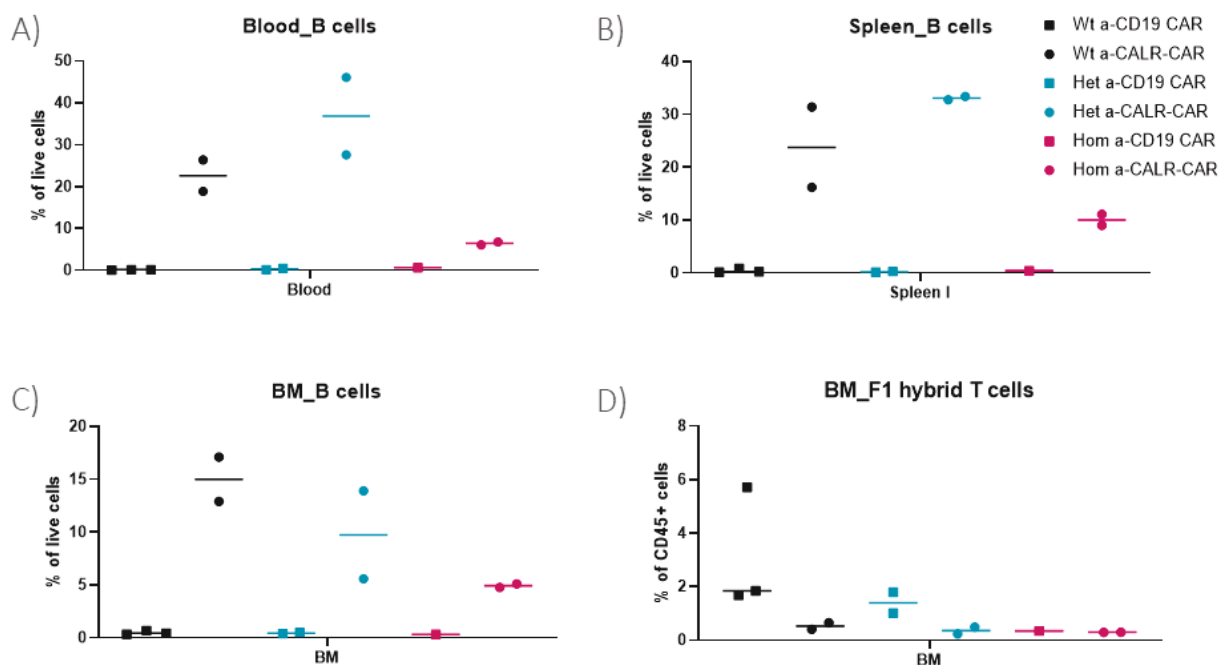


Figure 16: CD19-specific CAR-T cells are fully functional in Wt as well as *Calr* mutated mice. Mice were conditioned by nonmyeloablative irradiation (5 Gy) the day before CAR-T cell injection. 5 Mio CAR-T cells were injected with a CAR-positivity of around 20%. Animals were sacrificed two weeks post T cell injection. Depletion of B cells was shown in PB (A), spleen (B) and BM (C). D) Analysis of CAR-T cell infiltration.

While CD19-specific CAR-T cells were functional in all genotypes, we concluded that limited efficacy is rather caused by cell-contact-specific or antigen-specific factors than a general immune suppression. PD-L1 expression is STAT-driven and thus can be induced by oncogenic signaling downstream of MPN driver mutations. We measured PD-L1 expression in total bone marrow and megakaryocytes, as an example for MPL-expressing cells in KI mice and transplanted mice. PD-L1 expression of WT, heterozygous and homozygous KI mice was

comparable with a slight trend of increased expression in homozygous Calr mutant mice (Figure 17 A). Transplanted mice, however, showed increased PD-L1 expression compared to a non-transplanted WT control at four weeks post transplant (Figure 17 B). Thus, the cytokine storm seems to be a strong driver of PD-L1 expression in the BMT model, while the Calr mutation only had a minimum effect on PD-L1 surface levels.

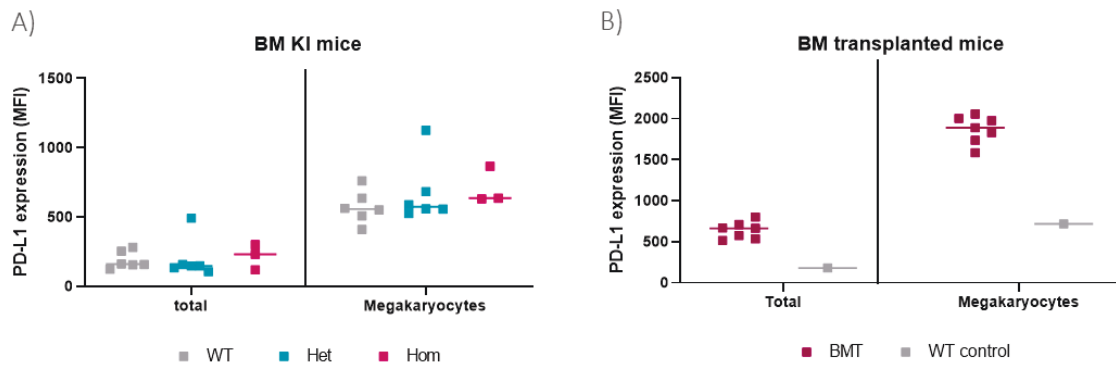


Figure 17: PD-L1 expression is cell type specific and is increased after BMT. PD-L1 expression was analyzed by FACS in Calrdel52 KI mice (A) and mice four weeks post BMT (B).

We further tested analyzed the expression of exhaustion markers after adoptive transfer of CAR-T cells in these two systems (KI model and BMT model). In the KI mice, we observed increased expression of PD-1, TIM-3 and LAG-3 in CALR-specific CAR-T cells compared to CD19-specific CAR-T cells in the spleen of homozygous mice (Figure 18 A-C). Interestingly, this was not the case in WT or heterozygous mice. In the BM, anti-CALR CAR T cells also showed a tendency towards increased expression of exhaustion markers when injected into homozygous mice compared to WT or heterozygous mice (Figure 18 D-E). Notably, expression of PD-1 and LAG-3 was higher in CD19-specific compared to CALR-specific cells and expression of exhaustion markers was not influenced by the recipients' genotype in a-CD19 CAR-T cells. CAR-T cells co-injected during BMT showed increased expression of PD-1 and LAG-3 in spleen and BM compared to Mock T cells (Figure 19 A-F). We further observed that adoptively transferred T cells (F1 hybrid) showed a higher expression of exhaustion markers compared to T cells generated from the BM graft (CD45.2) irrespective of the CAR expression.

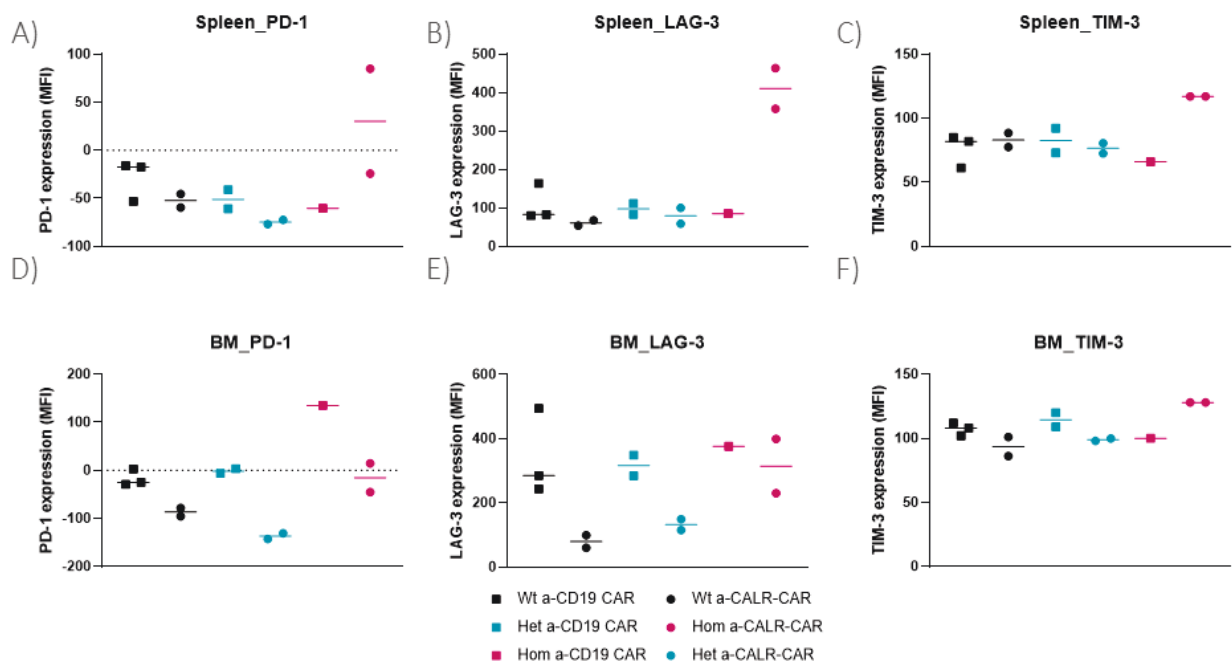


Figure 18: Expression of exhaustion markers in a-mutCALR CAR-T cells depends on the recipients' genotype. Expression of early (PD-1), mid (LAG-3) and late (TIM-3) activation markers was analyzed by FACS two weeks post CAR-T cell injection. T cells were isolated from spleen (A-C) or BM (D-F) and only adoptively transferred T cells (F1-hybrid) were included in the analysis. CD19- and mutCALR-specific CAR-T cells were tested in WT, Calrdel52 *f/+* vav-iCre (het) and Calrdel52 *f/f* vav-iCre (hom) mice.

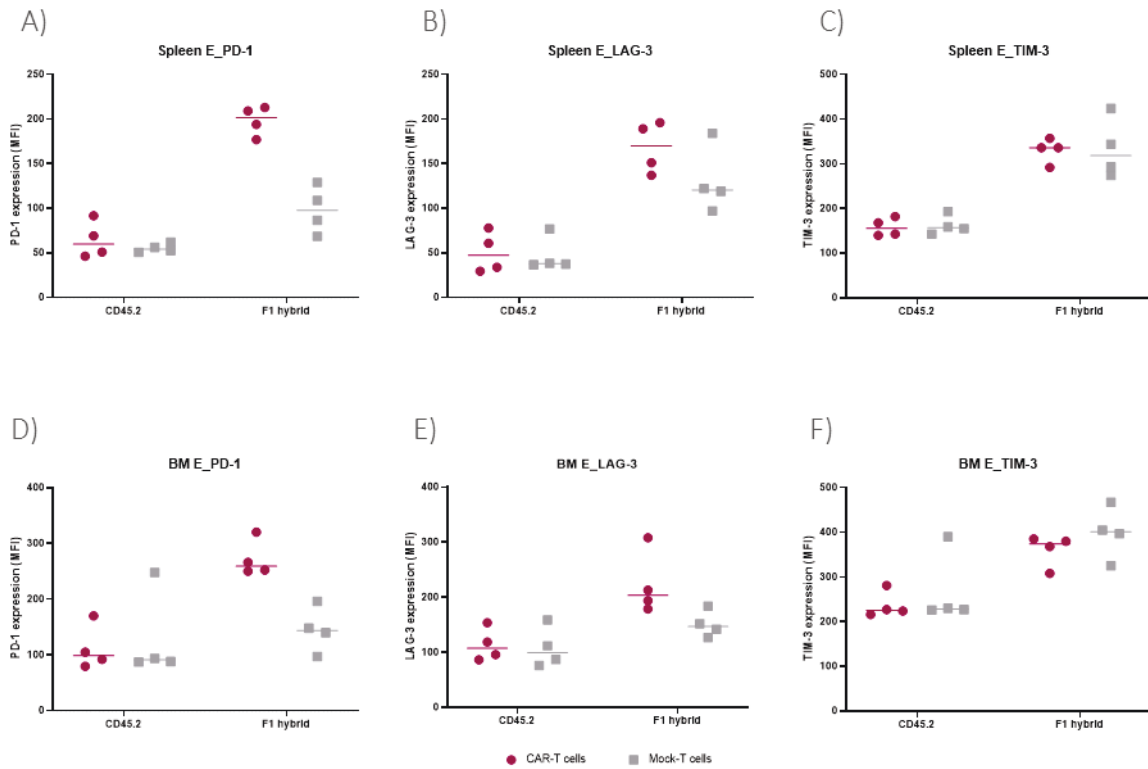


Figure 19: Expression of exhaustion markers is increased in CAR-T cells compared to Mock-T cells. Expression of early (PD-1), mid (LAG-3) and late (TIM-3) activation markers was analyzed by FACS four weeks post CAR-T cell co-injection with the stem cell graft. T cells were isolated from spleen (A-C) or BM (D-F). Adoptively transferred T cells (F1 hybrid) with (CAR-T cells) or without CAR (Mock-T cells) were compared to endogenous T cells (CD45.2) derived from the BM graft in these mice.

Next, we wanted to assess the potential of secreted Calr to block CARs and test the influence of depleting the soluble protein by antibody pre-treatment. We compared no pre-treatment, antibody alone and antibody plus sublethal irradiation. Irradiation substantially increased the percentage of CAR-T cells within PB, spleen and BM due to its toxic effect on dividing cells (Figure 20 B). We observed a 3-fold increase of “free CAR”, which we determined by staining with a peptide mimicking the mutant part of CALR in spleen and BM of mice that received pre-treatment. CAR-T cells in the spleen and especially in the BM of pre-treated mice also showed higher CD25 expression, indicative of increased activation (Figure 20 C). However, CD69 expression was comparable in conditioned and unconditioned mice (Figure 20 D).

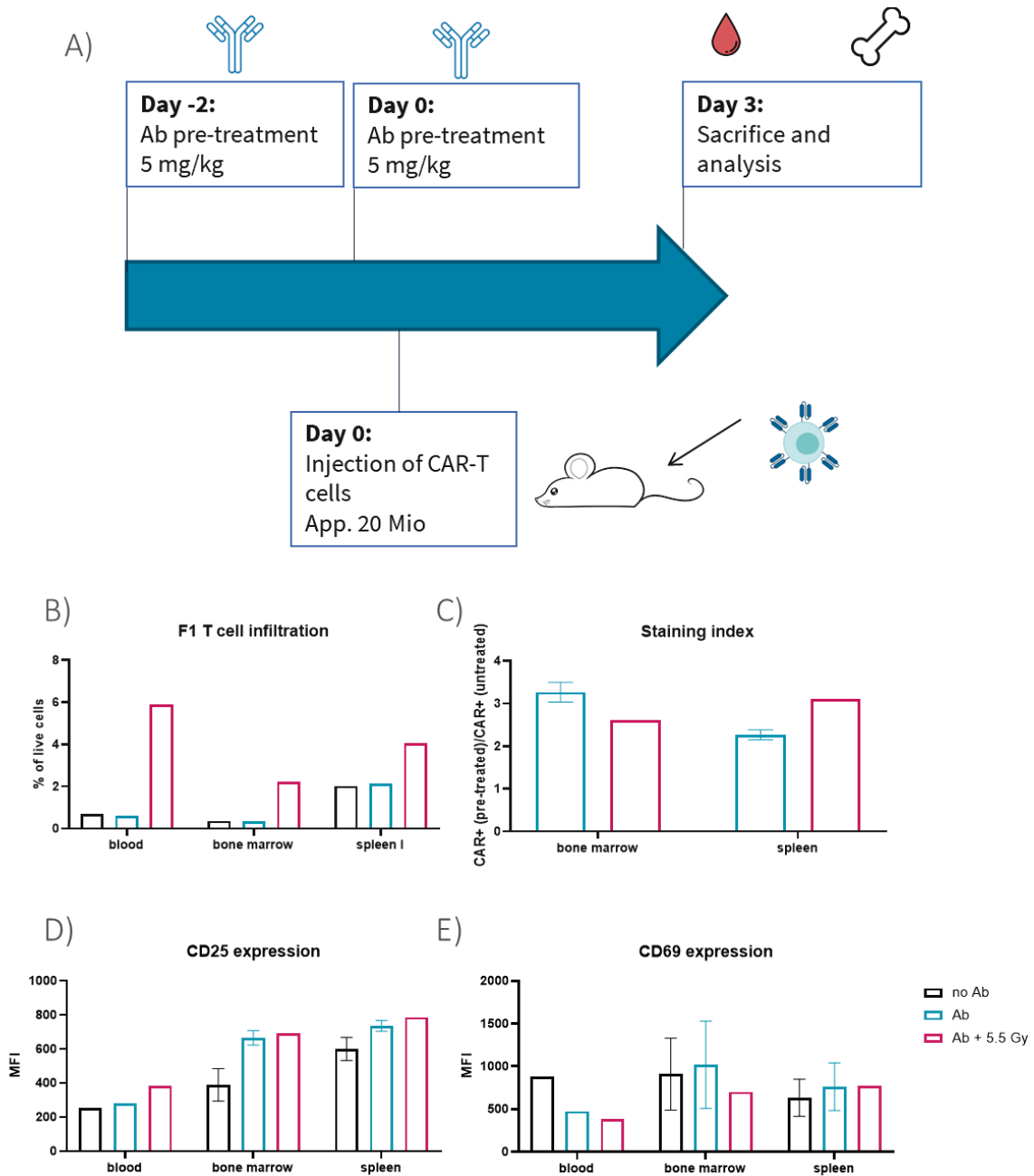


Figure 20: Antibody pre-treatment leads to increased availability of the CAR epitope. A) Schematic overview of the experimental setup. Mice were pre-treated with two antibody doses and a high number of CAR-T cells was injected. The isolated CAR-T cells were analyzed three days post injection. B) Quantification of the F1-hybrid T cell infiltration in blood, BM and spleen. C) The staining index was determined as the ratio of % CAR+ cells in with pre-treated to % CAR+ cells without pre-treatment. D-E) Expression of activation markers (CD25 – D, CD69 – E) by CAR-T cells.

3. DISCUSSION

While Dameshek categorized different hematological malignancies as myeloproliferative disorders based on a common stimulus as early as in 1951, the mechanism underlying these disorders was yet unknown. Since then, substantial knowledge has been generated elucidating the oncogenic mechanism of MPNs. The discoveries of the JAK2, MPL and CALR driver mutations between 2005 and 2013 were major milestones in MPN research, which led to better comprehension of the pathophysiology and provided invaluable diagnostic relevance. While these driver mutations were thought to be mutually exclusive, co-occurrence of two or more driver mutations was observed in a subset of MPN patients. In this thesis we present the first mouse model for Calr/Jak2 co-mutated MPN in which we determined the influence of double mutation on a systemic as well as the stem cell level. Apart from their role as diagnostic tools, driver mutations and their downstream effects represent MPN-specific points of attack for treatment. Whereas JAK2 and MPL mutations are point mutations resulting in a single amino acid substitution, frameshift mutations in the CALR gene generate a large stretch of novel amino acid sequence. In addition, the presence of mutCALR at the cell surface enables distinction of mutant from healthy cells by this distinct surface molecule. Thus, the second part of this thesis was focused on therapeutic targeting of mutCALR. We generated CARs targeting mutCALR and explored their therapeutic potential for MPN *in vitro* and *in vivo*.

3.1 Co-expression of Jak2 and Calr oncogenes

In the past, MPN driver mutations were defined as mutually exclusive^{43,44}. However, mutational analysis of large patient cohorts and improvement of the detection methods led to numerous reports about patients harboring two or even three concomitant driver mutations^{42,45-67}. In “Co-expression of mutated Jak2 and Calr enhances myeloproliferative phenotype in mice without loss of stem cell fitness”, published in American Journal of Hematology in 2022, we introduced a novel mouse model, in which Jak2-V617F and Calr-del52 are co-expressed in hematopoietic tissues by using the vav-iCre system. With this model we investigated the influence of Jak2/Calr double mutation on disease phenotype as well as HSC functionality.

In two studies by Usseglio and colleagues and Mansier et al. co-occurrence of JAK2V617F and MPL or CALR mutations was associated with increased thrombocytosis compared to single mutated MPN, while no difference in the frequency of thrombotic events or disease progression was observed. Lim et al. on the other hand reported an increased risk for thrombotic events in JAK2/CALR double mutated versus single mutated patients. Albeit partially contradicting, these reports indicate that acquisition of two driver mutations might

aggravate the disease. However, patient cohorts included different combinations of mutations and the allelic burden of each mutation was highly variable. Further, it is unknown whether these patients carried the co-occurring driver mutations in the same clone or in two independent clones. Therefore, double mutant MPN could be divided in subgroups, which might differ in disease phenotype and risk profile. Nishimura et al. recently published a case report of an ET patient who acquired a *JAK2V617F* mutation into a *CALRdel52* mutated clone 18 years post diagnosis. To our knowledge, this is the only report with proof for co-expression of both mutations in a single clone. While this patient progressed to post-ET MF after acquisition of the secondary mutation, there is no sizable patient cohort available to systematically evaluate the effect of *JAK2/CALR* double mutation on disease outcome. Therefore, we set out to investigate the phenotype of *Jak2/Calr* double mutated MPN in our mouse model.

We compared disease phenotype of *Jak2-V617F/Calr-del52* double mutated mice to single mutated mice and included WT mice as a control. Double-positive mice developed a severely aggravated disease compared to single mutated animals characterized by higher PLT counts, increased leukocytosis, and more pronounced splenomegaly. We hypothesize that increased PB counts are a result of synergistic receptor activation. This was also reflected in the gene expression profile of double mutated LSK cells. Gene set enrichment analysis showed increased expression of genes associated with IL-2/STAT-5 and IL-6/JAK/STAT3 signaling in double mutated compared to *Calr* single mutated mice. Further, STAT5-induced genes, such as *Cish* and *Socs2*, were upregulated in double compared to single mutated mice. Mutant *Calr* and *Jak2* both act on MPL, which drives HSC proliferation and megakaryopoiesis. The combination of both mutations seems to enhance MPL downstream signaling, which explains the increased frequency of megakaryocytes in the BM and consecutive thrombocytosis. Leukocytosis was mainly attributed to increased granulocyte and monocyte counts. MutCALR has been shown to induce activation of the G-CSFR albeit at a much weaker extent compared to MPL^{29,30}. In γ 2a cells mutCALR specifically induced constitutive STAT5 activation of MPL and G-CSFR but not of the EPOR²⁹. Presumably because G-CSFR only contains one extracellular domain as opposed to MPL with two, G-CSFR activation by mutant *Calr* is much weaker and does not render cells cytokine independent. However, *Jak2* is known to act on all three homodimeric type I cytokine receptors, MPL, EPOR and G-CSFR^{5,6,230,231}. Therefore, we believe that there is a synergistic effect of G-CSFR activation by *Calr* and *Jak2*. Erythrocytosis is driven by the *Jak2* mutation in single mutated as well as double mutated mice without an additive effect of mutCALR, thus explaining similar hematocrit and Hb values observed in both lines. The observation time was limited by the premature death of *Jak2/Calr* double mutated mice. Interestingly, additive effects of both mutations were visible in 8- to 9-week old mice, a time point at which heterozygous *Calr-del52* animals were comparable to WT mice apart from

very mild thrombocytosis. While *CALR* mutations are associated with higher platelet counts than *JAK2* mutations in patients, this is not the case for the *Jak2* and *Calr* single mutated mice²³². Heterozygous *Calr-del52* animals show a relatively mild phenotype with isolated thrombocytosis in aged mice¹⁰⁰. This might be caused by the weaker interaction of the chimeric *Calr-del52* protein with the murine MPL. The young age might also explain why we did not observe signs of myelofibrosis in our experiments.

Notably, the aggravated disease phenotype culminated in significantly reduced survival. Double positive as well as *Jak2* single mutated mice died spontaneously. Given the excessive expansion of thrombocytes and erythrocytes, early mortality is most likely associated with thromboembolic events. In addition, double mutated mice developed significant leukocytosis, which was also associated with increased thrombotic risk²³³. We observed an approximately 4-fold increase of granulocytes in *Jak2/Calr* mice compared to WT or *Calr* single mutated mice. Wolach et al., reported that granulocytes of *Jak2V617F* mice were prone to neutrophil extracellular net formation, which promoted thrombosis²³⁴. The hematocrit of double mutant mice was around 80-90%, which decreases blood flow. Together with high thrombocyte counts (app. $5000 \times 10^3/\mu\text{L}$) and leukocytosis with increased granulocytes this leads to an extremely high risk for thrombotic events. These have also been reported as cause of lethality in *Jak2V617F* mouse models, i.e. cardiac thrombosis in homozygous mice and gangrenous bowel, and are the leading cause of death in *JAK2V617F*-positive patients²³⁵⁻²³⁷.

The mere detection of two mutations from bulk cells does not provide information about the distribution of these genetic aberrations. It has been shown that acquisition of an additional driver or passenger mutation can lead to separate clones expanding side by side. Interestingly, patients with a low *JAK2V617F* burden frequently have an additional *JAK2* exon12, *CALR* or *MPL* mutation^{48,55-57,61,63,68}. In two studies, Mansier et al. also observed a lower *CALR* mutational burden in double mutated patients compared to those with a single *CALR* mutation^{56,63}. This might be explained by competition of two separate clones. Only two groups assessed clonality of patients harboring multiple mutations by performing colony formation assays and analysis of individual colonies or by single cell sequencing^{42,72}. Both publications revealed that *JAK2* and *CALR* mutations were acquired in independent clones, thus indicating that *JAK2* and *CALR* mutations might be mutually exclusive on the single cell level. Mutual exclusivity can be caused by a synthetic lethal interaction. Such synthetic lethality has been described in splicing factor mutated myeloid malignancies showing that *Sf3b1* and *Srsf2* double mutant HSCs have reduced fitness *in vivo* providing explanation why such patients are never observed²³⁸. Recently, the first report of a patient who acquired a *JAK2V617F* mutation in addition to a *CALR* type 1 mutation in the same clone, was released²³⁹. Although this publication showed that *JAK2V617F* and *CALRdel52* mutations can co-exist in a single clone, the effect on HSC

fitness remained elusive. While both mutations were detected in HSCs as well as myeloid progenitors, HSCs had the lowest VAF. Synthetic lethality can cause cell death or decreased competitive fitness over time in HSCs and therefore the best indicator for HSC fitness is their repopulation capacity in BMT experiments.

We compared the outgrowth of HSCs from double or single mutated mice against WT cells in competitive primary and secondary BMT. Double mutant stem cells engrafted well and induced a disease phenotype comparable to the KI mice. The chimerism (% of mutant cells) of myeloid cells in PB increased over time in all groups with the most pronounced expansion in the double mutated group and weakest expansion in the *Calr* single mutated group. Outgrowth on the HSCs level in primary and secondary transplants showed a similar pattern. Two and three out of four animals of the *Jak2* or *Jak2/Calr* group, respectively, reached full chimerism in the secondary transplant, which indicates that double mutated stem cells do not have reduced fitness. Competitive advantage of HSCs from *Calr*-del52 or *Jak2*-V617F single mutated knock-in mice tested in previous publications is comparable with our results. Mullaly et al. identified the LSK compartment as the MPN-initiating population and reported a minimal increase of *Jak2*V617F mutant stem cells over time after competitive transplantation of LSK cells¹³⁷. Hasan and colleagues, however, showed that *Jak2*-V617F positive cells expand and reach almost full chimerism 18 weeks post transplantation⁹⁶. Our group as well as Li, Prins and colleagues showed that HSCs of mice with a heterozygous *Calr*del52 mutation properly engraft lethally irradiated recipients in primary and secondary transplantation experiments. However, these cells did not show a significant proliferative advantage compared to the WT competitor^{100,101}. Likewise, we observed increased outgrowth of double mutated and *Jak2* mutated over *Calr* mutated cells.

Our data suggest that the co-expression of *JAK2* and *CALR* mutations lead to a compound phenotype with increased myelopoiesis, massive thrombocytosis and reduced survival. This is in line with recent case reports, where acquisition of a secondary driver mutation into a previously mutated clone was associated with a high-risk phenotype, disease progression or unresponsiveness to treatment^{65,66,73}. These studies delivered proof that two driver mutations can co-exist within the same clone and our study further ruled out that double mutation negatively affects HSC fitness. Based on our study and the available case reports, we hypothesize that secondary mutations might be an indicator for increased risk. Yet, they are rarely detected as driver mutations are usually screened in a sequential manner starting with the most frequent, the *JAK2*V617F mutation, and *JAK2*V617F⁺ patients are often not screened for additional mutations. Further, the studies by Nishimura et al. and Partouche and colleagues showed that a second driver mutation can arise years or decades after initial diagnosis. This hinders identification of double mutated patients, since driver mutations are usually not re-

analyzed during follow up. While the co-occurrence of *JAK2* and *CALR* mutations is frequently reported, the clonality is rarely analyzed. Formal proof for the co-expression of two mutations in one clone can only be provided by genotyping single colonies or single cell sequencing. However, these methods are time and cost-intensive and thus rarely performed. Thus, the true frequency of patients carrying two driver mutations in the same clone remains unknown.

3.2 CAR-T cells targeting mutCALR

With the main causative mutations being elucidated, MPNs belong to the genetically solved malignancies. Hence, now the time has come to find a specific therapy. Currently, there is a lack of disease modifying therapies and the only curative treatment is allogeneic HSCT, which is used for severe cases of myelofibrosis²⁴⁰. Classification by comprehensive genomic characterization allows for risk stratification in MPN²⁴¹. The most severe phenotype and worst prognosis is associated with MF with a ten-year risk of leukemic transformation of 20 %. Post-MPN AML is virtually untreatable with poor survival rates in the range of a few months²⁴². Therefore, patients with high risk for leukemic transformation or fibrosis urgently need targeted treatment.

There is strong evidence that immunotherapy might be an effective line of treatment in MPN patients harboring *CALR* mutations^{145–147,243}. With *CALR* being a neoantigen that is present at the cell surface and truly tumor specific, it is a promising target for antibody-based therapies or CAR-T cell therapy. Taking into account that studies failed to isolate HLA I-restricted neoantigen presentation and to isolate reactive CD8⁺ T lymphocytes from patients, one major advantage of antibodies or CARs is independence of MHC I. Downregulation of MHC class I molecules is a common way of tumor immune evasion, and their assembly might be impaired by mutation of *CALR*. Compared to conventional antibodies, CARs require a lower antigen density and showed functionality in a range of a few 100 molecules per cell¹⁶¹. This is an important aspect to consider when targeting mutCALR as the antigen surface density is limited by presentation via MPL, a protein that is weakly expressed. Further, *CALR* is partially secreted, which might generate a sink depleting the free antibody, whereas CARs can be re-expressed by T cells^{244,245}. Moreover, their CAR-T cell safety and efficacy can be improved by further genetic engineering, e.g. PD-1 knock-out for resistance to PD-L1-dependent suppression; expression of dominant negative TGFbRII for resistance to TGFb-dependent suppression; GM-CSF knock-out to eliminate the trigger of cytokine release syndrome^{213,246,247}. Therefore, we hypothesized that the use of CAR-T cells is a suitable mode of action for the treatment of *CALR* mutated MPN and developed the first mutCALR-specific CARs.

As mutCALR is presented at the cell surface in complex with MPL, epitope accessibility is sterically limited. Therefore, it is crucial to test binding to the antigen in its conformation on

target cells. Further, binding capacities of antibodies do not directly correlate to the suitability of their scFv in CARs. Therefore, we chose to screen multiple scFvs by using Jurkat CAR-T cells as effectors and UT7-Tpo CALR^{mut/mut} cells as targets to identify functional CARs from the library. The Jurkat cell line was derived from leukemic human T lymphocytes and has been extensively used to study T cell receptor signaling and screen CAR-T cells^{248–251}. In Jurkat cells, engagement of a CAR with its target antigen leads to activation, which can be assessed by CD69 expression. Using a cell line, allowed us to transform a very homogeneous cell population with the library leading to comparability of activation by different CAR molecules. Based on this initial screen, we could verify the proper expression and antigen binding of the scFv by staining with a peptide mimicking the mutant tail of mutCALR and by measuring CAR functionality in regard to T cell activation.

In co-culture assays with primary T cells, we could show that human anti-mutCALR CAR-T cells specifically lyse mutCALR expressing cells *in vitro*. Both UT7/Tpo as well as patient-derived CD34+ cells were recognized. We could achieve eradication of UT7/Tpo cells with minimum residual cells within 24 hours, while in co-culture assays with CD34+ cells, we achieved a reduction of about 50%. We did not analyze the composition of the remaining cell population. Yet, we hypothesize that the high percentage might be caused by the presence of WT cells and/or MPL-negative cells in the initial CD34+ cell mass. Due to the low expression of MPL, MPL-positive and negative cells are hard to distinguish by FACS. Thus, we plan to increase the sensitivity of the cytotoxicity assay for primary human CD34+ cells by measuring the VAF pre- and post CAR-T cell addition. Experiments were repeated with several T cell donors, including patient-derived T cells (data not shown). CAR-T cells generated from CALR mutated patients did not show any signs of reduced functionality. Thus, we generated a sensitive and specific receptor targeting mutCALR. Cytotoxicity towards primary CD34+ cells and functionality of patient-derived CAR T cells suggest that autologous CAR-T cell therapy is a potential line of treatment of CALR mutated MPN.

While *in vitro* experiments were performed under optimal media conditions, certain factors present in patient plasma might influence CAR-T cell functionality *in vivo*. For example, it was reported that the cytokine profile of MPN patients is altered compared to healthy individuals²⁵². Further, secreted CALR might bind to CARs, which could block their paratope and thus result in decreased activity, or lead to unspecific activation. Therefore, we performed experiments with cell culture supernatants, patient plasma and recombinantly produced mutCALR. In patients carrying CALR type 1 or type 2 mutations, mean serum mutCALR levels are 27 to 30 ng/ml (range 0-70 ng/ml)²⁵³. To see a maximum effect, we supplemented recombinant CALRins5 at a high concentration (200 ng/mL) exceeding the maximum levels seen in patients. We further performed assays with cell culture supernatant and patient plasma. While in these

conditions, mutCALR levels were in the low range (2-10 ng/mL), this ensured the native conformation of soluble CALR. By using patient plasma, we could further evaluate the influence of other factors present in patient plasma. We did not observe activation of anti-mutCALR CAR-T cells when incubated with recombinant mutCALR alone or parental UT7/Tpo cells with the recombinant protein at a high concentration (200 ng/ml). This suggests that the antigen is not "dressing up" the wild type cells. An important aspect for *in vivo* administration of anti-mutCALR CAR-T cells, indicating that secreted CALR does not induce off-target killing. We further excluded that the patient cytokine profile has an inhibitory effect of CAR-T cells by supplementing plasma from different donors. With these assays we could show, that soluble factors occurring in a patients' blood do not seem to hinder CAR-T cell functionality. Yet, *in vitro* experiments cannot recapitulate conditions at the target cell site. While patient plasma is a good indicator as a first approach, local concentrations might be different.

In vitro experiments are the first step in testing different therapies. However, the complex interplay of CAR-T cells, tumor cells and surrounding factors can only be recapitulated in *in vivo* models. The most commonly used models to provide proof-of-concept for CAR-T cell functionality are cell line-based xenograft models in NOD/SCID/IL2Rgc-KO (NSG) mice²⁵⁴. NSG mice are severely immunocompromised with a complete lack of innate immunity (B and T cells) and NK cells. They enable engraftment of a wide spectrum of human cell lines and allow testing of human CAR-T cells. Engraftment of patient-derived cells (patient derived xenograft, PDX) results in a model with a more physiologically relevant target cell population. While the feasibility of using human T cells against human target cells is a significant advantage of immunodeficient models, lack of immunity also brings its limitations. In these models, the crosstalk of immune cells cannot be addressed due to the lack of certain immune cells and cross-species incompatibility of cellular and soluble factors. These may influence T cell trafficking and persistence. In addition, human stromal cells and thus the tumor microenvironment is not well represented. Immunocompetent murine mouse models, such as KI models, allow assessment of CAR-T cells in the presence of a physiological environment. Their drawback, however, is the need for a fully murine system including murine effector and target cells. We established several models for preclinical testing of anti-mutCALR CAR-T cells. UT7/Tpo cells robustly engraft NSG mice after intravenous as well as subcutaneous injection and thus a UT7/Tpo xenograft models could be used for testing of human CAR-T cells. However, our human candidate CAR anti-mutCALR CAR 7, although specific for mutCALR in the human system, showed cross-reactivity with murine cells. Blast search of the targeted epitope revealed an overlap with antigens ubiquitous in murine bone marrow. Thus, application of CAR-T cells expressing anti-mutCALR CAR 7 would lead to on-target/off-tumor toxicity and this CAR is therefore not suitable for *in vivo* testing in murine models. Therefore, we focused on generating fully murine CAR-T cells, which allows testing in an

immunocompetent model, which enables to evaluate CAR-T cells in presence of the MPN immunophenotype. We performed competitive BMT with a mixture of WT and *Calr* mutated BM cells. This model mimicks many features of patients, including presence of WT and mutant cells. Target cells reside in their physiological environment, i.e. the bone marrow, and thus effects of the bone marrow niche including penetrance, soluble factors and influence of stromal cells can be assessed. Mutant HSCs differentiate and give rise to mature blood cells *in vivo*, thus all differentiation states and cell populations and the physiological MPL expression pattern are represented with the actual target population embedded in a mass of non-target cells.

Murine anti-mutCALR CAR-T cells completely eradicate Ba/F3 cells. We observed increased functionality of these cells compared to human cells, which might be caused by several factors. First, antigen expression in Ba/F3 cells is higher than in UT-7 or human CD34+ cells as this target cell line was generated by overexpression of human MPL and mutCALR. Second, CAR expression is higher in murine T cells, likely owing to the fact that these cells were generated by retroviral transduction as opposed to human T cells, which were lentivirally transduced. Third, the murine CAR includes a different antigen-recognition domain as the human CAR. Interestingly, while the same scFv incorporated in a human second-generation CAR backbone did lead to specific cytotoxicity towards CALR mutated UT7/Tpo cells, expansion of these CAR T cells was significantly reduced compared to anti-mutCALR CAR 7. Fine tuning of the human CAR with the murine scFv by varying the hinge region and linker length, the costimulatory domain also did not result in improved CAR-T cell expansion.

Murine anti-mutCALR CAR-T cells recognize primary mutant cells *ex vivo* and enable the depletion of mutant cells from a mixture of progenitor cells. While we primarily used transplantation as a sensitive readout for the presence of HSCs, this “cleanup” step might bring a therapeutic opportunity: There is no other therapy for severe cases of myelofibrosis than allogeneic stem cell transplantation. *Ex vivo* treatment might allow the depletion of mutant cells from a patient’s own bone marrow, thereby allowing autologous transplantation. The major benefit of this setup is that it substantially decreases the risk of HSCT, where severe side effects occur due to graft-versus-host disease.

Notably, we saw a partial response in one of the animal experiments, in which we treated chimeric animals. In two mice the myeloid chimerism in PB decreased. These two mice also had the lowest BM chimerism and highest number of infiltrating lymphocytes. However, it is unclear what caused the differences in the CAR-T cell group. It has been reported that insertional mutagenesis caused by random integration of the CAR sequence after viral transduction might influence the T cell phenotype. Fraietta et al., for example, reported that knock out of *Tet2* by random virus integration led to improved T cell proliferation. The CAR-T cell response in this patient was dominated by this clone. The clonality of a T cell pool can be

analyzed by TCR screening. In case T cells isolated from the two responder these mice are highly clonal, integration site analysis could be interesting and might help to understand the different responses of individual mice in the CAR-T cell group.

Although we could validate murine CAR-T cells *ex vivo*, we observed no or very limited efficacy in the BMT model *in vivo* with only two partial responses. We aimed at optimizing CAR-T cell dosing and injection time point. Lymphodepleting conditioning has been shown to be an essential step for proper engraftment and expansion of adoptively transferred T cells^{255–258}. Apart from anti-tumor activity such chemotherapeutic regimens can induce a favorable environment for CAR-T cells. The depletion of B, T and NK cells lead to the elimination of homeostatic cytokine sinks and increase the availability of cytokines, like IL-2, IL-7 and IL-15 for transferred T cells. Further, lymphodepletion can decrease the number of immune suppressive cells, such as Tregs and MDSCs. Kochenderfer et al., and Jacoby and colleagues also showed that lymphodepletion is vital for the activity of murine anti-CD19 CAR-T cells in immunocompetent mouse models^{228,259}. Therefore, we initially chose an early time after bone marrow transplantation, to ensure ongoing lymphodepletion at the time of CAR-T cell injection. We further tested co-injection of CAR-T cells together with the stem cell graft, as well as treatment of established chimeras after lymphodepleting sublethal irradiation (5 Gy). Yet, we only observed a partial response in one single experiment. Therefore, we set out to determine factors hindering CAR-T cell efficacy in this model.

To assess the overall effect of the MPN immunophenotype on CAR-T cell functionality we tested established CD19 CAR-T cells in heterozygous and homozygous *Calrdel52* *vav-iCre* KI mice. CD19 CAR-T cells completely eradicated B cells in blood, spleen and bone marrow in all mice. Especially the complete lack of bone marrow-resident B cells in *Calr* mutated mice indicated that the bone marrow of these mice is accessible for CAR-T cells and that the niche does not prevent T cell functionality. These results validated our CAR-T cell preparation protocol and showed that CAR-T cells can penetrate the bone marrow. As CD19-CAR T cells were functional in all genotypes, we could exclude a general immunosuppressive effect in these mice. However, the comparison of anti-CD19 and anti-mutCALR is limited by several factors. CD19 is a highly expressed antigen and thus signaling strength of the anti-CD19 and anti-mutCALR CAR are different. Increased signaling by the CD19 CAR might overcome inhibitory signals, which pose an obstacle for anti-mutCALR CARs. Although both CARs target hematopoietic cells, the target cells differ in their abundance, distribution and cell-intrinsic properties. Therefore, we aimed at expressing the murine CD19 exodomain in *Calrdel52* KI murine HSCs to generate a model in which CD19 CARs target the same population. However, low transduction efficiency and the lack of competitive advantage provided by the CD19 construct resulted in insufficient CD19-labelled HSCs.

Trafficking of T cells to the target cell site is of utmost importance for the efficacy of CAR-T cells. Detection of F1- T cells in the BM and the control experiment with CD19 CAR-T cells indicated that CAR-T cells reach the BM in WT as well as *Calr* mutated mice. However, the number of CAR-T cells in the BM was low (1-2 %). Despite the fact that this low number was enough to deplete B cells in the BM, further engineering of T cells by expressing BM-specific chemokine receptors or intrafemoral injection might improve the results.

T cell exhaustion is a factor frequently limiting T cell responses towards tumors. Exhaustion of CAR-T cells can be caused by several factors including tonic signaling due to suboptimal CAR-T cell design, chronic exposure to the antigen, soluble factors and increased expression of inhibitory receptors on target cells. It has been reported that PD-1 and CTLA-4 are promising candidates for checkpoint inhibition in MPN²⁶⁰. We assessed the expression of PD-L1 in the bone marrow of chimeric and non-transplanted mice and found a significant difference in these models. While non-transplanted homozygous *Calr* mutated mice only showed a trend towards increased PD-L1 expression. PD-L1 was 2-4-fold more expressed in total bone marrow and megakaryocytes in chimeric mice four weeks post transplantation. This indicates that the cytokine storm associated with transplantation might influence PD-L1 expression and thus early injection of CAR-T cells might complicate CAR-T cell efficacy. We do not know the dynamics of this PD-L1 expression and it would be interesting to analyze, whether this PD-L1 induction decays over time. Further, we yet have to test CTLA-4 expression in our model. We evaluated the exhaustion status of CAR-T cells by FACS analysis, i.e. staining for the early, mid and late exhaustion markers PD-1, LAG-3 and TIM-3, at the end of the experiment. FACS analysis showed increased expression of exhaustion markers by anti-mutCALR CAR-T cells in dependence of the recipient's genotype. CAR-T cells isolated from spleens of homozygous but not heterozygous or WT KI mice showed increased expression of PD-1, LAG-3 and TIM-3 compared to CD19-specific CAR-T cells. Expression of these markers in the BM was also highest in cells isolated from homozygous KI mice, but did not exceed the expression of these markers in anti-CD19 CAR-T cells. Notably, expression of exhaustion markers in CD19-specific CAR-T cells was not influenced by the recipient's genotype. The fact that the expression of exhaustion markers did not differ between the two different CAR constructs in WT and heterozygous mice, indicates that exhaustion might be triggered in an antigen-dependent manner and further shows that tonic signaling due to suboptimal CAR design is unlikely. The observed differences between the genotypes and CAR constructs could either be explained by increased expression of inhibitory receptors by mutCALR-expressing cells compared to B cells or by the effect of secreted CALR. The analysis of co-injected CAR-T cells at the time of BMT, also showed increased expression of PD-L1 and LAG-3 compared to Mock T cells. Interestingly, adoptively transferred T cells showed increased expression of PD-1, LAG-3 and TIM-3 compared to endogenously produced T cells. This might indicate an

exhausted phenotype caused by T cell culture conditions or the cytokine storm caused by lethal irradiation and BMT. Nevertheless, CD19-specific CAR-T cells generated under the same conditions were functional. Thus, the CAR-T cell generation protocol seems to be suitable to obtain functional CARs. However, we did not test the anti-CD19 CAR-T cells under BMT conditions yet. This might reveal transplantation-related changes in the T cell phenotype. Although we detected increased expression of exhaustion markers in anti-mutCALR CARs, one cannot draw strong conclusions from these data. Increased expression of exhaustion markers can also be a sign of activation and definitive proof of an exhaustive phenotype could only be obtained by testing the functionality CAR-T cells isolated from treated mice. A lack of functionality in addition to expression of exhaustion markers indicates T cell exhaustion. However, the little number of F1-hybrid T cells that can be isolated from the BM hindered such assays.

While *in vitro* experiments in the human system showed no influence of soluble mutCALR, this might not be the case for the murine model. The influence of secreted target protein on CAR-T cell efficacy is dependent on the antigen. Some studies reported that CAR T cells were insensitive to secreted antigen^{244,245}. In contrast, Chang et al., designed CARs that are specifically activated by soluble factors and determined essential factors for CAR-T cell activation by soluble ligands²⁶¹. Only antigens that can cross-link CAR receptors and are stable enough to transmit tensile force to the signaling domains of the CAR can induce cell-independent CAR-T cell activation. For some antigens, the soluble antigen interferes with CAR-T cell efficacy. Shed antigen blocked CAR-T cells specific for glypican-3 in a preclinical model for hepatocellular carcinoma²⁶². For BCMA CARs it was shown that antigen modulation by shedding decreases CAR-T cell efficacy and use of a γ -secretase inhibitor that prevented cleavage increased the CAR-T cell response. Inhibition of cleavage does not only increase the antigen surface density but also decreases the concentration of soluble BCMA in patients^{263,264}. This is an important factor to prevent blockade of CAR-T cells as it was shown that increasing concentrations of soluble BCMA can inhibit CAR-T cell activation²⁰⁶. Another antigen that is cleaved off the cell surface is mesothelin. Liu et al. showed that targeting an epitope that binds before the cleavage site can prevent blocking by the cleaved part of the antigen and recognize cleaved as well as non-cleaved antigen at the cell surface²⁶⁵. Similarly, Kihara et al. reported that part of mutCALR was cleaved off the cell-surface, which could be detected in cell-culture supernatants and they designed their antibody so that cleavage does not result in the loss of binding¹⁵¹. Thus, we revised the influence of secreted mutCALR in regard to the murine model.

During treatment of *CALR* mutated mice, we observed immune-complex formation of soluble mutCALR with anti-mutCALR antibodies¹⁰⁰. Such immune complexes deplete the secreted antigen, as well as the available antibody in the plasma. Thus, soluble mutCALR serves as an

antibody sink and therefore frequent administration of the therapeutic antibody is required. Here, we utilized this immune complex formation to deplete soluble CALR from the plasma as an analytic tool. After antibody treatment we detected 3-times more CAR-T cells binding the antigen compared to mice without pre-treatment. Mice with pre-treatment also showed a trend towards increased CD25 expression, which might be indicative of increased activation. Therefore, we hypothesize that secreted CALR binds to CAR-T cells and thereby blocks their epitope.

In conclusion, we could show that both human and murine CAR-T cells specifically recognize mutCALR expressing cells and lead to their clearance. Nonetheless, we did not obtain robust efficacy *in vivo*. Although primary HSCs were depleted in a mutCALR-specific manner by murine T cells *ex vivo*, they failed to eradicate mutant stem cells *in vivo*. Therefore, we analyzed several factors, which might lead to inhibition of T cells *in vivo*. We validated our CAR-T cell generation protocol and functionality of CAR-T cells *Calr* mutated mice with a CD19-specific control CAR. Although differences in the CD19 and mutCALR antigen limit the comparability of both CAR constructs, functionality of the CD19 CAR indicates that target-cell or target-antigen specific factors are likely responsible for the lack of efficacy of anti-mutCALR CAR-T cells. We observed increased PD-L1 expression of target cells, especially in the context of BMT, which might hamper CAR-T cell functionality. Further, mutCALR-specific CAR-T cells showed increased expression of PD-1 and LAG-3, which might be in line with an exhausted phenotype resulting from increased PD-1/PD-L1 signaling. In addition, we identified secreted mutCALR as a potential inhibitor of CAR-T cell functionality.

We are currently establishing a simplified Ba/F3 xenograft model for testing murine CAR-T cells *in vivo*. Preliminary data from treatment of mice with subcutaneous Ba/F3 tumors indicate that CAR-T cells are functional *in vivo*. Although Ba/F3 cells express the antigen at a higher density and xenograft models are less physiologically relevant, this is the first indication that anti-mutCALR CAR-T cells can deliver robust efficacy *in vivo* and the subcutaneous tumors might recapitulate a tumor environment with increased concentrations of soluble CALR. Yet, we plan to further elucidate mechanisms, which hinder the efficacy of the CAR-T cells in our immunocompetent BMT model. Thus, we will analyze the expression of CTLA-4 on target cells and test combination therapies of PD-1 or CTLA-4 blockade and CAR-T cells. Further, a main effort of the lab is the generation of novel conformation-specific antibodies. Thereby, we aim at finding an antibody, which specifically recognizes mutCALR in complex with MPL. This would prevent blocking of the paratope on CAR-T cells by secreted mutCALR.

4. METHODS

Generation of CAR constructs

CAR constructs were generated using NEBuilder HiFi DNA assembly.

Human CAR library for screening in Jurkat cells. ScFv sequences were provided by and are proprietary to MyeloPro Diagnostics and Research GmbH. Different scFvs were incorporated into a second-generation 28z CAR provided by the Christoph Bock Lab, CeMM. A CROPseq vector was used as a backbone, which included mCherry linked to the CAR via a T2A sequence²⁶⁶.

Human CAR constructs for in vitro testing. CAR 7 was cloned into the pCDH vector, which included a Puromycin resistance gene linked to the CAR via a P2A sequence. scFv 7 was additionally cloned into a second-generation BBz CAR provided by the Christoph Bock Lab.

Murine CAR. An scFv derived from a mouse mAb was cloned into a murine CAR backbone in a retroviral vector (Addgene #107226)²²⁸.

Cell culture

UT7/Tpo cells were transduced to stably express a *Photinus pyralis* firefly luciferase reporter (Addgene #17477)²⁶⁷. Cells were cultured in IMDM (Gibco) + 10% FBS (Sigma) + Penicillin-Streptomycin (Gibco, 100 U/mL). CALR WT cells were supplemented by human TPO generated in our lab.

Ba/F3 cells were cultured in RPMI (Gibco) + 10% FBS (Sigma) + Penicillin-Streptomycin (Gibco, 100 U/mL). CALR WT cells were supplemented by human TPO generated in our lab.

Human primary T cells were isolated from a buffy coat obtained from the Austrian Red Cross using the Miltenyi human CD3 microbead kit. After activation with T cell TransAct (Miltenyi), cells were cultured up to three weeks in CTS™ OpTmizer™ T Cell Expansion SFM (Gibco) supplemented with Glutamax (Gibco, 1:100), 2% human serum (Sigma) and human IL-2 (Peprotech, 100 U/mL). CAR-positive cells were selected using Puromycin (Invitrogen) at 1 µg/mL.

For mouse T cell isolation, splenocytes were harvested from F1 hybrid C57BL/6 (CD45.1/CD45.2) donor mice and passed over a mouse CD3⁺ T cell enrichment column (Miltenyi Biotec). T cells were incubated in complete mouse media (RPMI + 10% FBS + Penicillin-Streptomycin + HEPES + non-essential aa + sodium pyruvate + Glutamax + β-mercaptoethanol; all from Gibco) and activated with Mouse T-Activator CD3/CD28 Dynabeads (Thermo Fisher) in the presence of human IL-2 (Peprotech, 100 U/mL).

CAR screening in Jurkat cells

The receptor library was expressed in Jurkat cells by lentiviral transduction. Successful DNA integration was detected by mCherry, which was included on the CAR-encoding plasmid. Unsorted cells were co-cultured with UT7/Tpo target cells at an effector to target ratio of 1:1 for 16 hours before staining for CD69.

***In vitro* testing of human CAR-T cells**

A mixed population of CD4⁺ and CD8⁺ T cells with approximately were transduced with the CAR construct and selected with puromycin. CAR expression was determined by staining with the 22-aa peptide mimicking the mutant C-terminus of CALR.

All cells were resuspended in Cytotoxicity Medium (RPMI without phenol red with 10% FBS, Penicillin-Streptomycin). Target cells (20000/well) were seeded in white polystyrene 96-well round bottom plates. CAR-T cells were added according to the desired effector to target ratio. The plates were centrifuged at 300g for 5 min and incubated for 24 hours at 37 °C. 50 µL of luciferin solution (0.45 mg/mL Xenolight D luciferin, Perkin Elmer) was added to each well and the plate was incubated for 20 min at room temperature in the dark. Luminescence was measured using BioTek Synergy2 plate reader. Supernatant from cytotoxicity assays was stored at -80 °C for cytokine analysis. IFN-g was quantified using ELISA Kits purchased from Biolegend.

***In vitro* testing of murine CAR-T cells**

On days 2 and 3 of T cell culture, retroviral supernatant was centrifuged at 2000g for 2 hours on Retronectin (Takara) coated plates. After virus supernatant removal, T cells were incubated for an additional 24 hours. A second transduction was performed to increase CAR-T cell frequency. On day seven after isolation, T cells were either co-cultured with target cells. GFP-positive Ba/F3 cells (40000/well) were seeded in polystyrene 96-well round bottom plates. CAR-T cells were added according to the desired effector to target ratio. The plates were centrifuged at 300g for 5 min and incubated for 24 hours at 37 °C. The frequency of GFP+ target cells was measured by FACS. Assay supernatant was stored at -80 °C for cytokine analysis.

Animal experiments

All animal experiments were approved by the Austrian Bundesministerium für Wissenschaft, Forschung und Wirtschaft.

We intend to perform competitive bone marrow transplantation in lethally irradiated Ly5.1 recipient mice. We will use an F1 hybrid of C57BL/6 vavCre (Ly5.2) and C57BL/6-Ly5.1 mice as donor for competitor cells, while target cells will be isolated from C57BL/6 vavCALRdel52

(Ly5.2) mice. Hence, Ly5.1/Ly5.2 competitors can be separated from CALRmut Ly5.2 target cells and Ly5.1 residual recipient cells. Different populations can be assessed by the use of CD45.1 and CD45.2 specific antibodies as an end-point measurement. For monitoring of disease progression we have further developed a digital droplet PCR assay that allows to quantify the fractional abundance of cells expressing CALRmut, which is equivalent of assessing allelic burden.

We will inject mouse CAR-T cells into transplanted mice with established disease. The effect of treatment will be monitored by regular measurements of peripheral blood parameters. At the experimental end point we further plan to isolate organs and analyze spleen and bone marrow composition by flow cytometry completed by histological analysis of the bone marrow.

References

1. DAMESHEK, W. Some speculations on the myeloproliferative syndromes. *Blood* **6**, 372–5 (1951).
2. Arber, D. A. *et al.* The 2016 revision to the World Health Organization classification of myeloid neoplasms and acute leukemia. *Blood* **127**, 2391–2405 (2016).
3. Vainchenker, W. & Kralovics, R. Genetic basis and molecular pathophysiology of classical myeloproliferative neoplasms. *Blood* **129**, 667–679 (2017).
4. James, C. *et al.* A unique clonal JAK2 mutation leading to constitutive signalling causes polycythaemia vera. *Nature* **434**, 1144 (2005).
5. Mesa, R. A. *et al.* Activating mutation in the tyrosine kinase JAK2 in polycythemia vera, essential thrombocythemia, and myeloid metaplasia with myelofibrosis. *Cancer Cell* **7**, 387–397 (2005).
6. Kralovics, R. *et al.* A Gain-of-Function Mutation of JAK2 in Myeloproliferative Disorders. *N. Engl. J. Med.* **352**, 1779–1790 (2005).
7. Scott, L. M. *et al.* JAK2 Exon 12 Mutations in Polycythemia Vera and Idiopathic. *N. Engl. J. Med.* **356**, 459–468 (2007).
8. Chaligne, R. *et al.* Evidence for MPL W515L/K mutations in hematopoietic stem cells in primitive myelofibrosis. *Blood* **110**, 3735–3743 (2007).
9. Pikman, Y. *et al.* MPLW515L Is a Novel Somatic Activating Mutation in Myelofibrosis with Myeloid Metaplasia. *PLoS Med.* **3**, e270 (2006).
10. Beer, P. A. *et al.* MPL mutations in myeloproliferative disorders: analysis of the PT-1 cohort. *Blood* **112**, 141–149 (2008).
11. Klampfl, T. *et al.* Somatic Mutations of Calreticulin in Myeloproliferative Neoplasms. *N. Engl. J. Med.* **369**, 2379–2390 (2013).
12. Nangalia, J. *et al.* Somatic CALR Mutations in Myeloproliferative Neoplasms with Nonmutated JAK2. *N. Engl. J. Med.* **369**, 2391–2405 (2013).

13. Ward, A. C., Touw, I. & Yoshimura, A. The Jak-Stat pathway in normal and perturbed hematopoiesis. *Blood* **95**, 19–29 (2000).
14. Merchant, S. The JAK2 mutation. *Int. Rev. Cell Mol. Biol.* **365**, 117–162 (2021).
15. Leroy, E. *et al.* Uncoupling JAK2 V617F activation from cytokine-induced signalling by modulation of JH2 α C helix. *Biochem. J.* **473**, 1579–1591 (2016).
16. Tiedt, R. *et al.* Ratio of mutant JAK2-V617F to wild-type Jak2 determines the MPD phenotypes in transgenic mice. *Blood* **111**, 3931–3940 (2008).
17. Teofili, L. *et al.* Different STAT-3 and STAT-5 phosphorylation discriminates among Ph-negative chronic myeloproliferative diseases and is independent of the V617F JAK-2 mutation. *Blood* **110**, 354–359 (2007).
18. Chen, E. *et al.* Distinct clinical phenotypes associated with JAK2V617F reflect differential STAT1 signaling. *Cancer Cell* **18**, 524–535 (2010).
19. Yan, D., Hutchison, R. E. & Mohi, G. Critical requirement for Stat5 in a mouse model of polycythemia vera. *Blood* **119**, 3539–3549 (2012).
20. Walz, C. *et al.* Essential role for Stat5a/b in myeloproliferative neoplasms induced by BCR-ABL1 and JAK2V617F in mice. *Blood* **119**, 3550–3560 (2012).
21. Grisouard, J. *et al.* Deletion of Stat3 in hematopoietic cells enhances thrombocytosis and shortens survival in a JAK2-V617F mouse model of MPN. *Blood* **125**, 2131–2140 (2015).
22. Duek, A. *et al.* Loss of Stat1 decreases megakaryopoiesis and favors erythropoiesis in a JAK2-V617F-driven mouse model of MPNs. *Blood* **123**, 3943–3950 (2014).
23. Greenfield, G., McMullin, M. F. & Mills, K. Molecular pathogenesis of the myeloproliferative neoplasms. *J. Hematol. Oncol. J Hematol Oncol* **14**, 103 (2021).
24. Guglielmelli, P. & Calabresi, L. The MPL mutation. *Int. Rev. Cell Mol. Biol.* **365**, 163–178 (2021).
25. Pardanani, A. D. *et al.* MPL515 mutations in myeloproliferative and other myeloid disorders: a study of 1182 patients. *Blood* **108**, 3472–3476 (2006).

26. Ding, J. *et al.* Familial essential thrombocythemia associated with a dominant-positive activating mutation of the c-MPL gene, which encodes for the receptor for thrombopoietin. *Blood* **103**, 4198–4200 (2004).
27. Michalak, M., Groenendyk, J., Szabo, E., Gold, L. I. & Opas, M. Calreticulin, a multi-process calcium-buffering chaperone of the endoplasmic reticulum. *Biochem. J.* **417**, 651–666 (2009).
28. Araki, M. *et al.* Activation of the thrombopoietin receptor by mutant calreticulin in CALR-mutant myeloproliferative neoplasms. *Blood* **127**, 1307–1316 (2016).
29. Chachoua, I. *et al.* Thrombopoietin receptor activation by myeloproliferative neoplasm associated calreticulin mutants. *Blood* **127**, 1325–1335 (2016).
30. Marty, C. *et al.* Calreticulin mutants in mice induce an MPL-dependent thrombocytosis with frequent progression to myelofibrosis. *Blood* **127**, 1317–1324 (2016).
31. Waters, M. J. & Brooks, A. J. JAK2 activation by growth hormone and other cytokines. *Biochem. J.* **466**, 1–11 (2015).
32. Elf, S. *et al.* Mutant Calreticulin Requires Both Its Mutant C-terminus and the Thrombopoietin Receptor for Oncogenic Transformation. *Cancer Discov.* **6**, 368–381 (2016).
33. Pecquet, C. *et al.* Calreticulin mutants as oncogenic rogue chaperones for TpoR and traffic-defective pathogenic TpoR mutants. *Blood* **133**, 2669–2681 (2019).
34. Araki, M. *et al.* Activation of the thrombopoietin receptor by mutant calreticulin in CALR-mutant myeloproliferative neoplasms. *Blood* **127**, 1307–1316 (2016).
35. Merlinsky, T. R., Levine, R. L. & Pronier, E. Unfolding the Role of Calreticulin in Myeloproliferative Neoplasm Pathogenesis. *Clin. Cancer Res.* clincanres.3777.2018 (2019) doi:10.1158/1078-0432.CCR-18-3777.
36. Pecquet, C. *et al.* Secreted Mutant Calreticulins As Rogue Cytokines Trigger Thrombopoietin Receptor Activation Specifically in CALR Mutated Cells: Perspectives for MPN Therapy. *Blood* **132**, 4–4 (2018).

37. Jaiswal, S. *et al.* Clonal Hematopoiesis and Risk of Atherosclerotic Cardiovascular Disease. *N. Engl. J. Med.* **377**, 111–121 (2017).
38. Avagyan, S. & Zon, L. I. Clonal hematopoiesis and inflammation – the perpetual cycle. *Trends Cell Biol.* (2022) doi:10.1016/j.tcb.2022.12.001.
39. Luque Paz, D., Kralovics, R. & Skoda, R. C. Genetic basis and molecular profiling in myeloproliferative neoplasms. *Blood* blood.2022017578 (2022) doi:10.1182/blood.2022017578.
40. Williams, N. *et al.* Life histories of myeloproliferative neoplasms inferred from phylogenies. *Nature* **602**, 162–168 (2022).
41. Van Egeren, D. *et al.* Reconstructing the Lineage Histories and Differentiation Trajectories of Individual Cancer Cells in Myeloproliferative Neoplasms. *Cell Stem Cell* **28**, 514-523.e9 (2021).
42. Lundberg, P. *et al.* Clonal evolution and clinical correlates of somatic mutations in myeloproliferative neoplasms. *Blood* **123**, 2220–2228 (2014).
43. Klampfl, T. *et al.* Somatic Mutations of Calreticulin in Myeloproliferative Neoplasms. *N. Engl. J. Med.* **369**, 2379–2390 (2013).
44. Nangalia, J. *et al.* Somatic *CALR* Mutations in Myeloproliferative Neoplasms with Nonmutated *JAK2*. *N. Engl. J. Med.* **369**, 2391–2405 (2013).
45. Fu, R. *et al.* Analysis of calreticulin mutations in Chinese patients with essential thrombocythemia: clinical implications in diagnosis, prognosis and treatment. *Leukemia* **28**, 1912–1914 (2014).
46. McGaffin, G., Harper, K., Stirling, D. & McLintock, L. *JAK2* V617F and *CALR* mutations are not mutually exclusive; findings from retrospective analysis of a small patient cohort. *Br. J. Haematol.* **167**, 276–278 (2014).
47. Tefferi, A. *et al.* *CALR* vs *JAK2* vs *MPL*-mutated or triple-negative myelofibrosis: clinical, cytogenetic and molecular comparisons. *Leukemia* **28**, 1472–1477 (2014).
48. Al Assaf, C. *et al.* Analysis of phenotype and outcome in essential thrombocythemia with *CALR* or *JAK2* mutations. *Haematologica* **100**, 893–897 (2015).

49. Ha, J.-S. & Kim, Y.-K. Calreticulin Exon 9 Mutations in Myeloproliferative Neoplasms. *Ann. Lab. Med.* **35**, 22–27 (2015).
50. Lim, K.-H. *et al.* Frequent CALR exon 9 alterations in JAK2 V617F-mutated essential thrombocythemia detected by high-resolution melting analysis. *Blood Cancer J.* **5**, e295–e295 (2015).
51. Lin, Y. *et al.* The Prevalence of *JAK2*, *MPL*, and *CALR* Mutations in Chinese Patients With *BCR-ABL1* –Negative Myeloproliferative Neoplasms. *Am. J. Clin. Pathol.* **144**, 165–171 (2015).
52. Shirane, S. *et al.* JAK2, CALR, and MPL mutation spectrum in Japanese patients with myeloproliferative neoplasms. *Haematologica* **100**, e46–e48 (2015).
53. Xu, N. *et al.* A report on the co-occurrence of JAK2V617F and CALR mutations in myeloproliferative neoplasm patients. *Ann. Hematol.* **94**, 865–867 (2015).
54. Zamora, L. *et al.* Co-existence of JAK2 V617F and CALR mutations in primary myelofibrosis. *Leuk. Lymphoma* **56**, 2973–2974 (2015).
55. Kang, M.-G. *et al.* Coexistence of JAK2 and CALR mutations and their clinical implications in patients with essential thrombocythemia. *Oncotarget* **7**, 57036–57049 (2016).
56. Mansier, O., Migeon, M., Etienne, G., Bidet, A. & Lippert, E. JAK2 V617F and CALR double mutations are more frequently encountered in patients with low JAK2 V617F allelic burdens. *Leuk. Lymphoma* **57**, 1949–1951 (2016).
57. Nussenzveig, R. H. *et al.* Increased frequency of co-existing JAK2 exon-12 or MPL exon-10 mutations in patients with low JAK2V617F allelic burden. *Leuk. Lymphoma* **57**, 1429–1435 (2016).
58. Rashid, M. *et al.* Coexisting JAK2V617F and CALR Exon 9 Mutation in Essential Thrombocythemia. *Indian J. Hematol. Blood Transfus.* **32**, 112–116 (2016).
59. Xing, C., Li, H., Wu, J. & Gao, S. Co-occurrence of JAK2 V617F and an uncommon CALR del (p.K368fs*51) mutation facilitates JAK2/STAT signaling in polycythemia vera. *Leuk. Lymphoma* **57**, 1743–1745 (2016).

60. Cleyrat, C. *et al.* Leukemic Transformation of Post-Essential Thrombocythemia Myelofibrosis: A Unique Case Presenting with Double MPL and CALR Mutations. *Blood* **130**, 4215 (2017).
61. Usseglio, F., Beauvils, N., Calleja, A., Raynaud, S. & Gabert, J. Detection of CALR and MPL Mutations in Low Allelic Burden JAK2 V617F Essential Thrombocythemia. *J. Mol. Diagn.* **19**, 92–98 (2017).
62. Boddu, P. *et al.* The co-occurrence of driver mutations in chronic myeloproliferative neoplasms. *Ann. Hematol.* **97**, 2071–2080 (2018).
63. Mansier, O. *et al.* Clinical and biological characterization of MPN patients harboring two driver mutations, a French intergroup of myeloproliferative neoplasms (FIM) study. *Am. J. Hematol.* **93**, E84–E86 (2018).
64. Kelkar, K. *et al.* Co-occurrence of CALR and MPL somatic mutations in an Indian patient with a Philadelphia-negative myeloproliferative neoplasm. *J. Hematop.* **12**, 163–168 (2019).
65. Zhou, F.-P., Wang, C.-C., Du, H.-P., Cao, S.-B. & Zhang, J. Primary myelofibrosis with concurrent CALR and MPL mutations: A case report. *World J. Clin. Cases* **8**, 5618–5624 (2020).
66. Nishimura, M. *et al.* Acquisition of JAK2 V617F to CALR -mutated clones accelerates disease progression and might enhance growth capacity. *Br. J. Haematol.* **194**, (2021).
67. Thomas, S. J. & Dash, D. P. A Rare Co-Occurrence of Triple Mutations in JAK2, CALR, and MPL in the Same Patient with Myelofibrosis. *Case Rep. Hematol.* **2022**, 1–6 (2022).
68. Lippert, E. *et al.* Clinical and biological characterization of patients with low (0.1–2%) JAK2V617F allele burden at diagnosis. *Haematologica* **99**, e098-e101 (2014).
69. Tefferi, A. *et al.* Low JAK2V617F allele burden in primary myelofibrosis, compared to either a higher allele burden or unmutated status, is associated with inferior overall and leukemia-free survival. *Leukemia* **22**, 756–761 (2008).

70. Guglielmelli, P. *et al.* Identification of patients with poorer survival in primary myelofibrosis based on the burden of JAK2V617F mutated allele. *Blood* **114**, 1477–1483 (2009).
71. Plo, I. “Mixed” Myeloproliferative Neoplasm Due to Co-Occurrence of Different Driver Mutations. *Acta Haematol.* **141**, 268–270 (2019).
72. Thompson, E. R. *et al.* Clonal independence of JAK2 and CALR or MPL mutations in comutated myeloproliferative neoplasms demonstrated by single cell DNA sequencing. *Haematologica* **106**, 313–315 (2020).
73. Partouche, N. *et al.* Emergence of MPLW515 mutation in a patient with CALR deletion: Evidence of secondary acquisition of MPL mutation in the CALR clone. *Hematol. Oncol.* **36**, 336–339 (2018).
74. Tashkandi, H., Moore, E. M., Tomlinson, B., Goebel, T. & Sadri, N. Co-occurrence of type I CALR and two MPL mutations in patient with primary myelofibrosis. *Ann. Hematol.* **96**, 1417–1418 (2017).
75. Tefferi, A. & Pardanani, A. CALR mutations and a new diagnostic algorithm for MPN. *Nat. Rev. Clin. Oncol.* **11**, 125–126 (2014).
76. Vainchenker, W. & Constantinescu, S. N. JAK/STAT signaling in hematological malignancies. *Oncogene* **32**, 2601–2613 (2013).
77. Stivala, S. *et al.* Targeting compensatory MEK/ERK activation increases JAK inhibitor efficacy in myeloproliferative neoplasms. *J. Clin. Invest.* **129**, 1596–1611 (2019).
78. Kollmann, K. *et al.* A novel signalling screen demonstrates that CALR mutations activate essential MAPK signalling and facilitate megakaryocyte differentiation. *Leukemia* **31**, 934–944 (2017).
79. Bartalucci, N., Guglielmelli, P. & Vannucchi, A. M. Rationale for Targeting the PI3K/Akt/mTOR Pathway in Myeloproliferative Neoplasms. *Clin. Lymphoma Myeloma Leuk.* **13**, S307–S309 (2013).
80. Fu, C. *et al.* AKT activation is a feature of CALR mutant myeloproliferative neoplasms. *Leukemia* **33**, 271–274 (2019).

81. Bartalucci, N. *et al.* Inhibitors of the PI3K/mTOR pathway prevent STAT5 phosphorylation in JAK2V617F mutated cells through PP2A/CIP2A axis. *Oncotarget* **8**, 96710–96724 (2017).
82. Benlabiod, C., Dagher, T., Marty, C. & Villeval, J.-L. Lessons from mouse models of MPN. in *International Review of Cell and Molecular Biology* vol. 366 125–185 (Elsevier, 2022).
83. Wernig, G. *et al.* Expression of Jak2V617F causes a polycythemia vera–like disease with associated myelofibrosis in a murine bone marrow transplant model. *Blood* **107**, 4274–4281 (2006).
84. Lacout, C. *et al.* JAK2V617F expression in murine hematopoietic cells leads to MPD mimicking human PV with secondary myelofibrosis. *Blood* **108**, 1652–1660 (2006).
85. Bumm, T. G. P. *et al.* Characterization of Murine JAK2V617F-Positive Myeloproliferative Disease. *Cancer Res.* **66**, 11156–11165 (2006).
86. Chapeau, E. A. *et al.* A conditional inducible JAK2V617F transgenic mouse model reveals myeloproliferative disease that is reversible upon switching off transgene expression. *PLOS ONE* **14**, e0221635 (2019).
87. Li, J. *et al.* JAK2V617F homozygosity drives a phenotypic switch in myeloproliferative neoplasms, but is insufficient to sustain disease. *Blood* **123**, 3139–3151 (2014).
88. Mansier, O. *et al.* Description of a knock-in mouse model of JAK2V617F MPN emerging from a minority of mutated hematopoietic stem cells. *Blood* **134**, 2383–2387 (2019).
89. Zaleskas, V. M. *et al.* Molecular Pathogenesis and Therapy of Polycythemia Induced in Mice by JAK2 V617F. *PLOS ONE* **1**, e18 (2006).
90. Xing, S. *et al.* Transgenic expression of JAK2V617F causes myeloproliferative disorders in mice. *Blood* **111**, 5109–5117 (2008).
91. Shide, K. *et al.* Development of ET, primary myelofibrosis and PV in mice expressing JAK2 V617F. *Leukemia* **22**, 87–95 (2008).
92. Marty, C. *et al.* Myeloproliferative neoplasm induced by constitutive expression of JAK2V617F in knock-in mice. *Blood* **116**, 783–787 (2010).

93. Mullally, A. *et al.* Physiological Jak2V617F Expression Causes a Lethal Myeloproliferative Neoplasm with Differential Effects on Hematopoietic Stem and Progenitor Cells. *Cancer Cell* **17**, 584–596 (2010).
94. Akada, H. *et al.* Conditional expression of heterozygous or homozygous Jak2V617F from its endogenous promoter induces a polycythemia vera–like disease. *Blood* **115**, 3589–3597 (2010).
95. Li, J. *et al.* JAK2 V617F impairs hematopoietic stem cell function in a conditional knock-in mouse model of JAK2 V617F–positive essential thrombocythemia. *Blood* **116**, 1528–1538 (2010).
96. Hasan, S. *et al.* JAK2V617F expression in mice amplifies early hematopoietic cells and gives them a competitive advantage that is hampered by IFN α . *Blood* **122**, 1464–1477 (2013).
97. Shide, K. *et al.* Calreticulin mutant mice develop essential thrombocythemia that is ameliorated by the JAK inhibitor ruxolitinib. *Leukemia* **31**, 1136–1144 (2017).
98. Mesaeli, N. *et al.* Calreticulin Is Essential for Cardiac Development. *J. Cell Biol.* **144**, 857–868 (1999).
99. Guo, L. *et al.* Cardiac-specific expression of calcineurin reverses embryonic lethality in calreticulin-deficient mouse. *J. Biol. Chem.* **277**, 50776–50779 (2002).
100. Achyutuni, S. *et al.* Hematopoietic expression of a chimeric murine-human CALR oncoprotein allows the assessment of ANTI-CALR antibody immunotherapies in vivo. *Am. J. Hematol.* **96**, 698–707 (2021).
101. Prins, D. *et al.* The stem/progenitor landscape is reshaped in a mouse model of essential thrombocythemia and causes excess megakaryocyte production. *Sci. Adv.* **6**, eabd3139 (2020).
102. Nguyen, T. K., Morse, S. J. & Fleischman, A. G. Transduction-Transplantation Mouse Model of Myeloproliferative Neoplasm. *J. Vis. Exp. JoVE* 54624 (2016)
doi:10.3791/54624.

103. Toppaldoddi, K. R. *et al.* Rare type 1-like and type 2-like calreticulin mutants induce similar myeloproliferative neoplasms as prevalent type 1 and 2 mutants in mice. *Oncogene* **38**, 1651–1660 (2019).
104. Shide, K. *et al.* Mice with Calr mutations homologous to human CALR mutations only exhibit mild thrombocytosis. *Blood Cancer J.* **9**, 42 (2019).
105. Li, J. *et al.* Mutant calreticulin knockin mice develop thrombocytosis and myelofibrosis without a stem cell self-renewal advantage. *Blood* **131**, 649–661 (2018).
106. Benlabiod, C. *et al.* Calreticulin del52 and ins5 knock-in mice recapitulate different myeloproliferative phenotypes observed in patients with MPN. *Nat. Commun.* **11**, 4886 (2020).
107. Balligand, T. *et al.* Knock-in of murine Calr del52 induces essential thrombocythemia with slow-rising dominance in mice and reveals key role of Calr exon 9 in cardiac development. *Leukemia* **34**, 510–521 (2020).
108. Michl, M. *BASICS Hämatologie*. (Elsevier, 2019).
109. Cerquozzi, S. & Tefferi, A. Blast transformation and fibrotic progression in polycythemia vera and essential thrombocythemia: a literature review of incidence and risk factors. *Blood Cancer J.* **5**, e366–e366 (2015).
110. Dunbar, A. J., Rampal, R. K. & Levine, R. Leukemia secondary to myeloproliferative neoplasms. *Blood* **136**, 61–70 (2020).
111. Barbui, T. *et al.* Philadelphia chromosome-negative classical myeloproliferative neoplasms: revised management recommendations from European LeukemiaNet. *Leukemia* **32**, 1057–1069 (2018).
112. Tefferi, A. & Barbui, T. Essential Thrombocythemia and Polycythemia Vera: Focus on Clinical Practice. *Mayo Clin. Proc.* **90**, 1283–1293 (2015).
113. Barbui, T. *et al.* Development and validation of an International Prognostic Score of thrombosis in World Health Organization–essential thrombocythemia (IPSET-thrombosis). *Blood* **120**, 5128–5133 (2012).

114. Barbui, T. *et al.* Practice-Relevant Revision of Ipset-Thrombosis Based on 1019 Patients with WHO-Defined Essential Thrombocythemia. *Blood* **126**, 4055 (2015).
115. Haider, M. *et al.* Validation of the revised International Prognostic Score of Thrombosis for Essential Thrombocythemia (IPSET-thrombosis) in 585 Mayo Clinic patients. *Am. J. Hematol.* **91**, 390–394 (2016).
116. Cervantes, F. *et al.* New prognostic scoring system for primary myelofibrosis based on a study of the International Working Group for Myelofibrosis Research and Treatment. *Blood* **113**, 2895–2901 (2009).
117. Gangat, N. *et al.* DIPSS Plus: A Refined Dynamic International Prognostic Scoring System for Primary Myelofibrosis That Incorporates Prognostic Information From Karyotype, Platelet Count, and Transfusion Status. *J. Clin. Oncol.* **29**, 392–397 (2011).
118. Alvarez-Larrán, A. *et al.* Impact of genotype on leukaemic transformation in polycythaemia vera and essential thrombocythaemia. *Br. J. Haematol.* **178**, 764–771 (2017).
119. Guglielmelli, P. *et al.* MIPSS70: Mutation-Enhanced International Prognostic Score System for Transplantation-Age Patients With Primary Myelofibrosis. *J. Clin. Oncol. Off. J. Am. Soc. Clin. Oncol.* **36**, 310–318 (2018).
120. Tefferi, A. *et al.* MIPSS70+ Version 2.0: Mutation and Karyotype-Enhanced International Prognostic Scoring System for Primary Myelofibrosis. *J. Clin. Oncol. Off. J. Am. Soc. Clin. Oncol.* **36**, 1769–1770 (2018).
121. Tefferi, A. *et al.* GIPSS: genetically inspired prognostic scoring system for primary myelofibrosis. *Leukemia* **32**, 1631–1642 (2018).
122. Barosi, G. *et al.* A unified definition of clinical resistance/intolerance to hydroxyurea in essential thrombocythemia: results of a consensus process by an international working group. *Leukemia* **21**, 277–280 (2007).
123. Stegelmann, F. *et al.* Significant association of cutaneous adverse events with hydroxyurea: results from a prospective non-interventional study in BCR-ABL1-negative

myeloproliferative neoplasms (MPN) - on behalf of the German Study Group-MPN.

Leukemia **35**, 628–631 (2021).

124. Sterkers, Y. *et al.* Acute myeloid leukemia and myelodysplastic syndromes following essential thrombocythemia treated with hydroxyurea: high proportion of cases with 17p deletion. *Blood* **91**, 616–622 (1998).
125. Spivak, J. L. An inconvenient truth. *Blood* **115**, 2727–2728 (2010).
126. Kiladjian, J.-J., Chevret, S., Dosquet, C., Chomienne, C. & Rain, J.-D. Treatment of polycythemia vera with hydroxyurea and pipobroman: final results of a randomized trial initiated in 1980. *J. Clin. Oncol. Off. J. Am. Soc. Clin. Oncol.* **29**, 3907–3913 (2011).
127. Passamonti, F. *et al.* Life expectancy and prognostic factors for survival in patients with polycythemia vera and essential thrombocythemia. *Am. J. Med.* **117**, 755–761 (2004).
128. Passamonti, F. *et al.* A prognostic model to predict survival in 867 World Health Organization-defined essential thrombocythemia at diagnosis: a study by the International Working Group on Myelofibrosis Research and Treatment. *Blood* **120**, 1197–1201 (2012).
129. Tefferi, A. *et al.* Survival and prognosis among 1545 patients with contemporary polycythemia vera: an international study. *Leukemia* **27**, 1874–1881 (2013).
130. Mazur, E. M., Rosmarin, A. G., Sohl, P. A., Newton, J. L. & Narendran, A. Analysis of the Mechanism of Anagrelide-Induced Thrombocytopenia in Humans. *Blood* **79**, 1931–1937 (1992).
131. Solberg Jr, L. A. *et al.* The effects of anagrelide on human megakaryocytopoiesis. *Br. J. Haematol.* **99**, 174–180 (1997).
132. Tomer, A. Effects of anagrelide on in vivo megakaryocyte proliferation and maturation in essential thrombocythemia. *Blood* **99**, 1602–1609 (2002).
133. Takaishi, K. *et al.* Suppressive effects of anagrelide on cell cycle progression and the maturation of megakaryocyte progenitor cell lines in human induced pluripotent stem cells. *Haematologica* **105**, e216–e220 (2020).

134. Harrison, C. N. *et al.* Hydroxyurea compared with anagrelide in high-risk essential thrombocythemia. *N. Engl. J. Med.* **353**, 33–45 (2005).
135. Gisslinger, H. *et al.* Anagrelide compared with hydroxyurea in WHO-classified essential thrombocythemia: the ANAHYDRET Study, a randomized controlled trial. *Blood* **121**, 1720–1728 (2013).
136. Lu, M. *et al.* Interferon-alpha targets JAK2V617F-positive hematopoietic progenitor cells and acts through the p38 MAPK pathway. *Exp. Hematol.* **38**, 472–480 (2010).
137. Mullally, A. *et al.* Depletion of Jak2V617F myeloproliferative neoplasm-propagating stem cells by interferon- α in a murine model of polycythemia vera. *Blood* **121**, 3692–3702 (2013).
138. How, J. & Hobbs, G. Use of Interferon Alfa in the Treatment of Myeloproliferative Neoplasms: Perspectives and Review of the Literature. *Cancers* **12**, 1954 (2020).
139. Hasselbalch, H. C. & Holmström, M. O. Perspectives on interferon-alpha in the treatment of polycythemia vera and related myeloproliferative neoplasms: minimal residual disease and cure? *Semin. Immunopathol.* **41**, 5–19 (2019).
140. Levy, G. *et al.* Targets in MPNs and potential therapeutics. in *International Review of Cell and Molecular Biology* vol. 366 41–81 (Elsevier, 2022).
141. Loscocco, G. G. & Vannucchi, A. M. Role of JAK inhibitors in myeloproliferative neoplasms: current point of view and perspectives. *Int. J. Hematol.* **115**, 626–644 (2022).
142. McLornan, D. P., Pope, J. E., Gotlib, J. & Harrison, C. N. Current and future status of JAK inhibitors. *Lancet Lond. Engl.* **398**, 803–816 (2021).
143. Talpaz, M. & Kiladjan, J.-J. Fedratinib, a newly approved treatment for patients with myeloproliferative neoplasm-associated myelofibrosis. *Leukemia* **35**, 1–17 (2021).
144. Zhang, L., Yang, F. & Feng, S. Allogeneic hematopoietic stem-cell transplantation for myelofibrosis. *Ther. Adv. Hematol.* **11**, 2040620720906002 (2020).
145. Holmström, M. O., Riley, C. H., Svane, I. M., Hasselbalch, H. C. & Andersen, M. H. The CALR exon 9 mutations are shared neoantigens in patients with CALR mutant chronic myeloproliferative neoplasms. *Leukemia* **30**, 2413–2416 (2016).

146. Holmström, M. O. *et al.* The calreticulin (CALR) exon 9 mutations are promising targets for cancer immune therapy. *Leukemia* **32**, 429–437 (2018).
147. Holmström, M. O. *et al.* High frequencies of circulating memory T cells specific for calreticulin exon 9 mutations in healthy individuals. *Blood Cancer J.* **9**, 8 (2019).
148. Tubb, V. M. *et al.* Isolation of T cell receptors targeting recurrent neoantigens in hematological malignancies. *J. Immunother. Cancer* **6**, 70 (2018).
149. Arshad, N. & Cresswell, P. Tumor-associated calreticulin variants functionally compromise the peptide loading complex and impair its recruitment of MHC-I. *J. Biol. Chem.* **293**, 9555–9569 (2018).
150. Liu, P. *et al.* Immunosuppression by Mutated Calreticulin Released from Malignant Cells. *Mol. Cell* **77**, 748-760.e9 (2020).
151. Kihara, Y. *et al.* Therapeutic Potential of an Antibody Targeting the Cleaved Form of Mutant Calreticulin in Myeloproliferative Neoplasms. *Blood* **136**, 9–10 (2020).
152. Tvorogov, D. *et al.* Targeting human CALR-mutated MPN progenitors with a neoepitope-directed monoclonal antibody. *EMBO Rep.* **23**, e52904 (2022).
153. Abbas, A. K., Lichtman, A. H., Pillai, S. & Baker, D. L. *Cellular and molecular immunology*. (Elsevier, 2022).
154. Smith-Garvin, J. E., Koretzky, G. A. & Jordan, M. S. T cell activation. *Annu. Rev. Immunol.* **27**, 591–619 (2009).
155. Rock, K. L., Reits, E. & Neefjes, J. Present Yourself! By MHC Class I and MHC Class II Molecules. *Trends Immunol.* **37**, 724–737 (2016).
156. Oiseth, S. J. & Aziz, M. S. Cancer immunotherapy: a brief review of the history, possibilities, and challenges ahead. *J. Cancer Metastasis Treat.* **3**, 250–261 (2017).
157. Whiteside, T. L. & Parmiani, G. Tumor-infiltrating lymphocytes: their phenotype, functions and clinical use. *Cancer Immunol. Immunother.* **39**, 15–21 (1994).
158. Brummel, K., Eerkens, A. L., de Bruyn, M. & Nijman, H. W. Tumour-infiltrating lymphocytes: from prognosis to treatment selection. *Br. J. Cancer* **128**, 451–458 (2023).

159. Nagarsheth, N., Wicha, M. S. & Zou, W. Chemokines in the cancer microenvironment and their relevance in cancer immunotherapy. *Nat. Rev. Immunol.* **17**, 559–572 (2017).
160. Anderson, K. G., Stromnes, I. M. & Greenberg, P. D. Obstacles Posed by the Tumor Microenvironment to T cell Activity: A Case for Synergistic Therapies. *Cancer Cell* **31**, 311–325 (2017).
161. Liu, X. *et al.* Affinity-tuned ErbB2 or EGFR chimeric antigen receptor T cells exhibit an increased therapeutic index against tumors in mice. *Cancer Res.* **75**, 3596–3607 (2015).
162. Fesnak, A. D., June, C. H. & Levine, B. L. Engineered T cells: the promise and challenges of cancer immunotherapy. *Nat. Rev. Cancer* **16**, 566–581 (2016).
163. Salzer, B. *et al.* Engineering AvidCARs for combinatorial antigen recognition and reversible control of CAR function. *Nat. Commun.* **11**, 4166 (2020).
164. Long, A. H. *et al.* 4-1BB costimulation ameliorates T cell exhaustion induced by tonic signaling of chimeric antigen receptors. *Nat. Med.* **21**, 581–590 (2015).
165. Landoni, E. *et al.* Modifications to the Framework Regions Eliminate Chimeric Antigen Receptor Tonic Signaling. *Cancer Immunol. Res.* **9**, 441–453 (2021).
166. Singh, N. *et al.* Antigen-independent activation enhances the efficacy of 4-1BB-costimulated CD22 CAR T cells. *Nat. Med.* **27**, 842–850 (2021).
167. Martin, T. *et al.* Ciltacabtagene Autoleucel, an Anti-B-cell Maturation Antigen Chimeric Antigen Receptor T-Cell Therapy, for Relapsed/Refractory Multiple Myeloma: CARTITUDE-1 2-Year Follow-Up. *J. Clin. Oncol. Off. J. Am. Soc. Clin. Oncol.* **41**, 1265–1274 (2023).
168. Brudno, J. N. *et al.* Safety and feasibility of anti-CD19 CAR T cells with fully human binding domains in patients with B-cell lymphoma. *Nat. Med.* **26**, 270–280 (2020).
169. Awasthi, R. *et al.* Tisagenlecleucel cellular kinetics, dose, and immunogenicity in relation to clinical factors in relapsed/refractory DLBCL. *Blood Adv.* **4**, 560–572 (2020).
170. Srivastava, S. & Riddell, S. R. Engineering CAR-T Cells: Design Concepts. *Trends Immunol.* **36**, 494–502 (2015).

171. Schäfer, D. *et al.* A Novel Siglec-4 Derived Spacer Improves the Functionality of CAR T Cells Against Membrane-Proximal Epitopes. *Front. Immunol.* **11**, 1704 (2020).
172. Smith, E. L. *et al.* GPRC5D is a target for the immunotherapy of multiple myeloma with rationally designed CAR T cells. *Sci. Transl. Med.* **11**, eaau7746 (2019).
173. Hudecek, M. *et al.* Receptor Affinity and Extracellular Domain Modifications Affect Tumor Recognition by ROR1-Specific Chimeric Antigen Receptor T Cells. *Clin. Cancer Res.* **19**, 3153–3164 (2013).
174. Hudecek, M. *et al.* The Nonsignaling Extracellular Spacer Domain of Chimeric Antigen Receptors Is Decisive for *In Vivo* Antitumor Activity. *Cancer Immunol. Res.* **3**, 125–135 (2015).
175. Leddon, S. A. *et al.* The CD28 Transmembrane Domain Contains an Essential Dimerization Motif. *Front. Immunol.* **11**, 1519 (2020).
176. Bridgeman, J. S. *et al.* The Optimal Antigen Response of Chimeric Antigen Receptors Harboring the CD3 ζ Transmembrane Domain Is Dependent upon Incorporation of the Receptor into the Endogenous TCR/CD3 Complex. *J. Immunol.* **184**, 6938–6949 (2010).
177. Fujiwara, K. *et al.* Hinge and Transmembrane Domains of Chimeric Antigen Receptor Regulate Receptor Expression and Signaling Threshold. *Cells* **9**, 1182 (2020).
178. Majzner, R. G. *et al.* Tuning the Antigen Density Requirement for CAR T-cell Activity. *Cancer Discov.* **10**, 702–723 (2020).
179. Heitzeneder, S. *et al.* GPC2-CAR T cells tuned for low antigen density mediate potent activity against neuroblastoma without toxicity. *Cancer Cell* **40**, 53-69.e9 (2022).
180. Eshhar, Z., Waks, T., Gross, G. & Schindler, D. G. Specific activation and targeting of cytotoxic lymphocytes through chimeric single chains consisting of antibody-binding domains and the gamma or zeta subunits of the immunoglobulin and T-cell receptors. *Proc. Natl. Acad. Sci. U. S. A.* **90**, 720–724 (1993).
181. Kershaw, M. H. *et al.* A Phase I Study on Adoptive Immunotherapy Using Gene-Modified T Cells for Ovarian Cancer. *Clin. Cancer Res. Off. J. Am. Assoc. Cancer Res.* **12**, 6106–6115 (2006).

182. Lamers, C. H. J. *et al.* Treatment of Metastatic Renal Cell Carcinoma With CAIX CAR-engineered T cells: Clinical Evaluation and Management of On-target Toxicity. *Mol. Ther.* **21**, 904–912 (2013).
183. Lamers, C. H. J. *et al.* Treatment of Metastatic Renal Cell Carcinoma With Autologous T-Lymphocytes Genetically Retargeted Against Carbonic Anhydrase IX: First Clinical Experience. *J. Clin. Oncol.* **24**, e20–e22 (2006).
184. Louis, C. U. *et al.* Antitumor activity and long-term fate of chimeric antigen receptor–positive T cells in patients with neuroblastoma. *Blood* **118**, 6050–6056 (2011).
185. Pule, M. A. *et al.* Virus-specific T cells engineered to coexpress tumor-specific receptors: persistence and antitumor activity in individuals with neuroblastoma. *Nat. Med.* **14**, 1264 (2008).
186. Gomes-Silva, D. *et al.* Tonic 4-1BB Costimulation in Chimeric Antigen Receptors Impedes T Cell Survival and Is Vector-Dependent. *Cell Rep.* **21**, 17–26 (2017).
187. Ying, Z. *et al.* Parallel Comparison of 4-1BB or CD28 Co-stimulated CD19-Targeted CAR-T Cells for B Cell Non-Hodgkin’s Lymphoma. *Mol. Ther. - Oncolytics* **15**, 60–68 (2019).
188. Bachy, E. *et al.* A real-world comparison of tisagenlecleucel and axicabtagene ciloleucel CAR T cells in relapsed or refractory diffuse large B cell lymphoma. *Nat. Med.* **28**, 2145–2154 (2022).
189. Cappell, K. M. & Kochenderfer, J. N. A comparison of chimeric antigen receptors containing CD28 versus 4-1BB costimulatory domains. *Nat. Rev. Clin. Oncol.* **18**, 715–727 (2021).
190. Zhong, X.-S., Matsushita, M., Plotkin, J., Riviere, I. & Sadelain, M. Chimeric antigen receptors combining 4-1BB and CD28 signaling domains augment PI3kinase/AKT/Bcl-XL activation and CD8+ T cell-mediated tumor eradication. *Mol. Ther. J. Am. Soc. Gene Ther.* **18**, 413–420 (2010).

191. Abate-Daga, D. *et al.* A novel chimeric antigen receptor against prostate stem cell antigen mediates tumor destruction in a humanized mouse model of pancreatic cancer. *Hum. Gene Ther.* **25**, 1003–1012 (2014).
192. Milone, M. C. *et al.* Chimeric receptors containing CD137 signal transduction domains mediate enhanced survival of T cells and increased antileukemic efficacy in vivo. *Mol. Ther. J. Am. Soc. Gene Ther.* **17**, 1453–1464 (2009).
193. Cappell, K. M. & Kochenderfer, J. N. Long-term outcomes following CAR T cell therapy: what we know so far. *Nat. Rev. Clin. Oncol.* 1–13 (2023) doi:10.1038/s41571-023-00754-1.
194. Morris, E. C., Neelapu, S. S., Giavridis, T. & Sadelain, M. Cytokine release syndrome and associated neurotoxicity in cancer immunotherapy. *Nat. Rev. Immunol.* **22**, 85–96 (2022).
195. Parker, K. R. *et al.* Single-cell analyses identify brain mural cells expressing CD19 as potential off-tumor targets for CAR-T immunotherapies. *Cell* **183**, 126–142.e17 (2020).
196. Van Oekelen, O. *et al.* Neurocognitive and hypokinetic movement disorder with features of parkinsonism following BCMA-targeting CAR-T cell therapy. *Nat. Med.* **27**, 2099–2103 (2021).
197. Morgan, R. A. *et al.* Case report of a serious adverse event following the administration of T cells transduced with a chimeric antigen receptor recognizing ERBB2. *Mol. Ther. J. Am. Soc. Gene Ther.* **18**, 843–851 (2010).
198. Labanieh, L. & Mackall, C. L. CAR immune cells: design principles, resistance and the next generation. *Nature* **614**, 635–648 (2023).
199. Brudno, J. N. & Kochenderfer, J. N. Chimeric antigen receptor T-cell therapies for lymphoma. *Nat. Rev. Clin. Oncol.* **15**, 31–46 (2018).
200. Shah, N. N. *et al.* Bispecific anti-CD20, anti-CD19 CAR T cells for relapsed B cell malignancies: a phase 1 dose escalation and expansion trial. *Nat. Med.* **26**, 1569–1575 (2020).

201. Zhang, Y. *et al.* Long-term activity of tandem CD19/CD20 CAR therapy in refractory/relapsed B-cell lymphoma: a single-arm, phase 1–2 trial. *Leukemia* **36**, 189–196 (2022).
202. Cordoba, S. *et al.* CAR T cells with dual targeting of CD19 and CD22 in pediatric and young adult patients with relapsed or refractory B cell acute lymphoblastic leukemia: a phase 1 trial. *Nat. Med.* **27**, 1797–1805 (2021).
203. Shalabi, H. *et al.* CD19/22 CAR T cells in children and young adults with B-ALL: phase 1 results and development of a novel bicistronic CAR. *Blood* **140**, 451–463 (2022).
204. Spiegel, J. Y. *et al.* CAR T cells with dual targeting of CD19 and CD22 in adult patients with recurrent or refractory B cell malignancies: a phase 1 trial. *Nat. Med.* **27**, 1419–1431 (2021).
205. Ramakrishna, S. *et al.* Modulation of Target Antigen Density Improves CAR T-cell Functionality and Persistence. *Clin. Cancer Res. Off. J. Am. Assoc. Cancer Res.* **25**, 5329–5341 (2019).
206. Pont, M. J. *et al.* γ -Secretase inhibition increases efficacy of BCMA-specific chimeric antigen receptor T cells in multiple myeloma. *Blood* **134**, 1585–1597 (2019).
207. Adachi, K. *et al.* IL-7 and CCL19 expression in CAR-T cells improves immune cell infiltration and CAR-T cell survival in the tumor. *Nat. Biotechnol.* **36**, 346–351 (2018).
208. Moon, E. K. *et al.* Expression of a Functional CCR2 Receptor Enhances Tumor Localization and Tumor Eradication by Retargeted Human T cells Expressing a Mesothelin-Specific Chimeric Antibody Receptor. *Clin. Cancer Res.* **17**, 4719–4730 (2011).
209. Caruana, I. *et al.* Heparanase promotes tumor infiltration and antitumor activity of CAR-redirectioned T lymphocytes. *Nat. Med.* **21**, 524–529 (2015).
210. Wang, L.-C. S. *et al.* Targeting fibroblast activation protein in tumor stroma with chimeric antigen receptor T cells can inhibit tumor growth and augment host immunity without severe toxicity. *Cancer Immunol. Res.* **2**, 154–166 (2014).

211. Majzner, R. G. *et al.* GD2-CAR T cell therapy for H3K27M-mutated diffuse midline gliomas. *Nature* **603**, 934–941 (2022).
212. Pegram, H. J. *et al.* Tumor-targeted T cells modified to secrete IL-12 eradicate systemic tumors without need for prior conditioning. *Blood* **119**, 4133–4141 (2012).
213. Kloss, C. C. *et al.* Dominant-Negative TGF- β Receptor Enhances PSMA-Targeted Human CAR T Cell Proliferation And Augments Prostate Cancer Eradication. *Mol. Ther.* **26**, 1855–1866 (2018).
214. Narayan, V. *et al.* PSMA-targeting TGF β -insensitive armored CAR T cells in metastatic castration-resistant prostate cancer: a phase 1 trial. *Nat. Med.* **28**, 724–734 (2022).
215. Cherkassky, L. *et al.* Human CAR T cells with cell-intrinsic PD-1 checkpoint blockade resist tumor-mediated inhibition. *J. Clin. Invest.* **126**, 3130–3144 (2016).
216. Ren, J. *et al.* A versatile system for rapid multiplex genome-edited CAR T cell generation. *Oncotarget* **8**, 17002–17011 (2017).
217. Yamamoto, T. N. *et al.* T cells genetically engineered to overcome death signaling enhance adoptive cancer immunotherapy. *J. Clin. Invest.* **129**, 1551–1565 (2019).
218. Grosser, R., Cherkassky, L., Chintala, N. & Adusumilli, P. S. Combination Immunotherapy with CAR T Cells and Checkpoint Blockade for the Treatment of Solid Tumors. *Cancer Cell* **36**, 471–482 (2019).
219. Yin, Y. *et al.* Checkpoint Blockade Reverses Anergy in IL-13R α 2 Humanized scFv-Based CAR T Cells to Treat Murine and Canine Gliomas. *Mol. Ther. Oncolytics* **11**, 20–38 (2018).
220. Li, A. M. *et al.* Checkpoint Inhibitors Augment CD19-Directed Chimeric Antigen Receptor (CAR) T Cell Therapy in Relapsed B-Cell Acute Lymphoblastic Leukemia. *Blood* **132**, 556–556 (2018).
221. Liu, X. *et al.* A Chimeric Switch-Receptor Targeting PD1 Augments the Efficacy of Second-Generation CAR T Cells in Advanced Solid Tumors. *Cancer Res.* **76**, 1578–1590 (2016).

222. Xue, Y. *et al.* CD19 and CD30 CAR T-Cell Immunotherapy for High-Risk Classical Hodgkin's Lymphoma. *Front. Oncol.* **10**, 607362 (2021).
223. Tzankov, A. *et al.* Expression of B-Cell Markers in Classical Hodgkin Lymphoma: A Tissue Microarray Analysis of 330 Cases. *Mod. Pathol.* **16**, 1141–1147 (2003).
224. Mikkilineni, L. & Kochenderfer, J. N. CAR T cell therapies for patients with multiple myeloma. *Nat. Rev. Clin. Oncol.* **18**, 71–84 (2021).
225. Pan, J. *et al.* Donor-Derived CD7 Chimeric Antigen Receptor T Cells for T-Cell Acute Lymphoblastic Leukemia: First-in-Human, Phase I Trial. *J. Clin. Oncol. Off. J. Am. Soc. Clin. Oncol.* **39**, 3340–3351 (2021).
226. Zhang, M. *et al.* Autologous Nanobody-Derived Fratricide-Resistant CD7-CAR T-cell Therapy for Patients with Relapsed and Refractory T-cell Acute Lymphoblastic Leukemia/Lymphoma. *Clin. Cancer Res. Off. J. Am. Assoc. Cancer Res.* **28**, 2830–2843 (2022).
227. Cui, Q. *et al.* CD38-directed CAR-T cell therapy: a novel immunotherapy strategy for relapsed acute myeloid leukemia after allogeneic hematopoietic stem cell transplantation. *J. Hematol. Oncol. J Hematol Oncol* **14**, 82 (2021).
228. Kochenderfer, J. N., Yu, Z., Frasheri, D., Restifo, N. P. & Rosenberg, S. A. Adoptive transfer of syngeneic T cells transduced with a chimeric antigen receptor that recognizes murine CD19 can eradicate lymphoma and normal B cells. *Blood* **116**, 3875–3886 (2010).
229. Kochenderfer, J. N., Yu, Z., Frasheri, D., Restifo, N. P. & Rosenberg, S. A. Adoptive transfer of syngeneic T cells transduced with a chimeric antigen receptor that recognizes murine CD19 can eradicate lymphoma and normal B cells. *Blood* **116**, 3875–3886 (2010).
230. James, C. *et al.* A unique clonal JAK2 mutation leading to constitutive signalling causes polycythaemia vera. *Nature* **434**, 1144–1148 (2005).
231. Baxter, E. J. *et al.* Acquired mutation of the tyrosine kinase JAK2 in human myeloproliferative disorders. *The Lancet* **365**, 1054–1061 (2005).

232. Rumi, E. *et al.* JAK2 or CALR mutation status defines subtypes of essential thrombocythemia with substantially different clinical course and outcomes. *Blood* **123**, 1544–1551 (2014).
233. Carobbio, A. *et al.* Leukocytosis and thrombosis in essential thrombocythemia and polycythemia vera: a systematic review and meta-analysis. *Blood Adv.* **3**, 1729–1737 (2019).
234. Wolach, O. *et al.* Increased neutrophil extracellular trap formation promotes thrombosis in myeloproliferative neoplasms. *Sci. Transl. Med.* **10**, eaan8292 (2018).
235. Mullally, A. *et al.* Physiological Jak2V617F Expression Causes a Lethal Myeloproliferative Neoplasm with Differential Effects on Hematopoietic Stem and Progenitor Cells. *Cancer Cell* **17**, 584–596 (2010).
236. Akada, H. *et al.* Conditional expression of heterozygous or homozygous Jak2V617F from its endogenous promoter induces a polycythemia vera–like disease. *Blood* **115**, 3589–3597 (2010).
237. Elf, S. E. JAK out of the box: myeloproliferative neoplasms--associated JAK2 V617F mutations contribute to aortic aneurysms. *Haematologica* **106**, 1783–1784 (2021).
238. Lee, S. C.-W. *et al.* Synthetic Lethal and Convergent Biological Effects of Cancer-Associated Spliceosomal Gene Mutations. *Cancer Cell* **34**, 225-241.e8 (2018).
239. Nishimura, M. *et al.* Acquisition of JAK2 V617F to CALR-mutated clones accelerates disease progression and might enhance growth capacity. *Br. J. Haematol.* **194**, e89–e92 (2021).
240. Vannucchi, A. M. & Harrison, C. N. Emerging treatments for classical myeloproliferative neoplasms. *Blood* **129**, 693–703 (2017).
241. Grinfeld, J. *et al.* Classification and Personalized Prognosis in Myeloproliferative Neoplasms. *N. Engl. J. Med.* **379**, 1416–1430 (2018).
242. Yogarajah, M. & Tefferi, A. Leukemic Transformation in Myeloproliferative Neoplasms. *Mayo Clin. Proc.* **92**, 1118–1128 (2017).

243. Tubb, V. M. *et al.* Isolation of T cell receptors targeting recurrent neoantigens in hematological malignancies. *J. Immunother. Cancer* **6**, 1–14 (2018).
244. Gilham, D. E. *et al.* Primary polyclonal human T lymphocytes targeted to carcino-embryonic antigens and neural cell adhesion molecule tumor antigens by CD3 ζ -based chimeric immune receptors. *J. Immunother.* **25**, 139–151 (2002).
245. Nolan, K. F. *et al.* Bypassing immunization: Optimized design of ‘designer T cells’ against carcinoembryonic antigen (CEA)-expressing tumors, and lack of suppression by soluble CEA. *Clin. Cancer Res.* **5**, 3928–3941 (1999).
246. Sterner, R. M. *et al.* GM-CSF inhibition reduces cytokine release syndrome and neuroinflammation but enhances CAR-T cell function in xenografts. *Blood* **133**, 697–709 (2019).
247. Sachdeva, M., Duchateau, P., Depil, S., Poirot, L. & Valton, J. Granulocyte macrophage colony-stimulating factor inactivation in CAR T-cells prevents monocyte-dependent release of key cytokine release syndrome mediators. *J. Biol. Chem.* **294**, 5430–5437 (2019).
248. Abraham, R. T. & Weiss, A. Jurkat T cells and development of the T-cell receptor signalling paradigm. *Nat. Rev. Immunol.* **4**, 301–308 (2004).
249. Lipowska-Bhalla, G., Gilham, D. E., Hawkins, R. E. & Rothwell, D. G. Isolation of tumor antigen-specific single-chain variable fragments using a chimeric antigen receptor bicistronic retroviral vector in a Mammalian screening protocol. *Hum. Gene Ther. Methods* **24**, 381–391 (2013).
250. Alonso-Camino, V. *et al.* CARbodies: Human Antibodies Against Cell Surface Tumor Antigens Selected From Repertoires Displayed on T Cell Chimeric Antigen Receptors. *Mol. Ther. Nucleic Acids* **2**, e93 (2013).
251. Rydzek, J. *et al.* Chimeric Antigen Receptor Library Screening Using a Novel NF- κ B/NFAT Reporter Cell Platform. *Mol. Ther.* **27**, 287–299 (2019).

252. Cacemiro, M. da C. *et al.* Philadelphia-negative myeloproliferative neoplasms as disorders marked by cytokine modulation. *Hematol. Transfus. Cell Ther.* **40**, 120–131 (2018).
253. Pecquet, C. *et al.* Secreted mutant calreticulins as rogue cytokines in myeloproliferative neoplasms. *Blood* **141**, 917–929 (2023).
254. Duncan, B. B., Dunbar, C. E. & Ishii, K. Applying a clinical lens to animal models of CAR-T cell therapies. *Mol. Ther. - Methods Clin. Dev.* **27**, 17–31 (2022).
255. Wrzesinski, C. *et al.* Increased Intensity Lymphodepletion Enhances Tumor Treatment Efficacy of Adoptively Transferred Tumor-specific T Cells. *J. Immunother.* **33**, 1–7 (2010).
256. Fabrizio, V. A. *et al.* Optimal fludarabine lymphodepletion is associated with improved outcomes after CAR T-cell therapy. *Blood Adv.* **6**, 1961–1968 (2022).
257. Amini, L. *et al.* Preparing for CAR T cell therapy: patient selection, bridging therapies and lymphodepletion. *Nat. Rev. Clin. Oncol.* **19**, 342–355 (2022).
258. Neelapu, S. S. CAR-T efficacy: is conditioning the key? *Blood* **133**, 1799–1800 (2019).
259. Jacoby, E. *et al.* Murine allogeneic CD19 CAR T cells harbor potent antileukemic activity but have the potential to mediate lethal GVHD. *Blood* **127**, 1361–1370 (2016).
260. Cimen Bozkus, C. *et al.* Immune Checkpoint Blockade Enhances Shared Neoantigen-Induced T-cell Immunity Directed against Mutated Calreticulin in Myeloproliferative Neoplasms. *Cancer Discov.* **9**, 1192–1207 (2019).
261. Chang, Z. L. *et al.* Rewiring T-cell responses to soluble factors with chimeric antigen receptors. *Nat. Chem. Biol.* **14**, 317–324 (2018).
262. Sun, L. *et al.* Shed antigen-induced blocking effect on CAR-T cells targeting Glypican-3 in Hepatocellular Carcinoma. *J. Immunother. Cancer* **9**, e001875 (2021).
263. Roex, G. *et al.* Safety and clinical efficacy of BCMA CAR-T-cell therapy in multiple myeloma. *J. Hematol. Oncol. J Hematol Oncol* **13**, 164 (2020).

264. Cowan, A. J. *et al.* Efficacy and Safety of Fully Human Bcma CAR T Cells in Combination with a Gamma Secretase Inhibitor to Increase Bcma Surface Expression in Patients with Relapsed or Refractory Multiple Myeloma. *Blood* **134**, 204 (2019).
265. Liu, X. *et al.* Highly active CAR T cells that bind to a juxtamembrane region of mesothelin and are not blocked by shed mesothelin. *Proc. Natl. Acad. Sci. U. S. A.* **119**, e2202439119 (2022).
266. Datlinger, P. *et al.* Pooled CRISPR screening with single-cell transcriptome read-out. *Nat. Methods* **14**, 297–301 (2017).
267. Smale, S. T. Luciferase Assay. *Cold Spring Harb. Protoc.* **2010**, pdb.prot5421-pdb.prot5421 (2010).

Curriculum vitae



CONTACT

- +43 650 3301193
- christinamaria.schueller@gmail.com
- Bloch-Bauer-Promenade 20/34, 1100 Wien
- Linkedin.com/in/cmschueller

SKILLS

Experimental

- Cell culture incl. primary human and murine cells
- In vivo experiments (Mus musculus) – FELASA B certified
- Plasmid design and cloning
- Viral transduction
- Cytotoxicity assays
- CRISPR gene editing
- Multicolor flow cytometry
- Western blot, ELISA
- GraphPad

Soft skills

- Strong presentation skills
- Knowledge in scientific illustration
- Communicative
- Used to working in an international, collaborative environment
- Delegation skills
- Strategic planning abilities
- Ability to remain calm under pressure
- Driving license B

Christina M. Schüller

SUMMARY

I am a proactive scientist who combined eight years of biotechnological research with a medical background.

PROFESSIONAL EXPERIENCE

PREDOCTORAL FELLOW | since 10/2018

Center for Molecular Medicine, Vienna | Robert Kralovics lab

- Generation of chimeric antigen receptors for myeloproliferative neoplasms
- Generation of a novel in vivo model for double mutated myeloproliferative neoplasms
- Funded by a DOC fellowship of the Austrian Academy of Sciences
- Supervision of undergraduate students
- Collaboration with MyeloPro Diagnostics and Research GmbH
- Graduation envisaged 09/2023

MASTER THESIS | 03/2017 - 03/2018

Sankt Anna Children's Cancer Research Institute, Vienna | Group of cellular therapeutics

- Engineering of chimeric antigen receptors with ON-switch and AND-gate function

RESEARCH INTERNSHIP | 06/2016 - 09/2016

Suranaree University of Technology, Nakhon Ratchasima, Thailand | Parinya Noisa lab

- Transdifferentiation of human fibroblasts into neurons
- Investigation of the effect of curcumin on neuroblastoma cells

RESEARCH ASSISTANT AND BACHELOR THESIS

University of Natural Resources and Life Sciences, Vienna | 08/2014 - 05/2016

- Fusarium graminearum secondary metabolism and lysine biosynthesis: the role of PPT1

PUBLICATIONS

Co-authored:
Engineering AvidCARs for combinatorial antigen recognition and reversible control of CAR function. Nature Communications, 2020

Hematopoietic expression of a chimeric murine-human CALR oncoprotein allows the assessment of anti-CALR antibody immunotherapies in vivo. American Journal of Hematology, 2021

First author:
Co-expression of mutated Jak2 and Calr enhances myeloproliferative phenotype in mice without loss of stem cell fitness. American Journal of Hematology, 2022

AWARDS

2013-2016, 2018 Performance Scholarship - University of Natural Resources and Life Sciences, Vienna

2015 Advancement Award - Allgemeine Hochschulstipendienstiftung

2021 DOC Fellowship – Austrian Academy of Sciences

2022 Performance Scholarship, Medical University of Vienna

LANGUAGES

German – Native

English – Fluent (C1)

Spanish – Basic (B1)

HOBBIES

Basketball

Dancing

Bouldering

Travel

PROFESSIONAL EXPERIENCE CONT.

INTERNSHIP QUALITY ASSURANCE | 07/2013 – 10/2013

Agrana Bioethanol GmbH, Pischelsdorf

- Routine diagnostics

EDUCATION

HUMAN MEDICINE | since 10/2019

Medical University of Vienna

- Preclinical part will be completed 06/2023
- Diploma thesis: Treosulfan and fludarabine for allogeneic hematopoietic stem cell transplantation – a retrospective study
- Internships
 - Primary care incl. pediatric care
 - Hematology
 - Bone marrow transplantation
 - Internal medicine

MASTER OF SCIENCE IN BIOTECHNOLOGY | 09/2015 – 05/2018

University of Natural Resources and Life Sciences, Vienna

- Graduation with distinction

BACHELOR OF SCIENCE IN BIOTECHNOLOGY AND FOOD SCIENCE | 09/2012 – 08/2015

University of Natural Resources and Life Sciences, Vienna

- Graduation with distinction

VOLUNTEERING

PHD REPRESENTATIVE | 2018-2019

Center for Molecular Medicine, Vienna

- Organization of social events and a career workshop
- Science outreach: children education program

REFERENCES

- Available upon request